

**CHARLES UNIVERSITY**

**Faculty of Science**

Study programme: Biology

Study field: Parasitology



**Bc. Alena Revalová**

**The skin immune response of mice infected with avian schistosomes**

Imunitná odpoveď v koži myší infikovaných vtáčimi schistosomami

MASTER'S THESIS

Supervisor: RNDr. Tomáš Macháček, Ph.D.

Advisor: Mgr. Martin Majer

Praha, 2022



**Prehlásenie:**

Prehlasujem, že som záverečnú prácu vypracovala samostatne a uviedla v nej všetky použité informačné zdroje a literatúru. Táto práca ani jej podstatná časť neboli predložené k získaniu iného alebo rovnakého akademického titulu

V ..... dňa .....

.....

Bc. Alena Revalová



## Acknowledgement/Poďakovanie

My greatest thanks go to Tomáš Macháček and Martin Majer for their endless patience, kindness, experimental guidance and for manifesting love for science. I am incredibly thankful to the lab mates, for the friendship that brightened every day. I would like to acknowledge Jozef Janda, for technical help and for allowing me to have fun with flow cytometry.

Ďakujem mojej rodine, kamarátom a, samozrejme, labríkom. Bez vás by to nešlo.

## Abstract

Invasion of the mammalian skin by cercariae of avian schistosomes of the genus *Trichobilharzia* is associated with the skin pathology called cercarial dermatitis (CD). Although the manifestation of CD, characterized by the presence of maculo-papular rash and pruritus, is believed to be linked with the previous sensitization, the role of the infection dose and the specific causative agent is rarely considered. Therefore the skin immune response in mouse pinnae infected by 100, 1000 or 4x100 (repeated infections) cercariae of two *Trichobilharzia* species – *T. regenti* and *T. szidati* – was examined in this work. To compare the effect of these factors (the infection dose and species), a complex approach was ensured by employing both *in vivo* and *in vitro* methods. Firstly, histopathological changes in the pinnae were examined by classical histology and infiltrated leukocytes were characterized by flow cytometry. Sera of mice were used to detect the systemic production of cytokines and parasite-specific antibodies. *In vitro* cultivation of mouse pinnae was used to detect the local production of cytokines. The most remarkable observation was that the infection dose largely impacted the course of the immune response, both locally and systematically. In primary infected mouse pinnae, 100 cercariae of both species evoked only a mild reaction which was almost undetectable. On the other hand, 1000 cercariae caused extensive skin pathology, induced rapid cellular influx, and triggered antibody production. Furthermore, penetration of *T. regenti* led to the increased local production of both pro-inflammatory and regulatory cytokines. The production of pro-inflammatory cytokines, including alarmin TSLP, seemed to be less pronounced during reinfections. Generally, in contrast to the primary-infected mice (100 cercariae), exposures to 4x100 cercariae led to a detectable immune response. While cercariae of *T. szidati* caused similar (histo)pathological changes as *T. regenti*, the flow cytometry and cytokine production analysis revealed a much weaker immune response against the former species, regardless of the infection dose, indicating the higher immunopathogenic potential of *T. regenti* during early phases of mammalian invasion. Altogether, the data indicate that the course of CD reflects not only the number of exposures but also infection dose and the specific causative agent.

**Key words:** avian schistosome, cercarial dermatitis, immune response, infection dose, pathology, skin, *Trichobilharzia*.

## Abstrakt

Invázia kože cicavcov cercáriami vtáčích schistosom rodu *Trichobilharzia* vedie k vzniku kožnej patológie nazývanej cercáriová dermatitída (CD). Hoci výskyt kožných prejavov CD, ako sú makuly, papuly a pruritus, je zvyčajne spájaný s predošlou senzitivizáciou infikovaného jedinca, len ojedinele sa zohľadňuje konkrétna infekčná dávka či špecifický pôvodca CD. V tejto práci sme preto skúmali imunitnú odpoveď v koži a to v ušniciach myší infikovaných cercáriami rodu *Trichobilharzia* – konkrétne druhmi *T. regenti* alebo *T. szidati* – za použitia infekčných dávok 100, 1000 alebo 4x100 cercárií. Pre komplexné porovnanie týchto faktorov sme zvolili využitie kombináciu *in vivo* a *in vitro* metód. Na sledovanie histopatologických zmien ušnic bola využitá klasická histológia a na identifikáciu leukocytov v tkanive prietoková cytometria. Zo séra myší sme detekovali cytokíny a špecifické protilátky voči parazitárnym antigénom a lokálna produkcia cytokínov v koži bola detekovaná z *in vitro* kultivácie ušnic. Naše výsledky preukázali výrazný vplyv infekčnej dávky na priebeh imunitnej odpovede a to ako aj na úrovni lokálnej, tak aj systémovej reakcie. Nízka infekčná dávkou (100 cercárií) vyvolala len slabú imunitnú odpoveď, ktorá bola takmer nedetekovateľná použitými metódami. Naopak, infekcia 1000 cercáriami viedla k výraznej kožnej patológii, masívnemu prílivu leukocytov, tvorbe špecifických protilátok a v prípade infekcie druhom *T. regenti* aj k zvýšenej cytokínovej produkcii. Zatiaľ čo primárna infekcia viedla k produkcii pro- aj proti-zápalových cytokínov, pri reinfekciách bola produkcia pro-zápalových mediátorov, vrátane TSLP, potlačená a prevažovali proti-zápalové cytokíny. Pri opakovanej infekcii 100 cercáriami (4x100) sa na rozdiel od primo-infekcie (100) prejavila detekovateľná imunitná odpoveď. Hoci oba druhy rodu *Trichobilharzia* viedli k podobným histopatologickým zmenám, *T. szidati* vyvolala zreteľne slabšiu infiltráciu leukocytov a cytokínovú produkciu, čo naznačuje slabší imunopatogenetický potenciál tohto druhu. V súhrne výsledky tejto práce naznačujú, že priebeh CD sa odvíja nie len od počtu predošlých expozícií ale aj od intenzity infekcie a od konkrétneho druhu, pôvodcu CD.

**Kľúčové slová:** vtáacie schistosomy, cercáriová dermatitída, imunitná odpoveď, infekčná dávka, patológia, koža, *Trichobilharzia*.

## List of contents

Abbreviations .....	1
1. Introduction and aims of the study.....	3
2. Literature review .....	4
2.1. Avian schistosomes .....	4
2.1.1. Biology of <i>T. regenti</i> and <i>T. szidati</i> , with a focus on the skin phase.....	4
2.1.1.3. Penetration rate and migration.....	7
2.2. Cercarial dermatitis .....	8
2.2.1. Etiological agents of CD .....	8
2.2.2. CD in humans.....	8
2.2.3. CD in mice.....	10
3. Material and methods.....	12
3.1. Chemicals, solution, and suspensions .....	12
3.1.1. Used for <i>in vivo</i> experiments.....	12
3.1.2. Used for <i>in vitro</i> experiments.....	16
3.2. Experimental design .....	16
3.3. Model organisms and experimental infections.....	17
3.3.1. Infection agents and infection dose .....	17
3.3.2. Infection of experimental animals.....	17
3.4. <i>In vivo</i> experiments .....	18
3.4.1. Histological processing of the mouse pinna.....	18
3.4.2. Immunophenotyping leukocytes from the mouse skin and parotid LNs.....	20
3.4.3. Measurement of serum cytokines by CBA .....	24
3.4.4. Measuring antibody immune response .....	26
3.5. <i>In vitro</i> cultivation of the mouse pinna .....	27
3.5.1. Cultivation of the mouse pinna and harvest of supernatant .....	27
3.5.2. Counting the released cells .....	28
3.5.3. Measuring levels of cytokines .....	28
3.6. Statistics.....	29
4. Results .....	30
4.1. Penetration rate .....	30
4.2. Systemic immune response.....	30
4.2.1. Serum antibodies.....	30
4.2.2. Serum cytokines .....	31
4.3. Skin pathology .....	33
4.3.1. Macroscopic observations of mouse pinnae.....	33

4.3.2. Histological examination of mouse pinnae .....	33
4.4. Immunophenotyping of leukocytes in mouse pinnae.....	39
4.5. Examination of parotid LNs .....	45
4.6. <i>In vitro</i> examination of mouse pinnae .....	48
4.6.1. Cell emigration from pinnae <i>in vitro</i> .....	48
4.6.2. <i>In vitro</i> cytokine secretion from cultivated mouse pinnae .....	49
5. Discussion .....	51
Limitations of the study.....	60
6. Conclusion .....	61
References.....	62

## Abbreviations

Ag	antigen
ATP	adenosine triphosphate
CBA	cytokine bead array
CD	cercarial dermatitis
cxcl	chemokine (C-X-C) motif ligand
DCs	dendritic cells
DEC	dermal exudate cells
dpi	days post infection
ELISA	enzyme-linked immunosorbent assay
ES	excretory-secretory
HBSS	Hank's balanced salt solution
hpi	hours post infection
IFN- $\gamma$	Interferon- $\gamma$
Ig	immunoglobulin
IL	interleukin
LC	Langerhans cells
LN	lymph nodes
mac	macrophages
MHCII	major histocompatibility complex type II
OD	optical density
PBS	phosphate buffer saline
PBS-T	phosphate buffer saline with Tween
PD-L1	programmed death ligand
PE	phycoerythrin
RPMI 1640	Roswell Park Memorial Institute 1640
SD	standard deviation
TNF	tumor necrosis factor
TSLP	thymic stromal lymphopoietin



## 1. Introduction and aims of the study

Percutaneous invasion of the mammalian host is an invasion strategy employed by several helminths, including schistosomes, hookworms, and filariae. Despite that in natural infection larvae of these helminths actively penetrate the skin, the first mechanical barrier, the skin immune response is often inadequately studied. Frequently, larvae are administered into experimental animals by distinct routes, most commonly by injection or, if possible, by ingestion, thus bypassing the natural skin migration of the parasites. In combination with the deficiency of suitable (and easily maintained) parasitic model species, the role of the skin immune system in the skin-penetrating helminths is underestimated, and more attention is concentrated on the subsequent pathologies. Although the skin phase might be partially neglected, probably because skin pathologies are only minor health issues, from the perspective of the helminths it is the essential site for host invasion where they must employ immune evasion strategies.

Cercariae of avian schistosomes are only partially able to escape from mammalian skin, likely being in shortage of powerful immune evasion strategies. As a consequence, their penetration (especially repeated) evokes an immune response which manifests as cercarial dermatitis (CD). Particularly, cercariae of the genus *Trichobilharzia* are the most frequently recognized causative agents of this skin condition. Despite the focus on the ecological factors combined with personal records of patients (Kolářová *et al.*, 1997; Soldánová *et al.*, 2013) there were virtually no attempts to link symptoms of CD to the specific CD-causing species. Moreover, regardless of numerous experimental infection and pathological observations, there is no clear connection between the infection dose and the skin pathologies. Therefore, we decided to study the immune response in the skin of mice experimentally infected by cercariae of *Trichobilharzia* spp. to extend the current knowledge of CD.

In this thesis, we aimed to:

- examine the role of the infection doses of cercariae (100 and 1000) on the course of immune reaction
- study the effect of previous sensitization (4x repeated infection by 100 cercariae) on the course of the immune reaction
- determine the effect of different *Trichobilharzia* species (*T. regenti* and *T. szidati*) on the course of the immune reaction
- define qualitatively and quantitatively the immune response (both local and systemic) by histopathological examination, immunophenotyping of the leukocytes, detection of cytokine production, and detection of parasite-specific antibodies

## 2. Literature review

### 2.1. Avian schistosomes

Avian schistosomes comprise the majority of genera in the family of Schistosomatidae. The family Schistosomatidae, well-known for human schistosomiasis-causing species, currently consists of 17 described genera among which 13 genera (with at least 85 described species) represent parasites of birds (Loker et al., 2022). Recent findings of the new species and genera (e.g. in Argentina (Lorenti et al., 2022), Chile (Oyarzún-Ruiz et al., 2022), or New Zealand (Davis et al., 2022)) but also recent findings of the well-known species in new areas (Ashrafi et al., 2018; Helmer et al., 2021; Juhász et al., 2022; Marszewska et al., 2018; Reier et al., 2020) highlight the diversity of the avian schistosomes and the abundant occurrence worldwide.

As already mentioned, CD is the pathological skin reaction of mammals to the penetrating larvae of avian schistosomes (2.2.). In such cases, mammals are considered accidental hosts restraining further maturation of parasites (Blažová and Horák, 2005). On the other hand, in the aquatic birds, penetrating cercariae transform to schistosomula, undergo species-specific migration, and sexually reproduce. Miracidia developing within the eggs are infectious for aquatic snails, which serve as intermediate hosts. In snails, asexual reproduction takes place resulting in the development of cercariae. This larval stage emerges from snails and maintains the life cycle by infecting the aquatic birds, the definitive hosts (Horák et al., 2002).

Whereas in Europe and North America, CD is noted mostly during seasonal outbreaks for causing economic loss in the affected recreational areas (Horák et al., 2015; Loker et al., 2022), in other areas it may cause long-lasting irritation in some vulnerable groups of inhabitants, such as rice-farmers (Hunter et al., 1951; Kia lashaki et al., 2021), or in poor communities living in the developing countries (Rao et al., 2007). Scanty reports of human infections from the latter areas are likely due to the difficult diagnosis of CD caused by avian schistosomes in schistosomiasis-endemic areas (Pinto et al. 2022; Rao et al. 2007). Out of avian schistosomes, the genus *Trichobilharzia* is noteworthy not only for its species-richness and wide distribution but also for its notoriety as the most frequent causative agent of CD (Horák et al., 2015). Two species of the genus, *T. regenti* and *T. szidati*, represent available laboratory models for studying not only the CD.

#### 2.1.1. Biology of *T. regenti* and *T. szidati*, with a focus on the skin phase

*T. regenti* (Horák et al., 1998a) and *T. szidati* (Neuhaus, 1952) (former *T. ocellata* (Aldhoun et al., 2016)) represent nasal and visceral species, respectively, of the genus *Trichobilharzia*. *T. regenti* is a neurotropic species whose schistosomula leave the skin by peripheral nerves, migrate through the spinal cord and reach the brain of definitive hosts (Hrádková and Horák, 2002). Adult worms and eggs are found in the nasal area where miracidia hatch (Horák et al., 1999) and they infect snails of the

genus *Radix* in the aquatic environment (Horák et al., 1998a, 1999). Migration of *T. szidati* within the vertebrate host differs significantly. Schistosomula of *T. szidati* enter the vasculature in the skin of birds and migrate to the lungs. In the lungs, schistosomula escape from the circulatory system but, to continue their migration, they must re-enter it to reach the vessels of the small intestine (Chanová et al., 2007). Adults are found firstly in the veins of the small intestine and later in the intestinal mucosa where they lay eggs. The eggs with miracidia are passed in the feces of the infected bird (Bourns et al., 1973) and miracidia hatch in the water to infect intermediate host, the snail *Lymnaea stagnalis* (Rudolfová et al., 2005).

#### 2.1.1.1. Cercariae

Cercariae can be shed from snails in large quantities. During summer months, under laboratory conditions, *L. stagnalis* shed in average > 2500 cercariae of *T. szidati* (Soldánová et al., 2016) with the highest observed emergence of 80 000 cercariae per snail in a day (Al-Jubury et al., 2020). In contrast, from different snail species, *Radix balthica*, Soldánová et al. (2022) noted the highest number of 1316 cercariae of *Trichobilharzia* sp. to be shed and the mean was around 450 cercariae. Cercariae shedding from both snail species occurred mostly at the beginning of the light-period (16/8 dark/light regime), which corresponded with sunrise (Soldánová et al., 2016, 2022). After emerging from snails, cercariae of *Trichobilharzia* sp. survive around 2-3 days, depending on the temperature (Al-Jubury et al., 2020; Neuhaus, 1952). Generally the infectivity of cercariae is known to be decreasing in age-dependent manner as shown in other (*S. mansoni* (Whitfield et al., 2003); *Plagiorchis elegans* (Lowenberger and Rau, 1994); *Diplostomum spathaceum* (Karvonen et al., 2003)), but such experiments were not performed with *Trichobilharzia* sp. cercariae. Despite that, Al-Jubury et al. (2020) suggested, that the short-lifespan and decreasing infection potential could lay behind the development of highly specific host-finding strategies.

#### 2.1.1.2. Skin-penetration

Reacting to chemical and physical stimuli, cercariae actively seek and invade their hosts. During the first hour after emerging from a snail, the cercariae of *T. szidati* search the definitive host by alternating between the swimming and sinking phase likely to increase the chance of an encounter (Haas, 1994). Swimming patterns thoroughly described by Feiler and Haas (1988a) are influenced by light and dark signals as well as physical contact. In the darkness, the cercariae exhibit negative geotaxis but if stimulated by light, they swim towards the light source (Al-Jubury et al., 2020; Feiler and Haas, 1988a; Grabe and Haas, 2004a). If they are present in water for a prolonged time, they rest in a horizontal position near the surface unless a shadow stimulates their movement (Haas, 1994). Staying near the water surface while responding quickly to the shade could be the adaptation of cercariae to easily reach floating birds (Al-Jubury et al., 2020; Feiler and Haas, 1988a; Haas, 1994). Encouraged by the

shade, cercariae react to the temperature gradient (Feiler and Haas, 1988a) and chemical stimuli such as ceramides and cholesterol (Feiler and Haas, 1988b) which enhance the likelihood of cercarial attachment. Nonetheless, the presence of fatty acids is necessary for penetration and emptying of penetration glands (experimentally tested for both *T. szidati* and *T. regenti*) (Haas and Van De Roemer, 1998; Mikeš et al., 2005; Řimnáčová et al., 2017). Due to the presence of the aforementioned molecules in the skin of both, birds and humans, cercariae do not properly distinguish between their final and accidental hosts. After attachment, the cercariae of *T. szidati* initiate the penetration of human skin in less than 80 seconds. The fastest cercariae can fully burrow into the human skin in 83 seconds, yet most of them penetrate in around 4 minutes (Haas and Van De Roemer, 1998).

During skin penetration, cercariae undergo morphological and metabolic changes. Tail-shedding of *T. szidati* occurs less than 1.5 minutes after the beginning of penetration (Haas and Van De Roemer, 1998) and fucose-rich glycocalyx is gradually reduced, revealing different set of saccharide epitopes on the surface of both species (Horák et al., 1998b; Řimnáčová et al., 2017). Apart from morphological changes, schistosomula of *T. regenti* switch their metabolic pathways from aerobic to mostly anaerobic (Leontovyč et al., 2016). Once in the tissue, schistosomula of visceral *T. szidati* are attracted by serum and they orientate towards the L-arginine, D-glucose (Grabe and Haas, 2004b), and the darkness (Grabe and Haas, 2004a). As the authors suggest, these signals might help schistosomula of *T. szidati* to migrate deeper into the dermis and to localize blood vessels. Stimuli for host-finding and penetration for *T. regenti* were not published, however signals seem to be partially uniform over the tested trematode species (reviewed by Haas (1994, 2003)).

Disruption of the skin during penetration is facilitated by the chemical content of penetration glands, and by the active forward movement of the penetrating cercariae. Cercariae, attached to the host by ventral sucker, invade the skin while secreting the content of the penetration glands (Haas and Van De Roemer, 1998). Penetration glands, occupying almost 1/3 of cercarial body (assessed in *T. regenti* by Ligasová et al. (2011)), contain peptidases, peptidase inhibitors and venom like-allergen proteins which, likely, facilitate breaching the skin barrier and parasite migration (Dolečková et al., 2010; Kašný et al., 2007; Vondráček et al., 2022). Cysteine peptidase activity was described in both species (Mikeš et al., 2005). Earlier, in glands of *T. regenti*, cathepsin B2 capable of skin protein degradation (keratin, collagen, elastin) was found (Dolečková et al., 2009; Kašný et al., 2007). Recently, proteomic analysis of *T. szidati* revealed the presence of broad spectrum of peptidases, including cathepsin B2, cathepsin L, elastase 2b, leishmanolysin and invadolysin that Vondráček et al., (2022) highlight in the context of host invasion. The functional tests with *T. szidati* recombinants have not been performed, thus, only possible functions of these proteins are discussed therein by the authors. Nevhutalu et al. (1993) suggest, that prostaglandins and leukotrienes, found in the excretory-secretory (ES) products, may also

interfere with the host immune system during the skin penetration. Interactions between the ES products and/or the surface of schistosomula with the host immune system could lay behind the different migration success of schistosomula in definitive and accidental hosts.

#### 2.1.1.3. Penetration rate and migration

The migration of schistosomula in the skin of mammals and the following host immune response depends on the number of exposures as well as immunological background of the host. Cercariae of *T. regenti* penetrated the skin of mice at higher rate in the case of repeatedly exposed animals, and, regardless of the exposures, more cercariae penetrated into the skin of immunocompetent hairless mice than into (shaved) immunodeficient mice (Kouřilová et al., 2004a). In the skin of immunocompetent mice (2.2.3.), inflammation and mostly damaged schistosomula are observed whereas in immunodeficient mice, only weak immune response is detected (Kouřilová et al., 2004a). Weaker immune response in skin of immunodeficient mice is likely a reason for faster and more successful migration of schistosomula (Hrádková and Horák, 2002; Kouřilová et al., 2004a). Further, only observations from immunocompetent individuals are reviewed.

After penetration, majority of schistosomula of *T. regenti* remain in the epidermis for around 6 hours post infection (hpi). At 12 hpi to 24 hpi, schistosomula are found mostly in dermis (Kouřilová et al., 2004a), from where, 1.5 days post infection (dpi), some of them successfully escape to the peripheral nerves (Hrádková and Horák, 2002). According to Kouřilová et al., (2004b), approximately 90% of (radiolabeled) larvae do not reach central nervous system but remain in the skin of primary-infected mice and die within 8 days. Similar observation was done with radiolabeled schistosomula of *T. szidati* by Haas and Pietsch (1991) who found living schistosomula in the skin of mice only until 5 dpi. Moreover, in their experiment, 36% of schistosomula were detected in other organs but skin.

In experimentally infected mammals, *Trichobilharzia* spp. do not mature, however, a proportion of schistosomula escape the skin and partially continue in the migration (Chanová et al., 2007; Haas and Pietsch, 1991; Hrádková and Horák, 2002; Kouřilová et al., 2004b; Olivier, 1953). Although majority of the schistosomula die in the skin (Kouřilová et al., 2004b), the role of the penetration site (specific skin region) in the further migration of parasites was not properly elucidated. Haas and Pietsch (1991) observed a difference in the speed of schistosomula migration between mice infected via the tail and via the shaved abdomen by the cercariae of *T. szidati*. However, due to discrepancies in the experimental design, e.g., mice of different ages, different duration of exposure, and usage of radiolabeled cercariae in one case but not in the other, the results are incomparable. For example, taking a closer look at the schistosomula in the lungs of mice infected by non-radiolabeled cercariae of *T. szidati*, in the study of Haas and Pietsch (Han NMRI mice 5 weeks; 200 cercariae; 30 min exposure of abdomen), schistosomula were present already at 10 hpi. In the study of Chanová et al., (2007)

(BALB/c mice 8-12 weeks; 300-1500 cercariae; 40-45 min exposure of legs and tail), schistosomula were found in lungs 2-4 dpi which is in accordance also with the observations of (Olivier, 1953). To find out whether it was the infection site that influenced the migration of schistosomula, or the abovementioned factors, comparative experiments need to be performed. And even if it was the site of penetration, whether it is a matter of the skin anatomy, skin immune response or the distance of the parasite's route, remains to be answered. Despite the skin phase of the infection (and the associated immune reaction) represent a critical step in the invasion of the host by avian schistosome, many essential gaps remain to be filled.

## 2.2. Cercarial dermatitis

### 2.2.1. Etiological agents of CD

Despite that several genera of avian schistosomes have been confirmed as the causative agents of CD (Kolářová, 2007), not all of the avian schistosomes are likely to take part in CD outbreak as evidence for their CD-causing potential is lacking (Loker et al., 2022). For example, in the recent experiments of Anderson et al. (2022), penetration of cercariae of *T. stagnicola* into human skin resulted in numerous papules formation whereas hardly any skin lesions were observed after exposure to a novel species – schistosomatid sp. C. Their experiments also showed different cercarial behavior pattern between these species which suggests, that distinct stimuli trigger the penetration, thus possibly resulting in unwillingness of schistosomatid sp. C to penetrate human skin. However, the real penetration success was not determined. On the other hand, common symptoms of CD, such as vasodilation and erythematous skin, can be elicited after experimental infection of mammals by the species yet unrecognized as etiological agent (Pinto et al., 2022). Moreover, infection by mammalian species (e.g., *S. douthitti* (Kagan and Meranze, 1955), *S. turkestanicum* (Juhász et al., 2016), *S. haematobium* (Mduluzza-Jokonya et al., 2021), *S. mansoni* (Langenberg et al., 2020)) are frequently accompanied by skin rash. Taking a closer look at the genus *Trichobilharzia*, while several species (e.g. *T. physellae*, *T. stagnicola*, *T. szidati* (Olivier, 1953), *T. regenti* ((Horák et al., 1999) *T. franki* (Gulyás et al., 2020), were found to readily penetrate the skin of mammals, the species identified in the outbreaks of CD in Europe are mostly *T. franki* (Caron et al., 2017; Gulyás et al., 2020; De Liberato et al., 2019; Selbach et al., 2016) and *T. szidati* (Kolářová et al., 1997; Korycińska et al., 2021).

### 2.2.2. CD in humans

The intensity of the CD symptoms exaggerates over the multiple exposures. In primo-infected individuals, transient itch, described as prickling sensation, occurs, and papules formation was noted (Macfarlane, 1949; Macháček et al., 2018; Olivier, 1949). The symptoms, if present, usually persist only for few days. Nevertheless, in some circumstances, primary infection seems to be completely asymptomatic, as was tested after experimental exposure to *T. franki* by (Gay et al., 1999) or by *T.*

*elvae* (Cort, 1928). In the repeatedly infected humans, apparent maculopapular rash, erythema and edema, along with the intense pruritus usually occur but the appearance, intensity and the development of symptoms in time vary between the individuals (Gay et al., 1999; Macfarlane, 1949; Macháček et al., 2018; Olivier, 1949; Tracz et al., 2019). Despite all the pathological observations and questionnaires, association between the number of exposures with the symptoms intensity is not always clear, as can be concluded from the case reports (Tracz et al., 2019). Al-Jubury et al. (2021) similarly to Macfarlane (1949), ascribed development of unusually strong reactions in primary-exposed individuals to their immunological status and/or to the possibility of the former unnoticed exposure. Nevertheless, a general consensus is that the stronger skin immune response, the faster the destruction of schistosomula.

Beyond the local skin pathology, systemic symptom may also occur in CD patients. In the experiments of Olivier (1949), volunteers were repeatedly exposed to the cercariae of *T. stagnicolae* on one arm before the final exposure on a different body part. At the penetration site of the final exposure, severe CD occurred, indicating that immune reaction may be partially systematic. Besides, symptoms of systemic inflammation (fever, lymph node swelling, nausea, diarrhea) accompany CD in some individuals (Al-Jubury et al., 2021; Appleton and Lethbridge, 1979; Kolářová et al., 1997), but do not seem to be typical (Macháček et al., 2018; Tracz et al., 2019).

The skin immune response during cercarial dermatitis is characterized as the allergic reaction. The nature of CD as an allergic immune response was previously based on the (histo)pathological observations (Macfarlane, 1949; Olivier, 1949) of exposed humans, but later also on the experimental evidence. Intradermal injection of cercarial antigen evoked stronger immune response in sensitized individuals (Macfarlane, 1949) and Lichtenbergová et al. (2008) proved *in vitro* secretion of interleukin 4 (IL-4) from human basophils in response to cercarial antigen of *T. regenti*. Higher production of IL-4, as one of the pivotal mediators of allergic reaction, was supported also *in vivo*, when the higher levels of IL-4 were detected in peripheral blood after the infection of *T. szidati* (Macháček et al., 2018). Although these observations suggest the characterization of CD as the allergic reaction, there is some ambiguity in the production of IgE. Significant increase of IgE in the sera of CD patients was not detected (Lichtenbergová et al., 2008) (Macháček et al., 2018) although in the study of Lichtenbergová et al. (2008), IgE antibodies reacting to the cercarial ES products of *T. regenti* were present. Locally, at the penetration site, Gay et al. (1999) did not observe binding of anti-IgE antibodies in the skin by means of immunohistochemistry. To study immune response during CD more deeply, the mouse model of cercarial dermatitis was established.

### 2.2.3. CD in mice

After the penetration of *T. regenti* cercariae into naïve immunocompetent mice, immediate thickening of the skin at the penetration site with significantly elevated histamine production indicates skin-inflammation (Kouřilová et al., 2004b). Already 4–6 hpi, the immune response is detectable by edema, vasodilation and cytokine production. Firstly, increased production of IL-1 $\beta$ , IL-6, IL-10 was detected. Later, when migrating schistosomula reach the dermis (around 12–24 hpi), the cytokine production persists and IL-6 significantly increases. Leukocytes, mostly neutrophils and eosinophils, accumulate in the proximity of the migrating schistosomula along with the increasing number of mast cells and macrophages at the infection site. Folliculitis, vasculitis (Kouřilová et al., 2004a) and infiltration of Antigen (Ag)-presenting cells (cells expressing major histocompatibility complex type II /MHCII+/ and also cells expressing F4/80+) was noticed 48 hpi (Kouřilová et al., 2004b). The cytokine production considerably changes at the later timepoints (4–8 dpi). The level of IL-6 rapidly decreases, but along with the ongoing production of several cytokines (IL-1 $\beta$ , IL-10, IFN- $\gamma$ ), the excretion of IL-12p40 and IL-4 begins, indicating mixed Th1/Th2 polarization of immune response (Kouřilová et al., 2004b). The mixed polarization was observed also on a systemic level, when similar levels of cercariae-specific IgG1 and IgG2a were detected in mouse sera 7 dpi (Majer et al., 2020).

In the skin of repeatedly infected mice (the proper model for CD), histopathological changes are more prominent comparing to the primary infected animals. Every other exposure to *T. regenti* cercariae causes the increase in the thickness of mouse pinna, resulting from mast cell degranulation and the extensive infiltration of leukocytes into the epidermis and dermis. The fast onset of immune response is marked by the significant production of IL-4, IL-10 and histamine. Interestingly, the production of IL-12 is down-regulated by the infection. Anti-inflammatory cytokines IL-4 and IL-10 dominate in the infected skin until chronic phase, resembling Th2 polarization of the immune response (Kouřilová et al., 2004b). Intraepidermal pustules are formed and infiltration consisting of macrophages, eosinophils, neutrophils and also lymphocytes enwrap schistosomula (Kouřilová et al., 2004a) and infiltrate surrounding tissue (Kouřilová et al., 2004b). Cellular immune response, with striking influx of Ag-presenting cells and mast cells, is much more evident than in primary-infected mice. Additionally, there is a large increase of CD4+ T-lymphocytes. As soon as 3 dpi, only damaged schistosomula or their remnants are found in the tissue (Kouřilová et al., 2004a). Later, anti-inflammatory cytokines significantly decrease 4 dpi and, in contrast, the production of inflammatory IL-12p40 enhances.

At the chronic phase, similarly to the primary-infected mice, processes of tissue repair occur along with detachment of skin abscesses (Kouřilová et al., 2004b). Consistently with the observation in humans, schistosomula were eliminated faster in the reinfected skin (Kouřilová et al., 2004b). The prevalent production of IgG1 towards cercarial antigens in sera of reinfected mice indicates systemic Th2

response (Lichtenbergová et al., 2008) (Kouřilová et al., 2004b). Also, overall levels of IgE antibodies were elevated and gradually increased with the subsequent exposures. The increased antibody production is unlikely due to the time-course of infection solely, as the onset of the production differed in the studies of Lichtenbergová et al. (2008) and Kouřilová et al. (2004b), although the same timepoints were used and analogous trends were observed. However, differences in infection site, duration of exposure and infection dose could take a role.

The reports of clinical observations are consistent but variability in the immune response against different genera was shown (Batten, 1956). Whereas the penetration of *S. douthitti* led to appearance of visible skin lesions and the destruction of cercariae in both epidermis and dermis of mouse, the penetration of *Gigantobilharzia huronensis* into the dermis was much faster, thus, only minority of schistosomula were destroyed in epidermis and no papules developed (Batten, 1956). Comparable histopathological changes were observed in humans and mice infected by *Trichobilharzia* over different authors and species but the uniformity in the composition of infiltrating leukocytes can not be found. As an example, in the skin of primary-infected mice, Appleton and Brock (1986) found mostly neutrophils, monocytes/macrophages, and lymphocytes but no eosinophils, however, those were seen in the histological sections examined by Kouřilová et al. (2004a) or Gay et al. (1999). Olivier (1953) performed a comparative study of skin immune response of rabbits to *T. szidati* and *T. stagnicola*. He observed stronger immune response after infection by *T. szidati* along with faster destruction of schistosomula. However, this comparison was based on the histological studies which allow only approximate quantification as the description largely depends on the quality of histological processing and examination (prone to personal bias). The cellular immune response towards cercariae in the infected tissue was not quantified and the mechanisms laying behind the schistosomula destruction were not defined.

To conclude, literature review revealed the paucity of the comparative studies of avian schistosomes. Published results were usually obtained from experiments with a single species of avian schistosomes, overlooking the possible diversity. Moreover, no consistency regarding mode of infection and infection dose can be found in experimental infections disallowing proper comparison. Given that not all of the avian schistosomes, neither all species out of the genus *Trichobilharzia*, were identified as the causative agents of CD during outbreaks, the factors involved in the occurrence of CD need to be examined.

### 3. Material and methods

#### 3.1. Chemicals, solution, and suspensions

**Phosphate-buffered saline** (PBS) was used in both *in vivo* and *in vitro* experiments. The working solution was either diluted from 10x stock solution or prepared fresh (Table 1).

**Table 1.** Composition of 0.1 M phosphate-buffered saline, pH 7.4 (PBS).

Chemicals	Final concentration	Manufacturer
NaCl	136.89 mM	Lach-Ner
KCl	2.68 mM	Sigma-Aldrich
Na <sub>2</sub> HPO <sub>4</sub>	4.23 mM	Sigma-Aldrich
KH <sub>2</sub> PO <sub>4</sub>	1.47 mM	Sigma-Aldrich
dH <sub>2</sub> O	Solvent	-

**PBS-Tween** (PBS-T) (Table 2) was used as a washing buffer in enzyme-linked immunosorbent assay (ELISA) for detection of serum antibodies as well as thymic stromal lymphopoietin (TSLP).

**Table 2.** Composition of PBS-0.05% Tween (PBS-T).

Component	Final Concentration	Manufacturer
Tween 20	0.05% (v/v)	Bio-Rad
PBS	Diluent	See Table 1

##### 3.1.1. Used for *in vivo* experiments

The fixative for histology, **formaldehyde** (Table 3), was prepared fresh by dissolving paraformaldehyde in PBS in a water bath of 72 °C. The solution was always used ice-cold.

**Table 3.** Composition of 4% formaldehyde.

Chemicals	Final concentration	Manufacturer
Paraformaldehyde	4% (m/v)	Sigma-Aldrich
PBS	0.1 M	See Table 1

**The anesthetics solution** (Table 4) for intraperitoneal administration was prepared fresh in an insulin syringe at room temperature.

**Table 4.** Composition of the anesthetics solution for intraperitoneal administration.

Chemicals	Final concentration	Manufacturer
Rometar	10% (v/v), final conc. of xylazine: 2 mg/ml	Bioveta
Narkamon	20% (v/v), final conc. of ketamine: 20 mg/ml	Vétoquinol
Sterile physiological saline	Diluent	Mayrhofer Pharmazeutika

**Absolute ethanol** (Table 5) was prepared by dehydration of ethanol by anhydrous CuSO<sub>4</sub> in a closed container for 1-2 weeks.

**Table 5.** *Preparation of absolute (100%) ethanol.*

Chemicals	Final concentration	Manufacturer
Anhydrous CuSO <sub>4</sub>	25% (m/v) solid	Sigma-Aldrich
96% ethanol	-	Lach-Ner

**Acid alcohol** (Table 6) was prepared by adding drops of concentrated HCl into ethanol.

**Table 6.** *Composition of acid alcohol.*

Chemicals	Final concentration	Manufacturer
Concentrated (37%) HCl	0.2% (v/v)	Lach-Ner
70% ethanol	Diluent	Lach-Ner

**Ehrlich's hematoxylin solution** (Table 7) was prepared by mixing hematoxylin solution with partially dissolved potassium aluminum sulphate. To obtain hematoxylin solution, hematoxylin powder was dissolved in 96% ethanol with added acetic acid. In a different beaker, potassium aluminum was added in excess (~17 g) to the solution of 50% (v/v) glycerol in dH<sub>2</sub>O. The prepared hematoxylin solution and the potassium alum suspension were mixed together and kept for 3-4 months in a bright place at room temperature with a cotton plug to allow natural oxidation. Before use, the mixture was filtered using filter paper to obtain the final working Ehrlich's hematoxylin solution that was used for histological staining.

**Table 7.** *Composition of Ehrlich's Hematoxylin solution.*

Chemicals	Amount	Manufacturer
Hematoxylin	2 g; 0,65 % (m/v)	Sigma-Aldrich
96% ethanol	100 ml	Lach-Ner
Potassium aluminum sulphate	excess ~ 17g	Sigma-Aldrich
dH <sub>2</sub> O	100 ml	-
Glycerol	100 ml	Lach-Ner
Glacial acetic acid	10 ml	Sigma-Aldrich

**Eosin Y stock solution** (Table 8) was prepared and it was used for the preparation the of **Eosin Y working solution** (Table 9.). First, Eosin Y powder was dissolved in dH<sub>2</sub>O and ethanol was added. Before use, the Eosin Y stock solution was diluted with ethanol and then glacial acetic acid was added. The solution was mixed well and kept at room temperature. The working solution of Eosin Y approximate concentration of 0.25% (v/v) was used for histological staining.

**Table 8.** *Composition of 1% Eosin Y stock solution.*

Chemicals	Final concentration	Manufacturer
Eosin Y powder	1% (m/v)	Sigma-Aldrich
dH <sub>2</sub> O	20% (v/v)	-
96% ethanol	80% (v/v)	Lach-Ner

**Table 9.** *Composition of ~0.25% Eosin Y working solution.*

Chemicals	Volume	Manufacturer
1% Eosin Y Stock solution	25 ml	See Table 8
80% ethanol	75 ml	Lach-Ner
Glacial acetic acid	0.5 ml	Sigma-Aldrich

Dispase II was dissolved, aliquoted as 100U/ml **Dispase II stock solution**. Later, **Dispase II working solution** (Table 10), used for enzymatic separation of epidermis and dermis of mouse pinna, was prepared by diluting the stock 1:50 with Hanks' Balanced Salt Solution (HBSS), no calcium, no magnesium, no phenol red.

**Table 10.** *Composition of 2 U/ml Dispase II working solution.*

Chemicals	Final concentration	Manufacturer
100 U/ml Dispase II stock solution (in dH <sub>2</sub> O)	2% (v/v); 2 U/ml	Sigma-Aldrich
HBSS, no Ca and Mg salts, no phenol red	Diluent	Thermo Fisher Scientific

Collagenase from *Clostridium histolyticum*, type IV was used to enzymatically isolate leukocytes from skin samples of mouse pinna. The collagenase was dissolved in Roswell Park Memorial Institute (RPMI) 1640 without supplements, aliquoted as **Collagenase IV stock solution** (Table 11). Later, the aliquot was used in Digest solution (Table 15) in its working concentration.

**Table 11.** *Composition of 9140 U/ml Collagenase IV stock solution.*

Component	Concentration	Manufacturer
Collagenase, from <i>Clostridium histolyticum</i> , type IV	9140 U/ml	Sigma-Aldrich
RPMI 1640	Solvent	Sigma-Aldrich

DNase II was used to prevent the clumping of the isolated cells. At first, **DNase II storage buffer** pH 7.5 (Table 12) was prepared. In this buffer, DNase II was dissolved, without vigorous shaking or vortexing, into the **DNase stock solution** (Table 13) and used later in the Digest solution (Table 14).

**Table 12.** *Composition of DNase II storage buffer pH 7.5.*

<b>Component</b>	<b>Final concentration</b>	<b>Manufacturer</b>
Tris buffer	20 mM	Trizma base (Sigma-Aldrich) in dH <sub>2</sub> O
MgCl <sub>2</sub>	1 mM	Sigma Aldrich
Glycerol	50% (v/v)	Lach-Ner
37% HCl for titration	Final pH 7.5	Lach-Ner

**Table 13.** *Composition of 31560 U/ml DNase II stock solution.*

<b>Component</b>	<b>Final concentration</b>	<b>Manufacturer</b>
DNase II	31560 U/ml	Sigma-Aldrich
DNase II storage buffer	Solvent	See Table 12

**Digest solution** (Table 14) was used as the working enzymatic solution of both Collagenase IV and DNase II to digest skin samples of mouse pinna hence enabling the isolation of leukocytes from the tissue.

**Table 14.** *Composition of Digest solution*

<b>Component</b>	<b>Final concentration</b>	<b>Manufacturer</b>
9140 U/ml Collagenase IV stock solution	2% (v/v); 182.8 U/ml	See Table 11
31560 U/ml DNase II stock solution	0.5% (v/v); 157.8 U/ml	See Table 13
RPMI 1640 supplemented with 10% (v/v) fetal bovine serum (FBS)	Diluent	Sigma-Aldrich

Stock solutions of enzymes (Table 11, 13) were stored at -20 °C. Repeated freeze-thaw cycles were avoided. Working solutions (Table 10, Table 14) were prepared just before use to ensure high effectivity and kept on ice if not stated otherwise.

**Carbonate buffer** (Table 15) was prepared as a coating buffer for ELISA.

**Table 15.** *Composition of Carbonate buffer pH 9.6*

<b>Component</b>	<b>Concentration</b>	<b>Manufacturer</b>
Na <sub>2</sub> HCO <sub>3</sub>	15 mM	Sigma-Aldrich
NaHCO <sub>3</sub>	35 mM	Sigma-Aldrich
dH <sub>2</sub> O	Solvent	-

**Non-fat dry milk** (Table 16) was used to block unspecific binding of proteins in ELISA.

**Table 16.** Composition of 5% non-fat dry milk

Component	Concentration	Manufacturer
Non-fat dry milk	5% (m/v)	Bio-Rad
PBS-T	Solvent	-

### 3.1.2. Used for *in vitro* experiments

Complete RPMI 1640 medium (Table 17) was prepared for the cultivation of mouse pinnae.

**Table 17.** Composition of Complete RPMI 1640 medium.

Component	Final concentration	Manufacturer
Fetal bovine serum	10% (v/v)	Lab-tech
Penicillin-streptomycin	1% (v/v); penicillin: 100 U/ml; streptomycin: 100µg/ml	Sigma-Aldrich
L-glutamine	1% (v/v); 2mM	Sigma-Aldrich
RPMI 1640 with phenol red, without L-glutamine	Diluent	Sigma-Aldrich

## 3.2. Experimental design

Both *in vivo* and *in vitro* approaches were employed to study the immune response in the skin of mice infected with different doses of *T. regenti* or *T. szidati* cercariae (see 3.3.). The *in vivo* part consisted of histological examination of the infected pinnae (see 3.4.1.), flow cytometry immunophenotyping of leukocytes in the infected pinnae and pinnae-draining (parotid) LNs (see 3.4.2.), and assessment of the systemic immune response – analysis of serum cytokines (cytokine bead array /CBA/, see 3.4.3.) and parasite-specific antibodies (ELISA, see 3.4.4.). The *in vitro* part included cultivation of infected pinnae (see 3.5.1.) followed by quantification of leukocyte emigration from the tissue (see 3.5.2.) and analysis of cytokine production (see 3.5.3.). The experimental design is summarized in Figure 1.

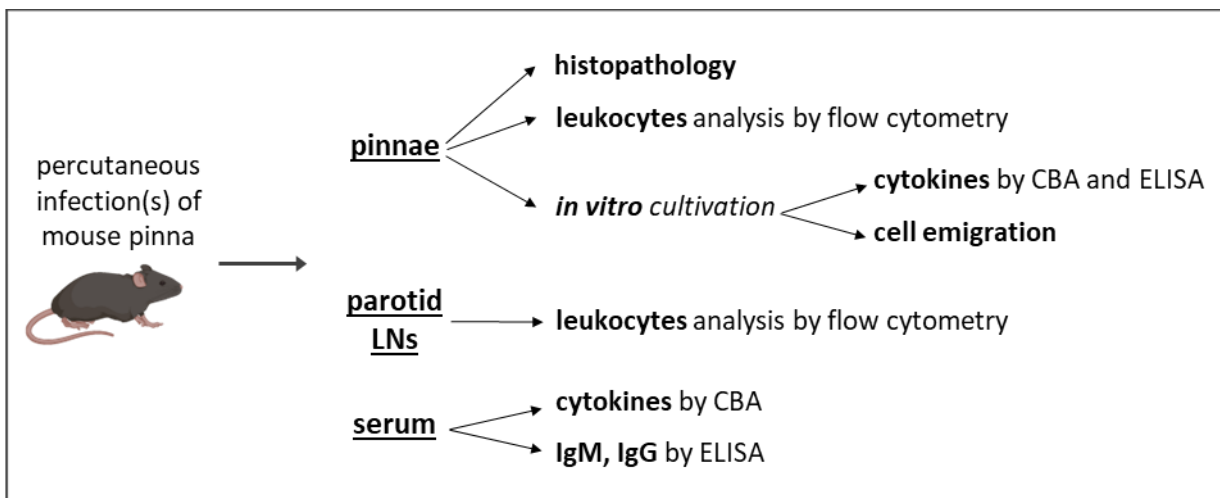


**Figure 1.** Schematic representation of the experimental design. Created with [BioRender.com](https://www.biorender.com)

### 3.3. Model organisms and experimental infections

#### 3.3.1. Infection agents and infection dose

*Trichobilharzia regenti* and *T. szidati* were used as model parasite species. Their life cycles are separately maintained in the Laboratory of Helminthology at Charles University, Prague. Freshwater snails (*Radix lagotis* and *Lymnaea stagnalis*, respectively) serve as the intermediate hosts and domestic ducks *Anas platyrhynchos f. domestica* serve as definitive hosts (Horák, 1995) (Horák et al., 1998a).

Cercariae, the infectious agents, were obtained from the snails as follows. The snails were exposed to an artificial light source in glasses filled with dechlorinated tap water for 40-60 min to initiate cercarial shedding. The cercariae were concentrated in Erlenmeyer flasks enwrapped in aluminum foil with a light source side-illuminating the top neck part, which was left transparent. From here, the positively phototactic cercariae were collected by Pasteur pipette into a 50 ml tube. The concentration of pooled cercariae was counted in 25 drops of 20 µl and the volume needed for the desired infection dose was determined by extrapolation. Infection doses of approximately 100 and 1000 cercariae were used.

To precisely determine the number of penetrating cercariae, the infection dose of 100 cercariae (range 90-112) was counted under a stereomicroscope and the exact number of cercariae (not the extrapolation as above) was noted. After percutaneous infection (3.3.2.), nonpenetrant cercariae were fixed by formaldehyde (see above Table 3.) and the number of the whole cercariae and separated heads were counted. The number of potentially penetrated cercariae was calculated by subtracting the nonpenetrant cercariae from the noted infection dose. The penetration rate was calculated as the ratio between the number of penetrant cercariae and the infection dose. For the assessment of penetration rate after infection by 1000 cercariae, extrapolation was used to determine the infection dose as well as to estimate the number of nonpenetrant cercariae. The penetration rate of cercariae was counted after primary infections.

#### 3.3.2. Infection of experimental animals

Female mice of C57BL/6J01aHsd strain (Envigo) were kept in the Centre for experimental biomodels (1<sup>st</sup> Faculty of Medicine, Charles University, Prague) under standard conditions (23 °C, 55% humidity, 12/12 h light/dark period). Mice aged 8–9 weeks were infected percutaneously via pinnae. Before the infection, they were anesthetized by intraperitoneal injection of 100 µl of anesthetics (see above Table 4). Anesthetized mice were laid on their lateral side on a microtube stand while having a pinna submerged for 30 min in the 2 ml tube containing the desired infection dose of cercariae. Specifically, mice were exposed to 100 or 1000 cercariae for a single infection (referred to as “100” or “1000”, respectively) or 4x reinfected by 100 cercariae in 10 days intervals at the same infection site by the same species (referred as “4x 100”). Groups of control mice, referred to as “0 hpi”, were once exposed to dechlorinated tap water without cercariae. Thus, every mouse had one pinna exposed and the other

pinna left untreated. After exposure, mice were transferred into corresponding boxes and regularly checked whether they recovered from anesthesia. In the experimental part of this thesis, a uniform group of mice is considered a group of individuals sharing (a) infectious agent, (b) infection dose, including a number of exposures, and (c) time point of processing post infection.

All experiments including animal handling were supervised or performed by the author authorized to design and perform the experiments with animals according to section 15d (3) of Act No. 246/1992 Coll. All experiments were accomplished in accordance with animal welfare laws of Czech Republic and the directives of the European Union. The project was approved by the Animal welfare committee of Charles University in Prague, Faculty of Science and the Animal welfare committee of the Ministry of Education, Youth and Sports of the Czech Republic (MSMT-33740/2017-2).

### 3.4. *In vivo* experiments

Mice were anesthetized, bled out and tissues of interest were collected. The animals were sampled and processed 5 hpi, 24 hpi, 48 hpi, and 7dpi after the single (1x) or repeated (4x) exposure to cercariae. Until tissue removal, all mice were handled in the same way.

Each mouse was anesthetized by inhalation of Isoflurine (Isoflurine inhalation vapour – active substance isofluranum 1000 mg/g; Vetpharma animal health) in a closed container and placed on a dissection pan in a fume hood. An inhalation mask prepared from a 50 ml conical tube with Isoflurine-soaked paper tissues was covering the head of a mouse to ensure continuous anesthesia. Blood was collected after cutting axillary veins and the mouse was terminally sacrificed by cervical dislocation. From each mouse, infected and control pinnae were cut above the cartilaginous part of the ears and placed in Petri dishes containing PBS on ice. The parotid LNs were dissected in mice intended for flow cytometry and processed concurrently (3.4.2.2.). Mouse pinnae were further processed according to the need of a specific method as described in the following chapters.

#### 3.4.1. Histological processing of the mouse pinna

Hematoxylin & eosin staining was used to localize schistosomula and examine the histopathology of the infected tissue. Mouse pinnae were fixed and embedded in paraffin blocks. Then, the blocks were sectioned and the slides were stained with hematoxylin & eosin. Pinnae of primary-infected mice by 100 or 1000 cercariae of either *T. regenti* or *T. szidati* were histologically processed 0, 5, 24, 48 hpi, 7dpi. For each of these groups, 2 mice per time point were used.

##### 3.4.1.1. Tissue processing

Mouse pinnae were fixed overnight at room temperature in formaldehyde (see above Table 3) in 20x excess and transferred to 4 °C for up to 7 days. The fixative was washed out of the tissue being followed

by dehydration, clearing, paraffin infiltration, and embedding. The steps were applied as follows in Table 18.

**Table 18.** *Processing of formaldehyde-fixed tissue samples for histology.*

<b>Process</b>	<b>Chemicals</b>	<b>Duration</b>
Washing out the fixative	PBS	3x 15 min
Dehydration	75% ethanol	3x 30 min
	95% ethanol	3x 30 min
	100% ethanol	3x 30 min
Clearing of the tissue	xylene – in a fume hood	2x 15 min
Paraffin infiltration (at 56 °C)	xylene/paraffin	1x 15 min
(Surgipath paraplast,	paraffin	1x 60 min
Sigma-Aldrich)	paraffin	1x 12 h
	paraffin	1x 60 min

Melted paraffin was poured into embedding molds into which tissue samples were placed. Special care was taken to avoid bubbles and early hardening of the paraffin by handling samples with pre-heated instruments. Molds were placed on ice for 4 hours to allow quick paraffin-hardening which was followed by hardening at room temperature overnight. Paraffin blocks were sectioned on the rotary microtome Microm HM355S (Thermo Fisher Scientific) at a thickness of 5 µm. Ribbons were placed on a 37 °C water bath to stretch out wrinkles and transferred onto the adhesive glass slides Superfrost (Thermo Fisher Scientific). Slides were placed on a hot plate at 37 °C for 1 hour and left to dry overnight at room temperature. Prolonged exposure to heat was causing the separation of skin layers due to ribbons stretching.

#### *3.4.1.2. Hematoxylin & eosin staining*

Combination of hematoxylin & eosin (see above Tables 7 and 9) was chosen to stain the slides after removal of the paraffin and rehydration. Between staining steps, slides were observed under a microscope to check the quality of staining. All the staining steps in Table 19 were performed in Hallendahl staining dishes. Slides were mounted in mounting medium, either DPX (Sigma-Aldrich) or Canada balsam (Sigma-Aldrich) and were left untouched to dry for a week at room temperature.

**Table 19.** *Steps of hematoxylin & eosin staining.*

<b>Processes</b>	<b>Chemicals</b>	<b>Duration</b>
Deparaffinization	Xylene	2x 5min
Rehydration	100% ethanol	1x 2 min
	96% ethanol	1x 2 min
	75% ethanol	1x 2 min
	dH <sub>2</sub> O	1x 2 min
Hematoxylin staining	Ehrlich's hematoxylin (See above Table 7)	1x 10 min
Bluing of nuclei	Running tap water	Checked under microscope
Differentiation of hematoxylin	Acid alcohol (See above Table 6)	1x dip
Eosin staining	Eosin Y working solution ~ 0.25% (see above Table 9)	1x 2 min
Dehydration	Tap water	1x dip
	75% ethanol	1x dip
	95% ethanol	1x dip
	100% ethanol	1x dip
	Xylene	1x dip

3.4.2. Immunophenotyping leukocytes from the mouse skin and parotid LNs  
Leukocytes from the skin of mouse pinnae and the parotid LNs were characterized and quantified by flow cytometry. Epidermis and dermis of both infected and control pinnae were processed separately as well as cells released during the separation of these layers. Cells from skin samples were stained for 2 sets of markers - "general set" and "Ag-presenting set". Concurrently with enzymatic digestion of skin (3.4.2.1.), parotid LNs from these mice were mechanically disrupted to isolate leukocytes (3.4.2.2.). These were stained solely for the "Ag-presenting set" of markers to focus on the immigration and maturation of the Ag-presenting cells. For these experiments, 4 mice per group (combination of species: *T. regenti*, *T. szidati*; infection doses: 1x 100, 1x 1000, 4x 100 cercariae; timepoints: 0, 5, 24, 48 hpi, 7 dpi). However, due to the unexpected death of one animal in each of the following groups -

*T. regenti* 4x 100 (48 hpi, 7 dpi) and *T. szidati* 4x 100 (48 hpi, 7 dpi), only 3 mice per group were processed.

#### 3.4.2.1. Isolation of the cells from mouse pinna

Enzymatic digestion was used to isolate cells from infected as well as untreated mouse pinnae. The protocol for cell isolation was adapted from Liu *et al.* (2020). Dorsal and ventral sides of the pinnae were separated by curved tweezers, and both parts of the same pinna were placed together into a 2 ml tube containing 1 ml of vortexed Dispase II working solution (see above Table 10) to allow separation of epidermis and dermis. Samples were incubated in the ThermoMixer C (Eppendorf) at 350 rpm, 37 °C for 90 min.

After the incubation, the epidermis was peeled from the dermis in PBS by curved tweezers under the stereomicroscope. Since separation, the epidermis and dermis of each pinna were processed as individual samples following an identical protocol. Samples were placed into 2 ml tubes containing 500 µl of the Digest solution (see above Table 14). PBS with released cells, in which half-pinna was separated, was kept on ice and was further processed as dermal exudate cells (DEC). Tissue samples were cut into small particles in the tubes and transferred into 12-well plates. Tubes were washed out and samples, in 1.5 ml of digest solution in total, were incubated in an incubator for 60 min at 37 °C. After the incubation, the well-plates were gently shaken and placed on ice to prevent further enzymatic digestion. Remnants of skin tissues were mechanically disrupted by pipetting.

Obtained cell suspensions of the epidermis, dermis as well as DEC were filtered through the 70 µm cell-strainer and centrifuged for 5 min at 380 *xg* at 4 °C. Supernatants were discarded, tubes were inverted for 1–2 min and the inner surface of tubes was dried manually to prevent dilution of the cell pellet. After enzymatic digestion, in total, 3 skin samples per mouse pinna were obtained: epidermis, dermis, and DEC. During all preparation (except for enzymatic incubation), the samples were kept on ice and ice-cold chemicals were used to prevent cell death.

#### 3.4.2.2. Isolation of cells from the mouse parotid LNs

Cells were mechanically isolated from the superficial parotid LNs that drain the area of the infection site, the mouse pinnae. The localization of pinnae-draining LNs was checked by intradermal application of 2% (m/v) Evans Blue (Sigma-Aldrich) (see Figure 11, p. 45) and the LNs were named according to Van den Broeck *et al.* (2006).

Cells from lymph nodes were isolated as described by Majer *et al.* (2020). After the removal of surrounding fat tissue, parotid LNs were harvested into a 1.5 ml tube with PBS. The tissue was homogenized by a polypropylene pestle in the tube, filtered via 70 µm cell-strainer, and centrifuged for 5 min at 380 *xg* at 4 °C.

### 3.4.2.3. Staining of leukocytes

Leukocytes were stained for extracellular markers of interest by fluorochrome-bound anti-mouse antibodies. The “general set” (Table 20) of antibodies aimed to identify common leukocytes in the infected skin such as neutrophils (CD45+ CD11b+ Ly6G+); eosinophils (CD45+ CD11b+ SiglecF+); monocytes (CD45+ CD11b+ Ly6C+); macrophages/DCs (CD45+ CD11b+ F4/80+), and CD4+ T-lymphocytes (CD45+ CD11b- CD4+). The “Ag-presenting set” (Table 21) aimed to examine the migration, maturation, and activation status of Ag-presenting cells, including Langerhans cells (LCs), both in the skin and parotid LNs. Both sets contained a viability dye Zombie aqua™ that stains cells with compromised membranes.

**Table 20.** Reagents for “General set” of antibodies including a viability dye.

Target	Fluorochrome	Clone	Final dilution	Manufacturer
Viability	Zombie Aqua™ dye	-	1:600	BioLegend
CD45	APC efluor 780	30F11	1:100	Invitrogen
CD11b	PE-Cy7	M1/70	1:100	BioLegend
Ly6G	APC	1A8	1:100	BioLegend
SiglecF	PE	S17007L	1:100	BioLegend
Ly6C	PE/Dazzle™ 594	HK1.4	1:100	BioLegend
F4/80	FITC	BM8	1:100	BioLegend
CD4	PerCP-Cy5.5	GK1.5	1:150	BioLegend
PBS	-	-	Diluent	Table 1

**Table 21.** Reagents for “Ag-presenting set” of antibodies including a viability dye.

Target	Fluorochrome	Clone	Final dilution	Manufacturer
Viability	Zombie Aqua™ dye	-	1:600	BioLegend
CD45	APC efluor 780	30F11	1:100	Invitrogen
CD11b	PE-Cy7	M1/70	1:100	BioLegend
CD11c	PE/Dazzle™ 594	N418	1:100	BioLegend
MHCII	PerCP-Cy5.5	M5/114	1:100	BioLegend
CD207	APC	4C7	1:100	BioLegend
CD80	FITC	16-10A1	1:100	BioLegend
PD-L1	PE	10F.9G2	1:80	BioLegend
PBS	-	-	Diluent	Table 1

Cell pellets obtained in [3.4.2.1.](#) and [3.4.2.2.](#) were resuspended in the desired volumes of PBS with Fc-receptors blocking antibody anti-CD16/32 (Invitrogen; dilution 1:100), to prevent unspecific binding of antibodies via their Fc receptor. From each sample, the volume needed for technical controls (see below) was preserved and the remaining volume of the sample was pipetted into corresponding wells

of 96-well round-bottom plate. After 20 min of incubation with anti-CD16/32 at 4 °C, the plate was centrifuged for 5 min at 380 *xg* at 4 °C and the supernatant was discarded by flicking the plate. Cell pellets were stained by 50 µl of the corresponding antibody set (see above) and incubated in the dark for 30 min at 4 °C. Before the acquisition, samples and controls were diluted with 250 µl of PBS.

For controls, unstained samples (blank) and fluorescence minus one (or minus two) samples were prepared during each flow cytometry experiment. Unstained controls of each tissue type were prepared to check for any autofluorescence of the cells. Fluorescence minus one (or minus two) samples were prepared for mixed-skin samples and separately for parotid LN samples. These samples were stained by the set of antibodies except for the one or two antibodies of choice (F4/80, CD207, PD-L1 /programmed death ligand/, CD80, CD11c, MHCII), to set the border for the negative and positive populations of the excluded markers while considering the fluorescence of other antibodies. For a calculation of the compensation matrix, single-stained controls were measured.

#### 3.4.2.4. *Measuring of cells by flow cytometry*

Flow cytometry measurements were performed in the Laboratory of cytometry (Faculty of Science, Charles University, Prague). Samples from mice infected by *T. szidati* were measured on the BD LSR II in high-throughput mode in which samples are measured directly from 96-well round-bottom plates. The acquisition was set to 100 µl per sample. Due to the technical problems with high-throughput mode, the samples from mice primary-infected by *T. regenti* were measured in a standard mode from tubes. In standard mode, setting the stopping gate to the acquired volume is not possible in BD LSR II and therefore the entire sample volume was measured. The measurements of samples from mice reinfected by *T. regenti* and the control group were measured on the CytoFLEX since BD LSR II was unexpectedly out of order. The entire volume was measured to acquire comparable data to the previous *T. regenti* measurements.

Before every measurement on BD LSR II, the daily cytometer performance was automatically adjusted according to the Cytometer Set-up and Tracking beads (BD Biosciences). The accuracy of the setting was further checked by running Quality Control beads (Beckman Coulter). CytoFLEX performance was checked before every measurement solely by Quality Control beads, which in the instrument substitute the previously mentioned Cytometer Set-up and Tracking beads. Analyses of acquired data, including the calculation of compensation values, were performed in FlowJo 10.8.1 (FlowJo). Samples that did not pass the quality criteria, mostly due to the fluidics or laser delay, were excluded from the analyses. No data were obtained for the “General set” of *T. szidati* 1000, 7dpi (even after the second attempt) because of laser failure. United gating strategy (see Figure S2-S5, p. 71-74) was applied per tissue per set of markers. DEC was gated in the same way as dermis.

### 3.4.3. Measurement of serum cytokines by CBA

BD LSR II was used to detect the amount of cytokines IL-4, IL-5, IL-6, IL-10, IL-17a, TNF, and IFN- $\gamma$  by Cytokine Bead Array (BD Bioscience). Cytokines in the samples are detected by cytokine-specific capture antibodies that are bound to the beads. Then, phycoerythrin (PE)-conjugated detection antibodies are used. Concentrations of cytokines in samples are calculated from the median fluorescence intensity (MFI) of PE of the cytokine-specific beads. All the reagents are provided by the manufacturer BD Biosciences in the BD CBA mouse flex set or in Mouse/rat soluble protein master buffer kit.

#### 3.4.3.1. Setting up the cytometer

As the CBA approach has been newly established in our laboratory, a brief technical background follows to provide sufficient details for reproducibility. First of all, the cytometer was set up following the BD Biosciences instructions ([https://www.bdbiosciences.com/content/dam/bdb/marketing-documents/facsdivabased\\_instr\\_setupguide.pdf](https://www.bdbiosciences.com/content/dam/bdb/marketing-documents/facsdivabased_instr_setupguide.pdf)) and the setting was performed using DIVA software. “Instrument setup bead A9” diluted 9x in CBA wash buffer was used to set up the voltages for forward-scatter area and side-scatter area to set the gate for the beads according to their size. Then, by these diluted “A9 beads”, APC and APC-Cy7 voltages were set to frame the outermost (“top-right”) position of the beads on the axes. PE voltage was set by 9x diluted “PE Instrument setup bead” combined with 4.5x diluted “PE Positive control detector”. Those are the beads bound with anti-antibodies and PE-conjugated antibodies, respectively, diluted in CBA wash buffer. Unstained “Instrument Setup Bead F1”, APC stained “Instrument Setup Bead F9” and APC-Cy7 stained “Instrument Setup Bead A1” (all these beads diluted 9x in CBA wash buffer) were used as the compensation controls. The aforementioned reagents were added in the total volume of 225  $\mu$ l in the final concentration noted in Table 22. Compensation values were calculated in DIVA and the acquired setting was saved for further measurements as acquisitions settings. Fluorescence of APC and APC-Cy7 distinguish individual bead-clusters which correlate to the specific cytokines (Figure 2, p. 25) while the fluorescence intensity of PE indicates the amount of the bound detection reagent mirroring the concentration of cytokines.

**Table 22.** Final concentration of reagents used for cytometer setup during CBA

Components	Diluent	Final dilution
Instrument setup bead A9	CBA wash buffer	25 $\mu$ l in 225 $\mu$ l
Instrument setup bead F1	CBA wash buffer	25 $\mu$ l in 225 $\mu$ l
Instrument setup bead F9	CBA wash buffer	25 $\mu$ l in 225 $\mu$ l
Instrument setup bead A1	CBA wash buffer	25 $\mu$ l in 225 $\mu$ l
PE Instrument setup bead	CBA wash buffer	25 $\mu$ l
PE Positive control detector		50 $\mu$ l in total of 225 $\mu$ l

### 3.4.3.2. Preparation of samples

The samples were processed according to the manufacturer’s instructions. Briefly, standards including blank and diluted sera (1:9 in PBS) were added to the 96-well round-bottom plate in the volume of 50  $\mu$ l to which 50  $\mu$ l of the vortexed “capture beads mixture” was added (each analyte in the 1x final concentration). After 5 min of shaking at 500 rpm on a plate shaker, plates were incubated in dark for 1 h at room temperature. “PE detection reagents” for all cytokines in a volume of 50  $\mu$ l (1x final concentration of each) were added. The plate was mixed at 500 rpm and incubated for 1 h at room temperature. The stained samples were pipetted into 1.5 ml tubes, wells were washed once by wash buffer and a total volume of 1 ml of wash buffer was added to the samples. The tubes were centrifuged for 5 min at 200  $xg$  at room temperature, supernatants were carefully aspirated and discarded. The samples were resuspended in 300  $\mu$ l of wash buffer and vortexed before the acquisition.

### 3.4.3.3. Acquisitions and analysis

The stopping gate was set to the beads according to their size (see Figure S1, p. 70 ) and 2100 events (~300 per analyte) were recorded. IL-17 was excluded from the analysis because the acquired levels were below the lowest standard. The acquisition was performed in DIVA software after the loading the application settings and compensation values. Analysis was performed in FlowJo 10.8.1. (FlowJo). Specific cytokine beads were gated according to the position defined by the manufacturer (Figure 2) Uniform gating for samples and standards was applied. The standard curve was calculated from the standards included. Assay diluent was used as a blank and the concentration of 0.02 pg/ml was set for acquired blank values of each cytokine to allow calculation of standards curves.

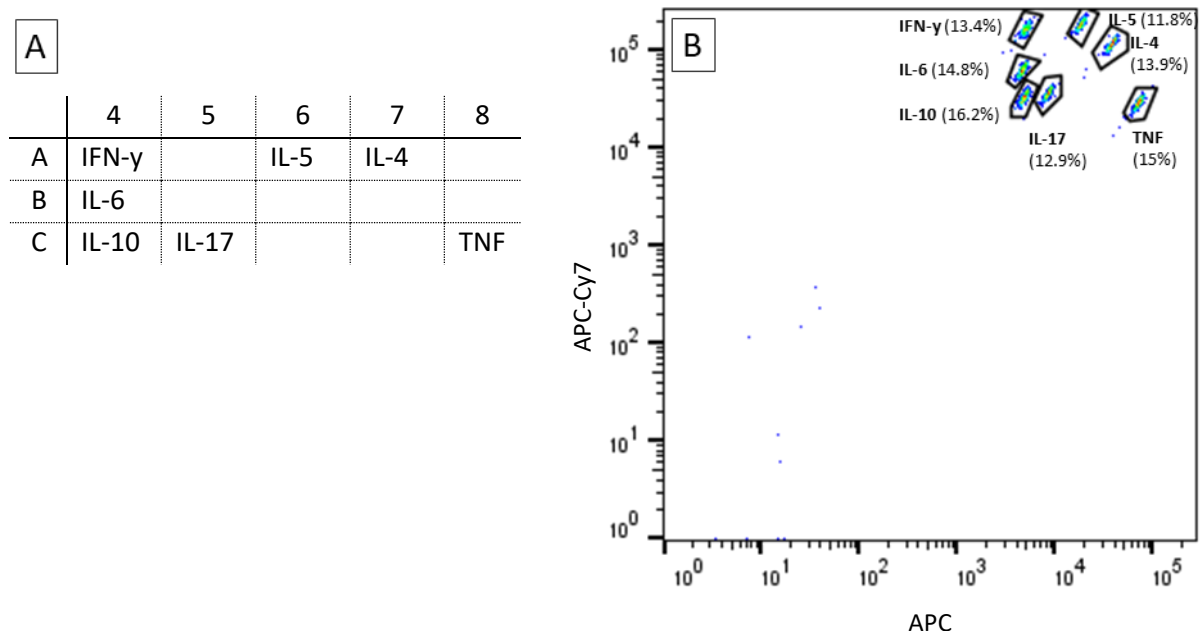


**Figure 2.** Position of the beads in the flex sets according to the manufacturer (A) and the real positions during acquisition (B).

#### 3.4.4. Measuring antibody immune response

Levels of parasite-specific IgG and IgM in sera of mice were measured by ELISA in order to detect the systemic immune response evoked by the infection. Antibodies were detected in sera of mice infected for immunophenotyping experiments (3.4.2) as well as from mice whose pinnae were used for *in vitro* cultivation (3.5) Protocols for sera processing, cercarial homogenate preparation, and ELISA were adapted from Majer et al. (2020).

##### 3.4.4.1. Serum and antigen preparation

To obtain serum, collected blood was left at room temperature for approximately 2 h to allow coagulation. It was centrifuged 2x for 10 min at 1500  $xg$  at 22 °C and pure serum was stored at -80 °C.

To detect the presence of parasite-specific antibodies, cercarial homogenates of *T. regenti* or *T. szidati* were prepared. Cercariae were collected as previously described (3.3.1) and concentrated on ice in a 50 ml tube covered by aluminum foil. Cercariae were transferred to the 1.5 ml tube, centrifuged 2x for 10 min at 1600  $xg$  at 4 °C, and washed with sterile PBS after each centrifugation. Cercariae were centrifuged one more time and washed with sterile PBS with the addition of peptidase inhibitors (Complete ultra tablets, Mini EDTA; 1 tablet/10 ml; Sigma-Aldrich). Cercariae were homogenized while kept on ice by the sonicator (Vibra Cell) 3x for 30 s, amplitude 30 W. Suspension was centrifuged for 20 min at 16 000  $xg$  at 4 °C. The final supernatant was filtered thorough 0.22  $\mu m$  strainer and the protein concentration was determined by Quant-iT Protein Assay Kit (Invitrogen) according to the manufacturer's instructions (<https://www.thermofisher.com/document-connect/document-connect.html?url=https://assets.thermofisher.com/TFS-Assets%2FMSG%2Fmanuals%2F33213.pdf>).

Based on the fluorescence measured by the microplate reader (Tecan Infinite M200), protein concentration was calculated as the average of technical triplicates while using standards as a reference. Homogenates were stored at -80 °C.

##### 3.4.4.2. IgM and IgG ELISA

Levels of parasite-specific IgM and IgG antibodies in sera of mice were detected by ELISA. All the reagents and their final concentrations are noted in Table 23. First, homogenate of *T. szidati* or *T. regenti* cercariae was diluted with carbonate buffer to the concentration of 6.25  $\mu l/ml$ . The wells of 96-well flat-bottom plate (Nunc MaxiSorp; Thermo Fisher Scientific) were coated with 100  $\mu l$  of the diluted homogenate. Sealed by adhesive sheet, the plate was left in a wet chamber at 4 °C overnight to allow adsorption of antigens to the surface of the wells. On the next day, to get rid of unbound proteins, the wells were washed 3x with 150  $\mu l$  of PBS-T (see above Table 2). All the washing steps in this protocol were performed in the same way (150  $\mu l$  of PBS-T; 1 min). In the next step, the wells were blocked with non-fat dry milk in PBS-T (see above Table 16) for 2 h while being shaken at 100 rpm (at room temperature for IgG, at 37 °C for IgM). The blocking solution was discarded by flicking the plate

and 100 µl of diluted sera (dilution of 1:80 in PBS-T or 1:500 in non-fat dry milk in PBS-T for measurements of IgG and IgM, respectively) was added. All the samples, including blank, were prepared in duplicates. After 2 h of incubation on the platform shaker (Innova 2000) at 100 rpm, the wells were washed 3x and the addition of 100 µl of diluted secondary antibody in PBS-T followed. Anti-mouse IgG (diluted 1:8000; Merck; A2554) or anti-mouse IgM (diluted 1:10 000; Abcam; ab97230) conjugated with peroxidase was added and incubated for 1.5 h in dark on the platform shaker at 100 rpm. Afterward, the wells were washed 6x followed by the incubation with 100 µl of TMB (3,3',5,5'-tetramethylbenzidine liquid substrate system for ELISA; Merck) in the dark to enable enzymatic reaction, visualized by color change. After the blue color developed, the ongoing enzymatic reaction was stopped by 1 M HCl. The optical density (OD) of samples was measured by a microplate reader (Tecan Infinite M200) at 450 nm. The values from the control group were used to calculate cut-off values with 99.9% confidence interval according to (Frey et al., 1998) and the concentration of specific antibodies reacting to cercarial antigen was assessed.

**Table 23.** Final concentration of antigens, sera, and antibodies used in IgM and IgG ELISA.

Components	Diluent	Final dilution	Manufacturer
Cercarial homogenate	Carbonate buffer 9.6 pH (see above Table 16)	6.25 µg/ml	(See 3.4.4.1.)
Serum for IgG measurement	PBS-T (see above Table 2)	1:80	-
Serum for IgM measurement	PBS-T (see above Table 2)	1:500	-
Anti-mouse IgG (A2554)	PBS-T (see above Table 2)	1:8000	Merck
Anti-mouse IgM (ab97230)	PBS-T (see above Table 2)	1:10 000	Abcam

### 3.5. *In vitro* cultivation of the mouse pinna

*In vitro* cultivation of mouse pinnae was used to acquire supernatants for the detection of cytokines by CBA and an alarmin – thymic stromal lymphopoietin (TSLP) by ELISA (3.5.3.). Also, the effect of infection on the number of cells released in the supernatant was examined. For these experiments, 4 mice per group (combination of species: *T. regenti*, *T. szidati*; dose: 1x 100, 1x 1000, 4x 100 cercariae; timepoints: 0, 5, 24, 48 hpi, 7 dpi) were processed. However, due to unexpected death of one animal in groups of *T. regenti* 1000, 48 hpi and *T. regenti* 1000, 7 dpi, only 3 mice were analyzed.

#### 3.5.1. Cultivation of the mouse pinna and harvest of supernatant

Mouse pinnae were washed in 70% ethanol to prevent contamination, moved to the laminar flow hood (Esco) and left in a Petri dish in 70% ethanol for 5 min. They were air-dried in the Petri dish and washed 2x by complete medium (Table 17). Dorsal and ventral sides of each pinna were separated and placed into separate wells of 24-well plate containing 0.5 ml of media by inner-side down. The half-pinnae were incubated for 18 h at 37 °C in CO<sub>2</sub> incubator (Esco). After 18 h of cultivation, the wells were

checked for contamination under the inverted microscope (Olympus IX50) using phase contrast. Half-pinnae were discarded and medium from both wells of single pinna was pooled into the single 1.5 ml tube. During collection, every well was washed 3x by its content. Tubes were centrifuged for 10 min at 300 *xg* at 4 °C and supernatant was collected into new 1.5 ml tubes. To ensure purity of supernatant, it was centrifuged for 5 min at 800 *xg* at 4 °C, collected, aliquoted, and stored at –80 °C.

### 3.5.2. Counting the released cells

The numbers of cells released during cultivation from control and infected mouse pinnae were determined after supernatant collection (see 3.5.1). Cell pellets were resuspended in remnants of supernatants and pooled for a single pinna. The volume of the suspension was carefully measured by pipette and noted. Cells were counted in the Bürker counting chamber. The total number of cells per sample (X) was calculated by dividing the average number of cells per square (A) by the volume of the square (S) and multiplied by the volume of the sample (V) in  $\mu\text{l}$  while knowing that the volume of the square is 0,1  $\mu\text{l}$ .

$$X = \frac{A \times V}{S}$$

### 3.5.3. Measuring levels of cytokines

A set of cytokines (IL-4, IL-5, IL-6, IL-10, IL-17, TNF, and IFN- $\gamma$ ) was measured by CBA in undiluted supernatant as previously described (3.4.3) IL-17 was excluded from the analysis because levels were below the lowest standard. Concentration of TSLP was determined by Mouse TSLP DuoSet ELISA (R&D Systems) following the instructions (<https://resources.rndsystems.com/pdfs/datasheets/dy555.pdf>). Final concentrations of reagents are noted in Table 24. Briefly, the wells were coated overnight, washed and blocked by 1%BSA-PBS. Afterward, capture antibody was added and incubation with standards, including blank, or undiluted samples followed. Supernatants were prepared in technical monoplicates and standards in duplicates. Then, incubation with detection antibody was followed by Streptavidin-Horseradish Peroxidase B. TMB (3,3',5,5'-Tetramethylbenzidine liquid substrate system for ELISA; Merck) was added and the reaction was stopped by 1M HCl. All the incubation steps lasted for 2 h. The OD was measured by the microplate reader (Tecan Infinite M200) at 450 nm wavelength.

**Table 24.** Final concentration of reagents used in Mouse TSLP DuoSet ELISA (R&D Systems)

Components	Solvent	Final concentration	Manufacturer
Capture antibody	PBS (see above Table 1.)	1 $\mu\text{g/ml}$	R&D Systems
Detection antibody	1% BSA-PBS (see above Table 19.)	50 ng/ml	R&D Systems
Top standard	1% BSA-PBS (see above Table 19.)	1000 pg/ml	R&D Systems
Streptavidin-Horseradish Peroxidase B	1% BSA-PBS (see above Table 20.)	1:40	R&D Systems
Sample (supernatant)	undiluted	-	-

### 3.6. Statistics

Statistical analysis was performed in GraphPad Prism 9. By one-way ANOVA, results from antibody-ELISA were analyzed. By two-way ANOVA, statistical significance was assessed for penetration rate, cytokine levels, flow cytometry and for cell-emigration during *in vitro* cultivation. The significance was determined according to Sidak test in both cases, P values are visualized by asterisk (\*) in graphs or by arrows in tables as follows: \*  $p \leq 0.05$ , \*\*  $\leq 0.01$ , \*\*\*  $\leq 0.001$ . Always, means of the group (visualized as mean  $\pm$  standard deviation /SD/) were compared. Statistical differences in levels of antibodies and in levels of cytokines are shown between infected groups and a control group (0 hpi). In flow cytometry and cell-emigration, significant differences are shown between infected and control samples of the same individuals.

## 4. Results

### 4.1. Penetration rate

Cercariae of both *T. regenti* and *T. szidati* penetrated in a similar rate into mouse pinnae when the infection dose of 100 was used. However, *T. regenti* showed higher penetration rate than *T. szidati* if the mouse pinnae were exposed to 1000 cercariae (Figure 3). As for *T. regenti*, penetration success also seems to be partially dependent on the number of cercariae as the infection by 1000 cercariae resulted in significantly higher penetration rate than the infection by 100 cercariae. However, in mice infected by 1000 cercariae of *T. szidati*, penetration rate was only slightly elevated in comparison with the lower infection dose.

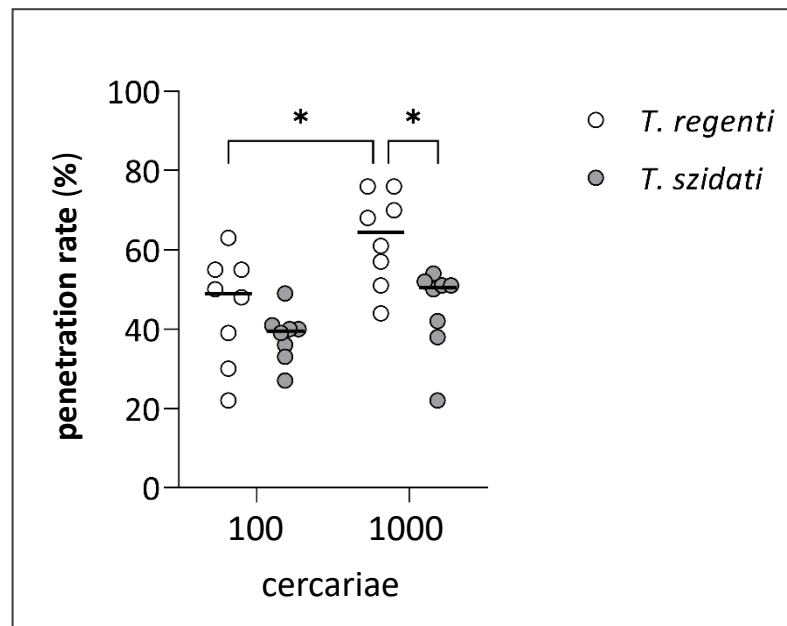


**Figure 3.** Cercarial penetration rate of *T. regenti* and *T. szidati* into mouse pinnae after 30 min of exposure. Mice were exposed to 100 or 1000 cercariae and the number of non-penetrating cercariae was assessed. Significant differences between the species as well as between the infection doses are shown. 2-way ANOVA; Sidak test;  $n = 8$

### 4.2. Systemic immune response

#### 4.2.1. Serum antibodies

Infection by 1000 and 4x100 cercariae of either species, *T. regenti* or *T. szidati*, induced the production of parasite-specific IgM antibodies 7 dpi (Figure 4A). Interestingly, the production was strengthened in mice repeatedly infected by *T. regenti* (compared to single exposure to 1000 cercariae), but this trend was not observed in *T. szidati*-infected mice. At the same time point (7 dpi), parasite-specific IgG were detected only in mice repeatedly (4x100) infected by *T. regenti* (Figure 4B). Although statistically significant elevation was found also in mice reinfected by *T. szidati*, none of the sera could have been considered positive as they did not reach the cut-off value. Infection dose of 100 cercariae had

negligible effects on antibody production in both species 7 dpi. Differences between the species were not statistically evaluated because of the possibly different quality of antigens.

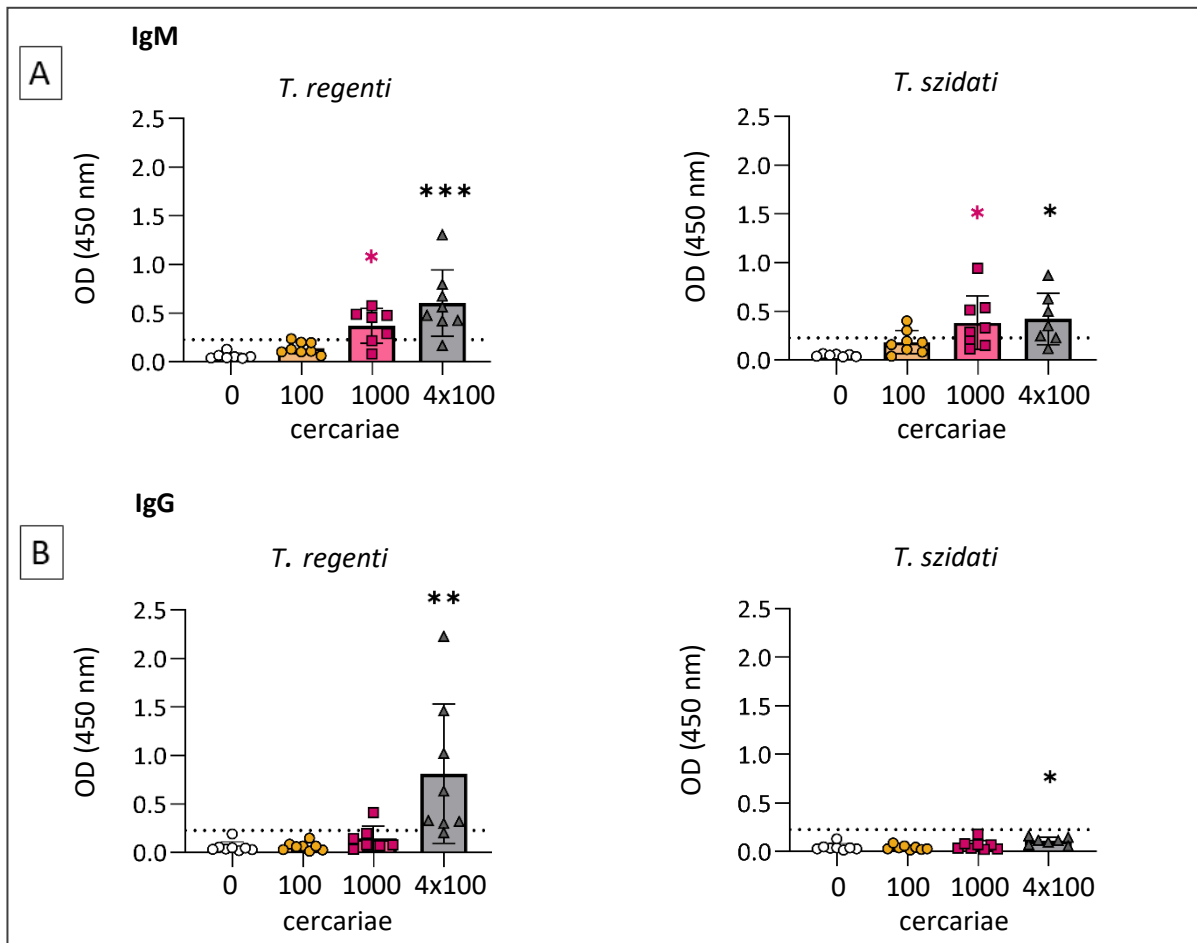


**Figure 4.** Levels of of parasite-specific IgM (A) and IgG (B) antibodies in sera of mice infected by *T. regenti* (left side) and *T. szidati* (right side) as detected by ELISA. Significant differences between the groups and the control group are shown. 1-way ANOVA; Sidak test; individual values as well as means  $\pm$  SD are shown;  $n = 6-8$ ; OD – optical density

#### 4.2.2. Serum cytokines

Levels of all examined cytokines (IFN- $\gamma$ , IL-4, IL-5, IL-10, IL-6, and TNF) were increased in sera of mice infected by both 1000 and 4x100 cercariae of *T. regenti* as soon as 5 hpi, but they remained elevated up to 7 dpi only in the repeatedly infected mice (Figure 5A). On the contrary, a hugely different pattern of serum cytokine dynamics was noticed in the mice infected by *T. szidati*. Specifically, only a single high infection dose of 1000 cercariae induced a minor elevation of cytokine levels (especially IL-4 and TNF) 7 dpi (Figure 5B). Multiple exposures (4x100 cercariae) did not trigger cytokine secretion detectable in sera. Based on the cytokine production in sera, *T. regenti* evoked stronger systemic immune response which is especially prominent and long-term in sensitized animals. Through the course of primary infection, systemic immune response was induced by *T. regenti* earlier than by *T. szidati*.

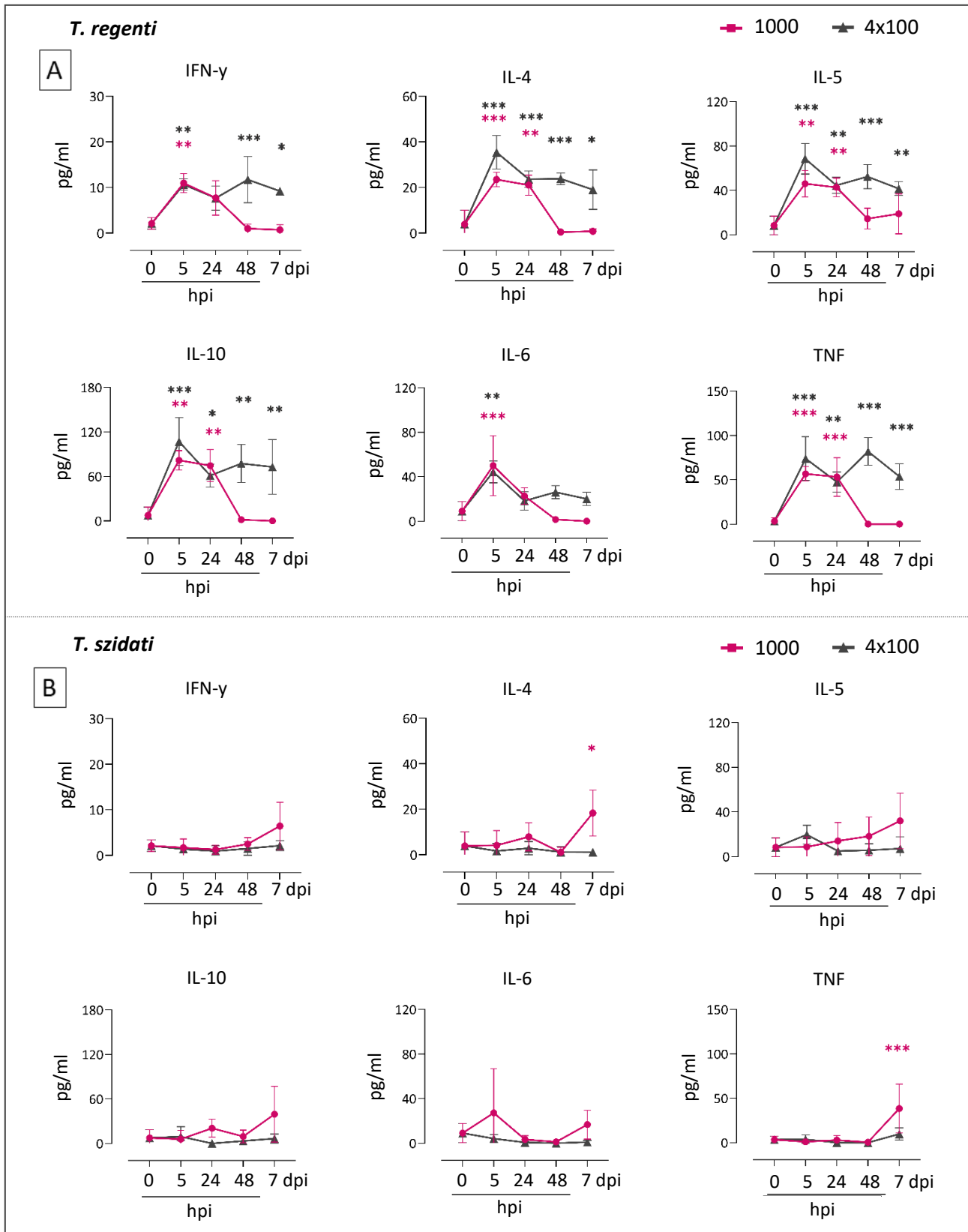


**Figure 5.** Concentration of cytokines in sera of mice infected by 1000 or 4x100 cercariae of *T. regenti* (A) and *T. szidati* (B). Cytokines IFN- $\gamma$ , IL-4, IL-5, IL-10, IL-6 and TNF were detected simultaneously by cytokine bead array. Significant mean difference between the groups at the particular timepoints and the control group (0 hpi) are shown with the corresponding color code. means  $\pm$  SD are shown; 2-way ANOVA; Sidak test;  $n = 3-4$ ; hpi – hours post infection; dpi – days post infection

### 4.3. Skin pathology

#### 4.3.1. Macroscopic observations of mouse pinnae

Immediately after the infection (after 30 min of exposure to 1000 cercariae of *T. regenti* or *T. szidati*), blood vessels in affected pinnae became more visible (Figure 6A; 6B, p. 34). Such effect was not present after the infection by 100 cercariae and neither after the last (4<sup>th</sup>) exposure in reinfection (Figure 6C; 6D). Vasodilation was assessed visually by comparing infected and unexposed pinnae of the same individual. Moreover, a control group, exposed to water only, was examined and did not show any signs of vasodilation (not shown), excluding the effect of the handling itself.

The pinnae were also observed throughout the course of the infection at all examined time points. Hyperemia of the pinnae fluctuated in time after infection by 1000 cercariae. Firstly, 5 hpi, vasodilation induced by the penetration of cercariae diminished, but became conspicuous 24 hpi and 48 hpi in mouse pinnae infected by *T. regenti* and *T. szidati* respectively (Figure 7, p. 35). It was the most prominent 48 hpi and pinnae, especially infected by *T. regenti*, were erythematous. Later, signs of hyperemia diminished and were unnoticeable 7 dpi. Although there was variability between individuals, the trend was clearly present over the groups. Infection dose of 100 cercariae neither during single nor multiple exposures evoked noticeable vasodilation at the timepoints of processing.

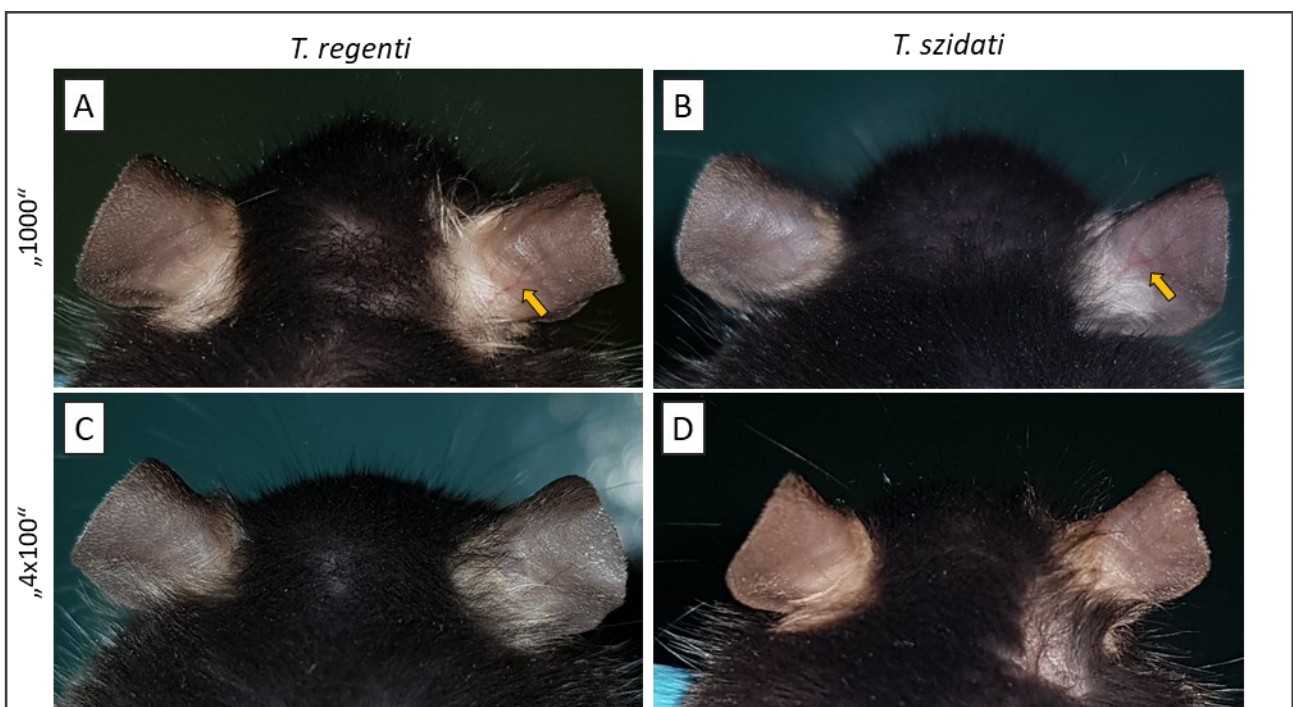
Examination of mouse pinnae under the stereomicroscope revealed skin lesions after infection by 1000 and 4x100 cercariae of *T. regenti* as well as *T. szidati*. Macules were not noticeable but blisters in small number appeared on the infected skin. Firstly, uplifted edges of the lesion appeared 24 hpi (not shown), and at 48 hpi, it developed into compact papule (Figure 8A; 8B, p. 36). At 48 hpi, the skin pathology was the most conspicuous. At 7 dpi, mostly flatten skin lesions resembling wheals remained (Figure 8C; 8D). On the reinfected pinnae, except skin eruptions (Figure 8E), also patches of previously sloughed skin with whitish appearance were noticed (Figure 8F). The skin pathology was comparable between the species.

#### 4.3.2. Histological examination of mouse pinnae

Histopathological changes developed similarly in the mouse pinnae infected by *T. regenti* and *T. szidati*. Histopathologies were only rarely observed in pinnae infected by 100 cercariae, thus pinnae infected by 1000 cercariae were used for the comparative examination. At 5 hpi, *stratum corneum* was disrupted and schistosomula were found underneath (Figure 9A; 9B, p. 37). Keratinocytes in *stratum basale* were compressed and elongated (Figure 9A, inset; 9B, inset). Cellular infiltration was not observed. Histopathology became apparent 24 hpi especially at dermal-epidermal junction where hypergranulosis and infiltration of cells occurred (Figure 9C; 9D). Intraepidermal pustules started to form. Subcorneal acantholysis was causing separation of epidermal layers (Figure 9C). At 48 hpi, suprabasal acantholysis occurred but large pustules and abscesses (Figure 9E; 9F), which formed from

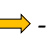
parakeratotic and hyperkeratotic epidermis, represented the most prominent features at this time point. The skin thickened also due to the proliferation of keratinocytes at *stratum basale* and infiltration of leukocytes into the dermis. Thickening of dermis was observed mostly under the epidermal pustules. Schistosomula were found rarely, but they were either entrapped in epidermis (Figure 10A; 10B, p. 38) or present in dermis (Figure 10C; 10D). Whereas in the epidermis schistosomula were enwrapped by the huge amount of cells, no cellular infiltration was observed in their close proximity in the dermis. Later (7 dpi), crust with clearly-defined borders were sloughing off (Figure 9G; 9H, p. 37) and epidermis was thicker than in the uninfected skin. Rarely present cellular debris in the dermis possibly indicated the area of schistosomula destruction (Figure 10E; 10F).

The abovementioned histopathological processes were alike in both species, but slight differences were noticed. At 5 hpi, few cercariae of *T. szidati* already breached *stratum basale* and reached the dermis (Figure 9B, inset) whereas schistosomula of *T. regenti* were found only under *stratum corneum*. In the skin infected by *T. regenti*, skin thickness and abscess appeared larger, especially 48 hpi, although this was not supported quantitatively. Overall thickness of mouse pinnae was dependent also on the sliced area. Therefore, the increase in pinnae thickness was always compared by the adjacent unaffected tissue on the same section.



**Figure 6.** Representative photographs of mouse pinnae immediately after 30 min of exposure to cercariae of *T. regenti* (left column) and *T. szidati* (right column). Mouse pinnae were exposed to 1000 cercariae (A,B) or to 4x100 cercariae (C, D), while the photograph was taken after the last exposure. yellow arrow → - indicates vasodilation



**Figure 7.** Representative photographs of the mouse pinnae infected by cercariae of *T. regenti* (left columns) and *T. szidati* (right column) 5 hpi (A, B), 24 hpi (C, D), 48 hpi (E, F), 7 dpi (G, H) by the infection dose of 1000 and 48 hpi by 4x100 cercariae (I, J). Each photo consists of the unexposed pinna (on the left side) and the infected pinna (on the right side). hpi – hours post infection; dpi – days post infection; yellow arrow  - indicates vasodilation

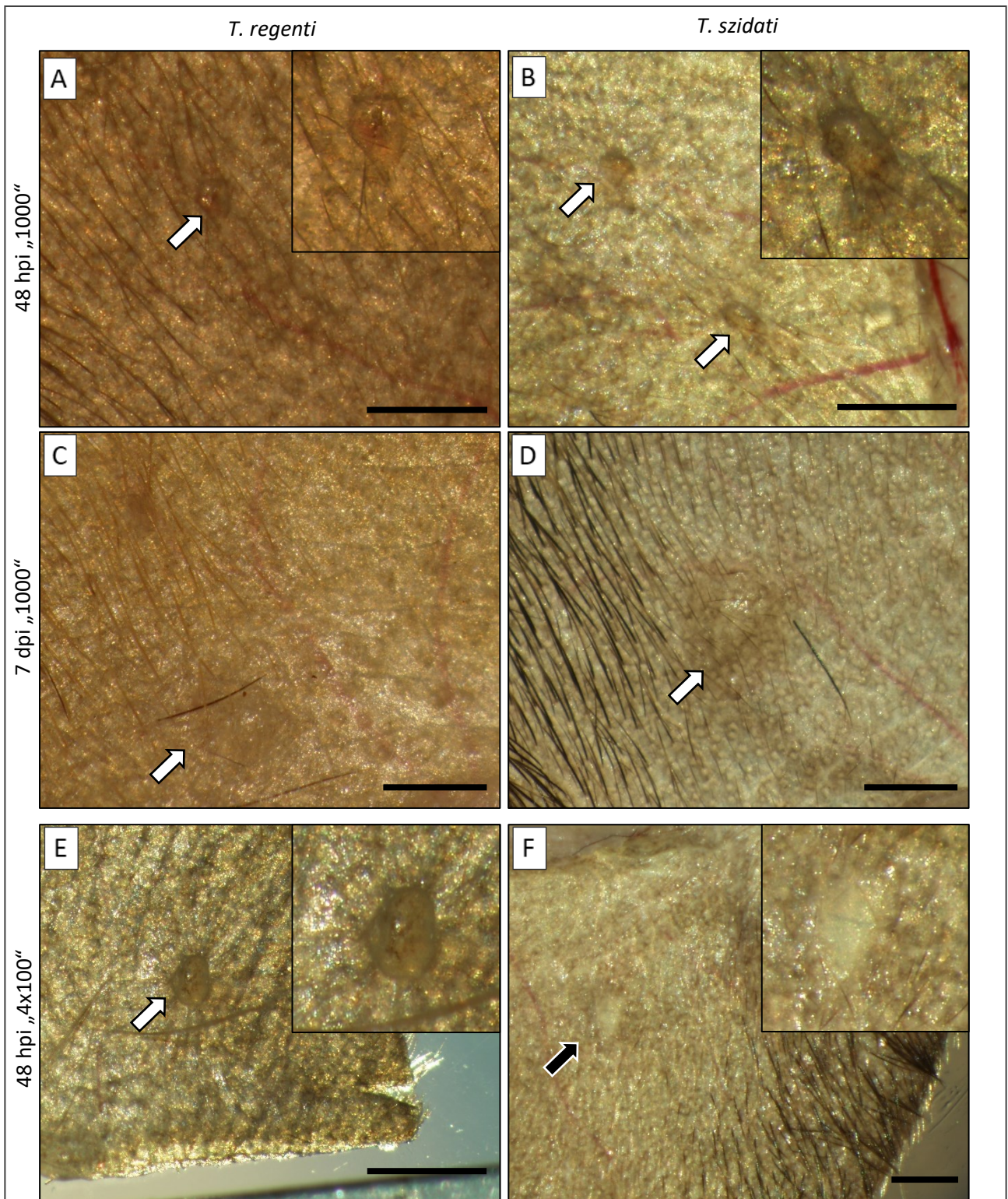


**Figure 8.** Representative photographs of skin pathology of the mouse pinnae infected by cercariae of *T. regenti* (left columns) and *T. szidati* (right column). Pinnae were photographed after infection by 1000 cercariae 48 hpi (A, B), 7 dpi (C, D) or after the last exposure of reinfection 4x100 (E, F). ⇨ white arrow - papules; ⇨ black arrow – area of previously sloughed skin; scale bar = 1 mm; hpi – hours post infection; dpi – days post infection

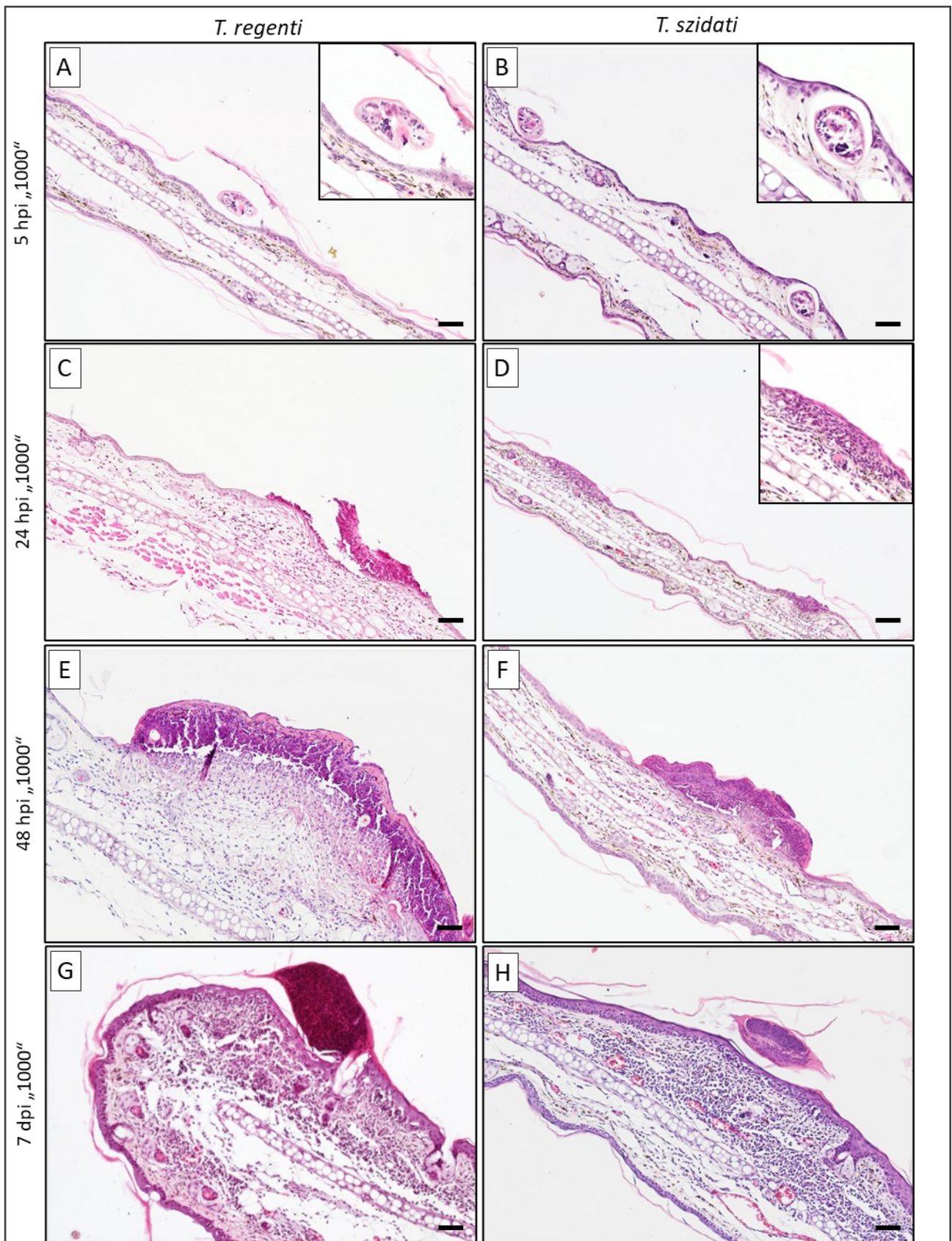


**Figure 9.** Histopathology of the mouse pinnae infected by 1000 cercariae of *T. regenti* (left columns) and *T. szidati* (right column) at 5 hpi (A,B), 24 hpi (C,D), 48 hpi (E,F) or 7dpi (G,H). hematoxylin & eosin staining; scale bar = 50 µm, hpi – hours post infection; dpi – days post infection

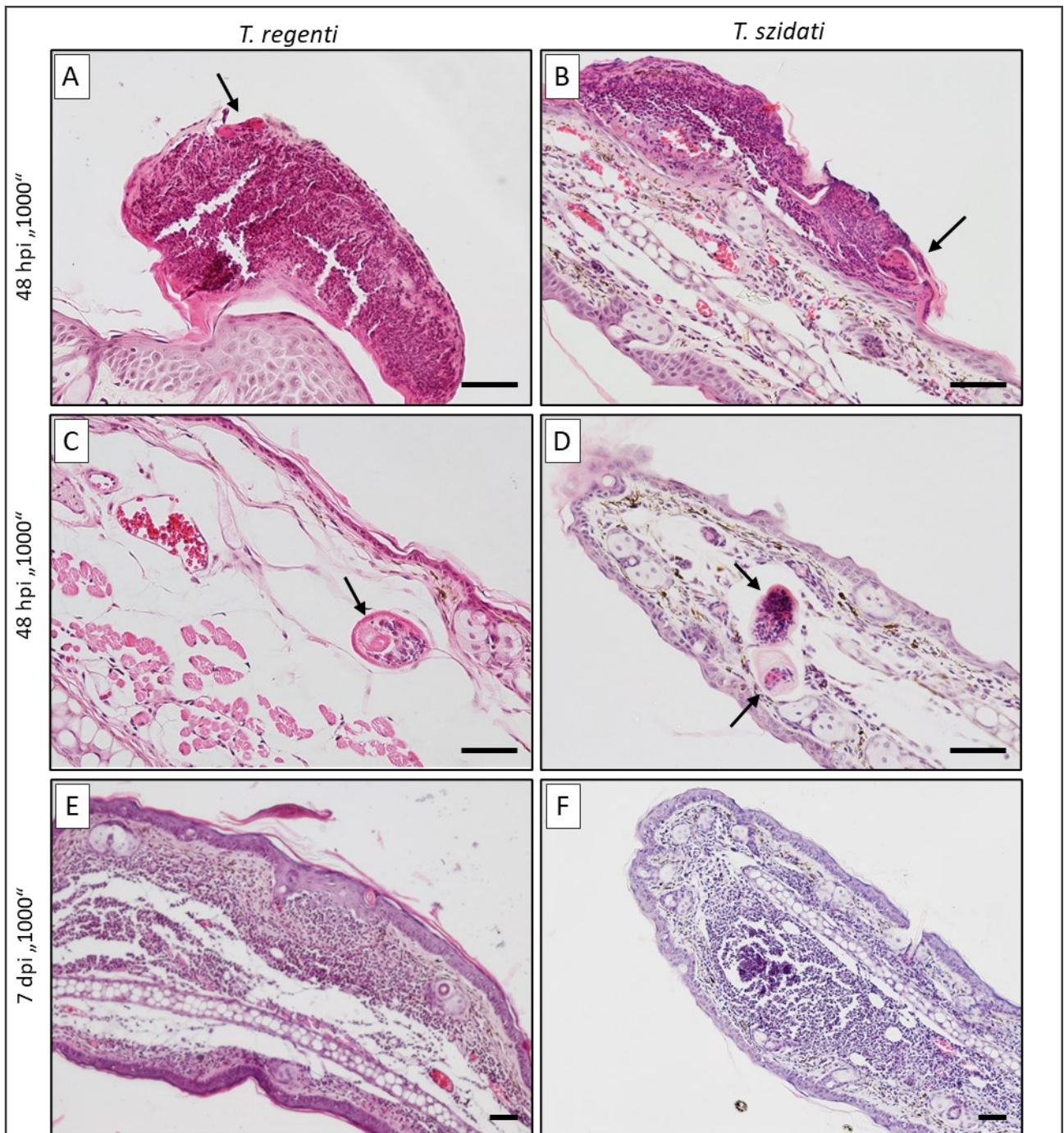


**Figure 10.** Histopathology of the mouse pinnae infected by 1000 cercariae of *T. regenti* (left columns) and *T. szidati* (right column) 48 hpi (A,B, C, D) or 7dpi (G,H). hematoxylin & eosin staining; → black arrow – schistosomulum; scale bar = 50  $\mu$ m, hpi – hours post infection; dpi – days post infection

#### 4.4. Immunophenotyping of leukocytes in mouse pinnae

Flow cytometry analysis revealed a strong effect of the infection by 1000 cercariae of both species on the cell influx into the affected pinnae. Of note, much stronger cellular immune response was detected following the exposure to *T. regenti*. Infection by 100 cercariae of both species induced only weak cellular infiltration detectable by flow cytometry. Reinfection (4x100) did not lead to dramatic increase of leukocytes (CD45+) but it changed their composition. This was evident mostly in control pinnae of mice infected by *T. szidati* indicating that the reinfection changed also the frequency of leukocytes in peripheral blood. Regarding the phenotype of leukocytes in reinfected skin, similar cell-types were observed as in primary infected pinnae. With reference to the aforementioned reasons and to keep this part clear, mostly the results obtained from mice infected by 1000 cercariae are further described if not stated otherwise. Summarized full data are shown in Tables 25–36 (p. 41–44), where significant differences between infected and control pinnae are noted. Complete graphs with individual values can be found in supplementary figures (Figure S6–S23, p. 75-92).

Cellular immune response in infected pinnae was marked by the infiltration of myeloid cells which was noteworthy since 24 hpi (Table 25; 26; 28; 29, p. 41; 42). Neutrophils (CD45+ CD11b+ Ly6G+) and monocytes (CD45+ CD11b+ Ly6C+) dominated the skin infected by both species 24 and 48 hpi. Additionally, at these timepoints, noticeable increase of eosinophils (CD45+ CD11b+ SiglecF+) occurred in mice infected by *T. szidati*. However, in *T. regenti*-infected mouse, major eosinophilic infiltration was observed later, 7 dpi. Whereas granulocytes (neutrophils and eosinophils) were attracted into the epidermis as well as dermis, monocytes infiltration was noted predominantly in dermis. Despite that 7 dpi cellular immune response weakened, elevated numbers of leukocytes were still detected in the infected tissue.

As for the professional Ag-presenting cells (CD45+ CD11c+ MHCII+), only minor changes were observed in the numbers of LCs (CD45+ CD11c+ MHCII+ CD207+) (Table 31; 34, p.43; 44) but counts of dermal DCs (CD45+ CD11c+ MHCII+) significantly increased 48 hpi and 7 dpi (Table 32; 35, p.43; 44). Absolute numbers of CD80+ DCs as well as PD-L1+ DCs mirrored total numbers of DCs (or LCs in epidermis). Therefore, frequency of positive cells was rather examined. Higher percentage of LCs was expressing PD-L1 24 and 48 hpi, although statistically significant only in *T. regenti*-infected epidermis. In reinfected epidermis by either species, PD-L1+ LCs were present in higher frequencies. On the contrary, changes in the proportion of PD-L1+ DCs in dermis were mostly unambiguous. Increased expression of co-receptor CD80+, indicating mature status of Ag-presenting cells, was observed at the later phase of infection. It was expressed on the larger proportion of LCs and DCs in mice infected by *T. regenti* and *T. szidati*, respectively. Lymphoid cells of interest were found only in low numbers (Table 25; 26; 28; 29, p. 41; 42).

The trends observed in DEC mostly mirrored the dynamics and phenotypes of leukocytes observed in the skin (Table 27; 30, p.41; 42). Interestingly, in DEC from pinnae reinfected by *T. regenti* 48 hpi, less F4/80+ macrophages/DCs was found but no change in maturation or activation status of DCs was observed (Table 33, 36, p. 41; 46). Notwithstanding, single high dose infection by *T. regenti* induced significantly higher expression of CD80 on DCs (possibly including also epidermal LCs).

**Table 25.** The effect of infection by 100, 1000 and 4x100 cercariae of *T. regenti* on the absolute numbers of leukocytes and specific leukocyte populations detected by flow cytometry in epidermis of mouse pinnae. Significant differences between the means of infected pinnae and contralateral control pinnae are shown pinnae are shown. hpi – hours post infection; dpi – days post infection; mac – macrophages; DCs – dendritic cells

<i>T. regenti</i>	100				1000				4x100			
<b>Epidermis</b>	5 hpi	24 hpi	48 hpi	7 dpi	5 hpi	24 hpi	48 hpi	7 dpi	5 hpi	24 hpi	48 hpi	7 dpi
leukocytes	-	-	-	-	-	-	↑	-	-	-	-	-
neutrophils	↑	-	-	-	-	↑↑	↑↑	-	-	-	-	-
eosinophils	-	-	-	-	-	-	-	↑	-	-	-	-
monocytes	-	-	-	-	-	-	↑↑↑	-	-	-	-	-
mac/DCs	-	-	-	-	-	-	-	-	-	-	-	-
CD4+ T-cells	-	-	-	-	-	-	-	-	-	-	-	-

**Table 26.** The effect of infection by 100, 1000 and 4x100 cercariae of *T. regenti* on the absolute numbers of leukocytes and specific leukocyte populations detected by flow cytometry in dermis of mouse pinnae. Significant differences between the means of infected pinnae and contralateral control pinnae are shown pinnae are shown. hpi – hours post infection; dpi – days post infection; mac – macrophages; DCs – dendritic cells

<i>T. regenti</i>	100				1000				4x100			
<b>Dermis</b>	5 hpi	24 hpi	48 hpi	7 dpi	5 hpi	24 hpi	48 hpi	7 dpi	5 hpi	24 hpi	48 hpi	7 dpi
leukocytes	-	-	-	-	-	↑↑↑	↑↑	↑↑↑	-	-	-	-
neutrophils	-	-	↑	-	-	↑↑↑	↑↑↑	-	-	-	-	-
eosinophils	-	-	↑↑↑	↑↑	-	-	-	↑↑↑	-	-	-	-
monocytes	-	-	↑↑	-	-	↑↑↑	↑↑↑	-	-	↑	-	-
mac/DCs	-	-	-	-	-	-	-	-	-	-	-	-
CD4+ T-cells	-	-	-	-	-	-	-	-	-	-	-	-

**Table 27.** The effect of infection by 100, 1000 and 4x100 cercariae of *T. regenti* on the absolute numbers of leukocytes and specific leukocyte populations detected by flow cytometry in DEC of mouse pinnae. Significant differences between the means of infected pinnae and contralateral control pinnae are shown pinnae are shown. hpi – hours post infection; dpi – days post infection; mac – macrophage; DCs – dendritic cells

<i>T. regenti</i>	100				1000				4x100			
<b>DEC</b>	5 hpi	24 hpi	48 hpi	7 dpi	5 hpi	24 hpi	48 hpi	7 dpi	5 hpi	24 hpi	48 hpi	7 dpi
leukocytes	-	-	-	-	-	↑↑↑	↑↑	↑↑↑	-	-	-	-
neutrophils	-	-	-	-	-	↑↑↑	-	-	-	-	-	-
eosinophils	-	-	-	-	-	↑↑↑	-	↑↑↑	-	-	-	-
monocytes	-	-	-	-	-	↑	↑	-	-	-	-	-
mac/DCs	-	-	-	-	-	↑	-	-	-	-	↓	-
CD4+ T-cells	-	-	-	-	-	-	-	-	-	-	-	-

**Table 28.** The effect of infection by 100, 1000 and 4x100 cercariae of *T. szidati* on the absolute numbers of leukocytes and specific leukocyte populations detected by flow cytometry in epidermis of mouse pinnae. Significant differences between the means of infected pinnae and contralateral control pinnae are shown pinnae are shown. hpi – hours post infection; dpi – days post infection; mac – macrophages; DCs – dendritic cells

<i>T. szidati</i>	100				1000				4x100			
<b>Epidermis</b>	5 hpi	24 hpi	48 hpi	7 dpi	5 hpi	24 hpi	48 hpi	7 dpi	5 hpi	24 hpi	48 hpi	7 dpi
leukocytes	-	-	-	-	-	-	-	-	-	-	-	-
neutrophils	-	-	-	-	-	↑↑↑	↑↑	NA	-	-	-	-
eosinophils	-	-	-	-	-	↑↑↑	-	NA	-	-	↑	-
monocytes	-	-	-	-	-	↑↑↑	-	NA	-	-	-	-
mac/DCs	-	-	-	-	-	-	-	NA	-	-	-	-
CD4+ T-cells	-	-	-	-	-	-	-	NA	-	-	-	-

**Table 29.** The effect of infection by 100, 1000 and 4x100 cercariae of *T. szidati* on the absolute numbers of leukocytes and specific leukocyte populations detected by flow cytometry in dermis of mouse pinnae. Significant differences between the means of infected pinnae and contralateral control pinnae are shown pinnae are shown. hpi – hours post infection; dpi – days post infection; mac- macrophages; DCs – dendritic cells

<i>T. szidati</i>	100				1000				4x100			
<b>Dermis</b>	5 hpi	24 hpi	48 hpi	7 dpi	5 hpi	24 hpi	48 hpi	7 dpi	5 hpi	24 hpi	48 hpi	7 dpi
leukocytes	-	-	-	-	-	-	-	↑↑	-	-	-	-
neutrophils	-	-	-	-	-	↑	↑↑↑	NA	-	-	-	-
eosinophils	-	-	-	-	-	↑	↑↑↑	NA	-	-	-	-
monocytes	-	-	-	-	-	↑↑	↑↑↑	NA	-	-	↑	-
mac/DCs	-	-	-	-	-	-	-	NA	-	-	-	-
CD4+ T-cells	-	-	-	-	-	-	↑	NA	-	-	-	-

**Table 30.** The effect of infection by 100, 1000 and 4x100 cercariae of *T. szidati* on the absolute numbers of leukocytes and specific leukocyte populations detected by flow cytometry in DEC of mouse pinnae. Significant differences between the means of infected pinnae and contralateral control pinnae are shown pinnae are shown. hpi – hours post infection; dpi – days post infection; mac – macrophages; DCs – dendritic cells

<i>T. szidati</i>	100				1000				4x100			
<b>DEC</b>	5 hpi	24 hpi	48 hpi	7 dpi	5 hpi	24 hpi	48 hpi	7 dpi	5 hpi	24 hpi	48 hpi	7 dpi
leukocytes	-	-	-	-	-	↑↑↑	-	-	-	-	-	-
neutrophils	-	-	-	-	-	-	-	-	-	-	-	-
eosinophils	-	-	-	-	↑	↑	↑	↑	↑	↑	↑	↑
monocytes	-	-	-	-	-	↑↑	-	-	-	↑	-	-
mac/DCs	-	-	-	-	-	-	-	-	-	-	-	-
CD4+ T-cells	-	-	-	-	-	-	-	-	-	-	-	-

**Table 31.** The effect of infection by 100, 1000 and 4x100 cercariae of *T. regenti* on the absolute numbers of LCs, on the frequency of CD80+ DLs, and on the frequency of PD-L1+ LCs detected by flow cytometry in epidermis of mouse pinnae. Significant differences between the means of infected pinnae and contralateral control pinnae are shown pinnae are shown. hpi – hours post infection; dpi – days post infection; LC – Langerhans cells; PD-L1 – programmed death ligand 1

<i>T. regenti</i>	100				1000				4x100			
<b>Epidermis</b>	5 hpi	24 hpi	48 hpi	7 dpi	5 hpi	24 hpi	48 hpi	7 dpi	5 hpi	24 hpi	48 hpi	7 dpi
LCs	-	-	-	-	-	-	-	-	-	-	-	-
% CD80+ LCs	-	-	-	-	-	-	↑↑↑	↑↑↑	-	-	-	-
% PD-L1+ LCs	-	-	-	-	-	-	↑	-	-	↑↑↑	-	-

**Table 32.** The effect of infection by 100, 1000 and 4x100 cercariae of *T. regenti* on the absolute numbers of DCs, on the frequency of CD80+ DCs, and on the frequency of PD-L1+ DCs detected by flow cytometry in dermis of mouse pinnae. Significant differences between the means of infected pinnae and contralateral control pinnae are shown pinnae are shown. hpi – hours post infection; dpi – days post infection; LC – Langerhans cells; PD-L1 – programmed death ligand 1

<i>T. regenti</i>	100				1000				4x100			
<b>Dermis</b>	5 hpi	24 hpi	48 hpi	7 dpi	5 hpi	24 hpi	48 hpi	7 dpi	5 hpi	24 hpi	48 hpi	7 dpi
DCs	-	-	-	-	-	-	↑↑	↑↑↑	-	-	-	-
% CD80+ DCs	-	-	-	-	-	-	-	-	-	↑	-	-
% PD-L1+ DCs	-	-	-	-	-	-	-	-	-	↓↓	-	-

**Table 33.** The effect of infection by 100, 1000 and 4x100 cercariae of *T. regenti* on the absolute numbers of DCs, on the frequency of CD80+ DCs, and on the frequency of PD-L1+ DCs detected by flow cytometry in DEC of mouse pinnae. Significant differences between the means of infected pinnae and contralateral control pinnae are shown pinnae are shown. hpi – hours post infection; dpi – days post infection; LC – Langerhans cells; PD-L1 – programmed death ligand 1

<i>T. regenti</i>	100				1000				4x100			
<b>DEC</b>	5 hpi	24 hpi	48 hpi	7 dpi	5 hpi	24 hpi	48 hpi	7 dpi	5 hpi	24 hpi	48 hpi	7 dpi
DCs	-	-	-	-	-	-	↑	↑↑↑	-	-	↓	-
% CD80+ DCs	-	-	-	-	↑	↑	↑	↑	-	-	-	-
% PD-L1+ DCs	-	-	-	-	-	-	-	-	-	-	-	-

**Table 34.** The effect of infection by 100, 1000 and 4x100 cercariae of *T. szidati* on the absolute numbers of LCs, on the frequency of CD80+ LCs, and on the frequency of PD-L1+ LCs detected by flow cytometry in epidermis of mouse pinnae. Significant differences between the means of infected pinnae and contralateral control pinnae are shown pinnae are shown. hpi – hours post infection; dpi – days post infection; LC – Langerhans cells; PD-L1 – programmed death ligand 1

<i>T. szidati</i>	100				1000				4x100			
Epidermis	5 hpi	24 hpi	48 hpi	7 dpi	5 hpi	24 hpi	48 hpi	7 dpi	5 hpi	24 hpi	48 hpi	7 dpi
LCs	-	-	-	-	-	-	-	-	-	-	-	-
% CD80+ LCs	-	-	-	-	-	-	-	-	-	-	-	-
% PD-L1+ LCs	-	-	-	-	-	-	-	-	↑	-	↑	-

**Table 35.** The effect of infection by 100, 1000 and 4x100 cercariae of *T. szidati* on the absolute numbers of DCs, on the frequency of CD80+ DCs, and on the frequency of PD-L1+ DCs detected by flow cytometry in dermis of mouse pinnae. Significant differences between the means of infected pinnae and contralateral control pinnae are shown pinnae are shown. hpi – hours post infection; dpi – days post infection; LC – Langerhans cells; PD-L1 – programmed death ligand 1

<i>T. szidati</i>	100				1000				4x100			
Dermis	5 hpi	24 hpi	48 hpi	7 dpi	5 hpi	24 hpi	48 hpi	7 dpi	5 hpi	24 hpi	48 hpi	7 dpi
DCs	-	-	-	-	-	-	-	↑	-	-	-	-
% CD80+ DCs	-	-	-	-	-	-	-	↑↑↑	-	-	-	-
% PD-L1+ DCs	-	-	-	-	-	-	-	-	-	-	-	-

**Table 36.** The effect of infection by 100, 1000 and 4x100 cercariae of *T. szidati* on the absolute numbers of DCs, on the frequency of CD80+ DCs, and on the frequency of PD-L1+ DCs detected by flow cytometry in DEC of mouse pinnae. Significant differences between the means of infected pinnae and contralateral control pinnae are shown pinnae are shown. hpi – hours post infection; dpi – days post infection; LC – Langerhans cells; PD-L1 – programmed death ligand 1

<i>T. szidati</i>	100				1000				4x100			
DEC	5 hpi	24 hpi	48 hpi	7 dpi	5 hpi	24 hpi	48 hpi	7 dpi	5 hpi	24 hpi	48 hpi	7 dpi
DCs	-	-	-	-	-	-	-	↑↑	-	-	-	↑
% CD80+ DCs	-	-	-	-	-	-	-	-	-	-	-	-
% PD-L1+ DCs	-	-	-	-	↑	↑	↑	↑	-	-	-	-

#### 4.5. Examination of parotid LNs

To complement the previous observations on the skin immunity, the host immune response was also assessed in the skin-draining lymph nodes. Striking enlargement of the parotid LN at the infected side was apparent in mice infected by 1000 cercariae of both species 7 dpi (Figure 11B; 11C). Comparing contralateral mouse LNs in reinfected mice, small increases in the size of parotid LNs could be observed 48 hpi and it became more prominent 7 dpi. However, the enlargement varied over the reinfected individuals. For precise evaluation, the number of the leukocytes in parotid LNs was quantified (Figure 12, p. 46).

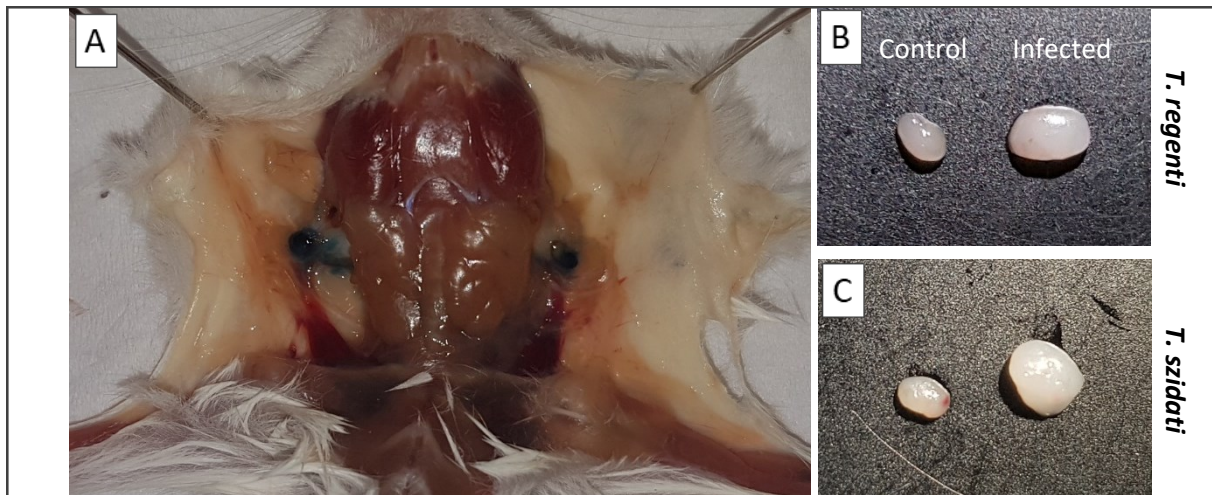


**Figure 11.** Mouse parotid LNs stained by Evans blue (A) and representative photographs of parotid LNs infected by *T. regenti* (B) and *T. szidati* (C). (A) – Detection of parotid LNs: 2% Evans Blue dissolved in PBS (m/v) was injected intradermally into pinnae of anesthetized mouse to verify localization of pinnae-draining LNs. Two consecutive administrations of 5  $\mu$ l were injected into each pinna. After 30 min, mice were sacrificed by cervical dislocation and dissected. (B,C) – Contralateral parotid LNs of mice exposed to cercariae via single pinna (7 dpi). On the photographs from infected mice (B, C), LN from control side is on the left side, LN from infected side on the right side.

Even though infection by 100 cercariae did not affect the LNs size (data not shown), the number of leukocytes in LN was significantly elevated in mice infected by *T. regenti*. Consistent with the parotid LN enlargement, leukocyte expansion occurred mostly 7 dpi in mice infected by 1000 cercariae. Primoinfection induced increase of DCs (CD45+ CD11c+ MHCII+) in the LNs at low rate 24hpi which was followed by the proliferation of B-cells (CD45+ CD11b- MHCII+) (Figure 13A, p. 47). The rate of expansion greatly increased 7 dpi. In sensitized mice (Figure 13B, 13C), the cells expanded at slower, but at more stable rate and again, B-cells dominated in the LNs. On the other hand, number of T-cells (CD45+ CD11b- MHCII-) increased only to a small extent and the fold increase did not change rapidly through the course of infection when either of the infection dose was used. Representation of the cells dynamics in the parotid LNs by fold increase was chosen to visualize the increase in cell numbers and also to compare the rate of expansion of the chosen leukocyte populations.

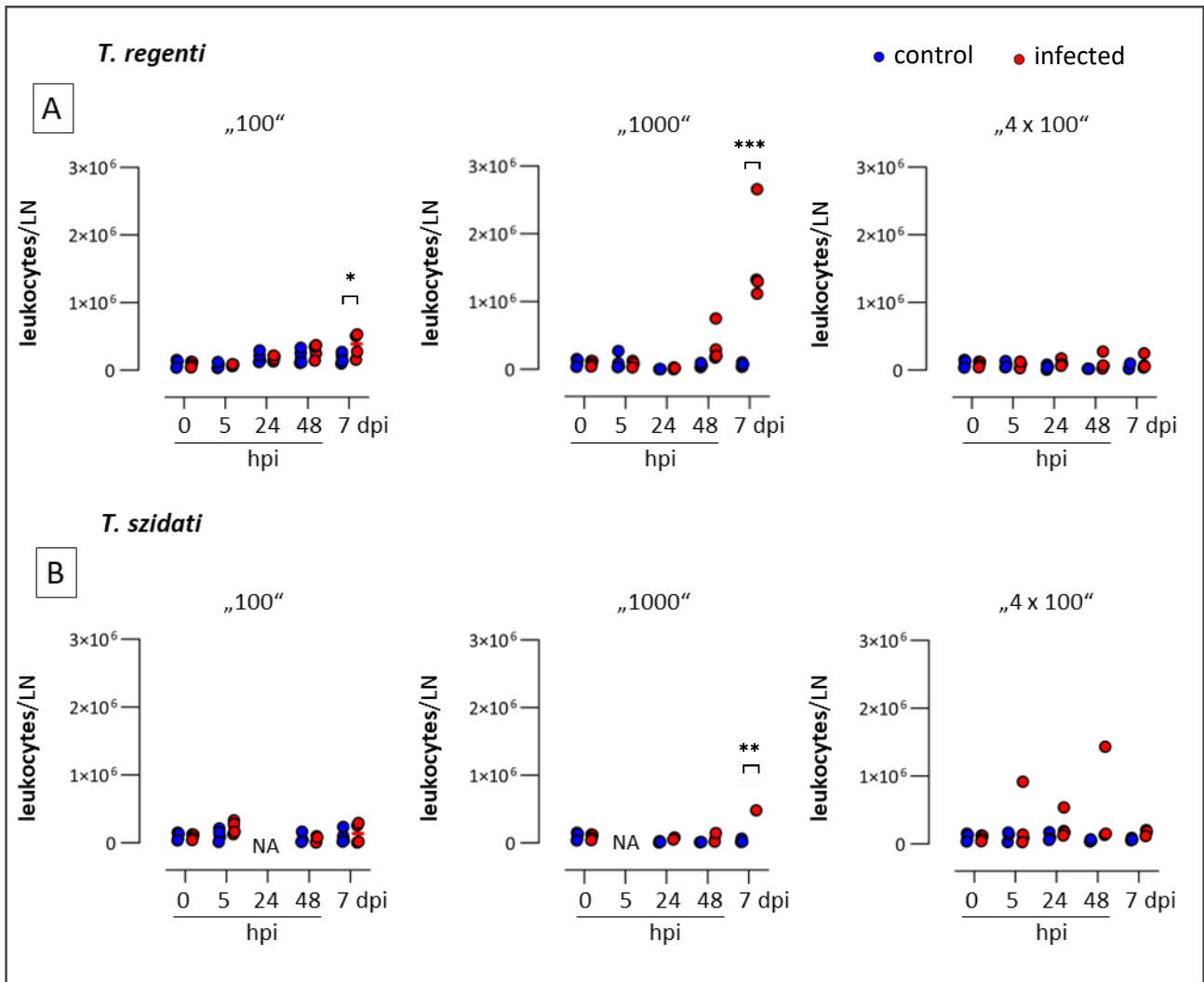


**Figure 12.** Dynamics of leukocytes detected by flow cytometry in parotid LNs of mice infected by 100, 1000 and 4x100 cercariae of *T. regenti* (A) and cercariae of *T. szidati* (B). Significant differences between the means of infected LNs and contralateral controls are shown. 1-way ANOVA; Sidak test;  $n = 0-4$ ; hpi – hours post infection; dpi – days post infection

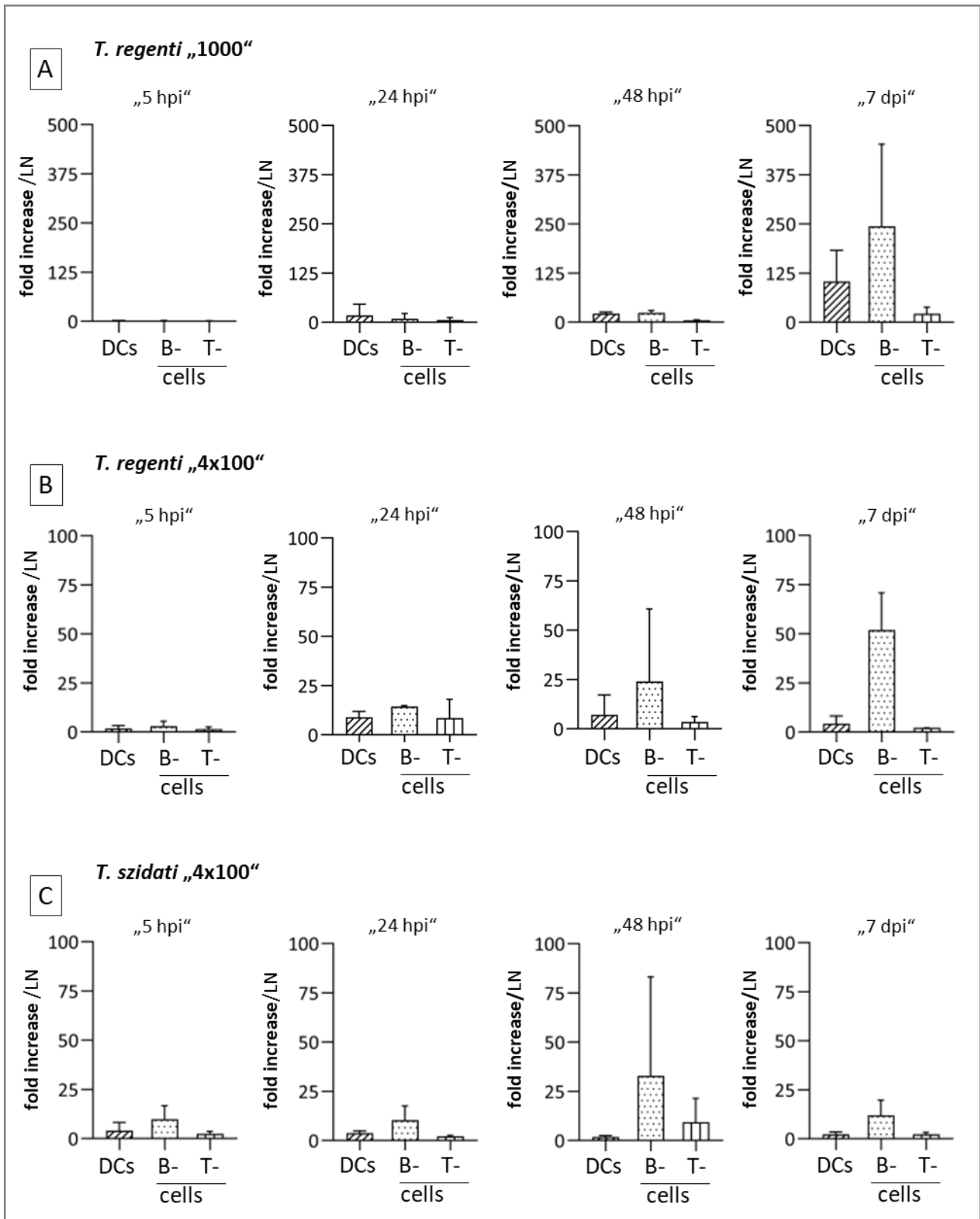


**Figure 13.** Fold increase of DCs (CD45+ CD11c+ MHCII+), B-cells (CD45+ CD11b- MHCII+) and T-cells (CD45+ CD11b- MHCII-) in the parotid LNs of mice infected by 1000 cercariae of *T. regenti* (A), 4x100 cercariae of *T. regenti* (B), 4x100 cercariae of *T. szidati* (C). Fold increase represents the ratio between the numbers of cells from infected LN compared to the contralateral control LN. *n* = 3-4; DCs – dendritic cells

## 4.6. *In vitro* examination of mouse pinnae

### 4.6.1. Cell emigration from pinnae *in vitro*

Emigration of cells from infected pinnae was assessed *in vitro*. Infection by *T. regenti* evoked earlier emigration of cells during *in vitro* cultivation of mouse pinnae. Significant number of cells was released from pinnae exposed to 1000 and 4x100 cercariae of *T. regenti* which were harvested for further *in vitro* cultivation 24 and 48 hpi (Figure 14A). Infection dose of 1000 cercariae induced significant cell emigration also from mouse pinnae infected by *T. szidati* but later, 7 dpi (Figure 14B). In response to *T. szidati*, cell emigration was slightly increased also at earlier timepoints but these counts were low and non-significant. Infection by 100 cercariae of only *T. szidati* caused significant although mild emigration 48 hpi. Generally, infection by 100 cercariae had almost no effect on the cell emigration.

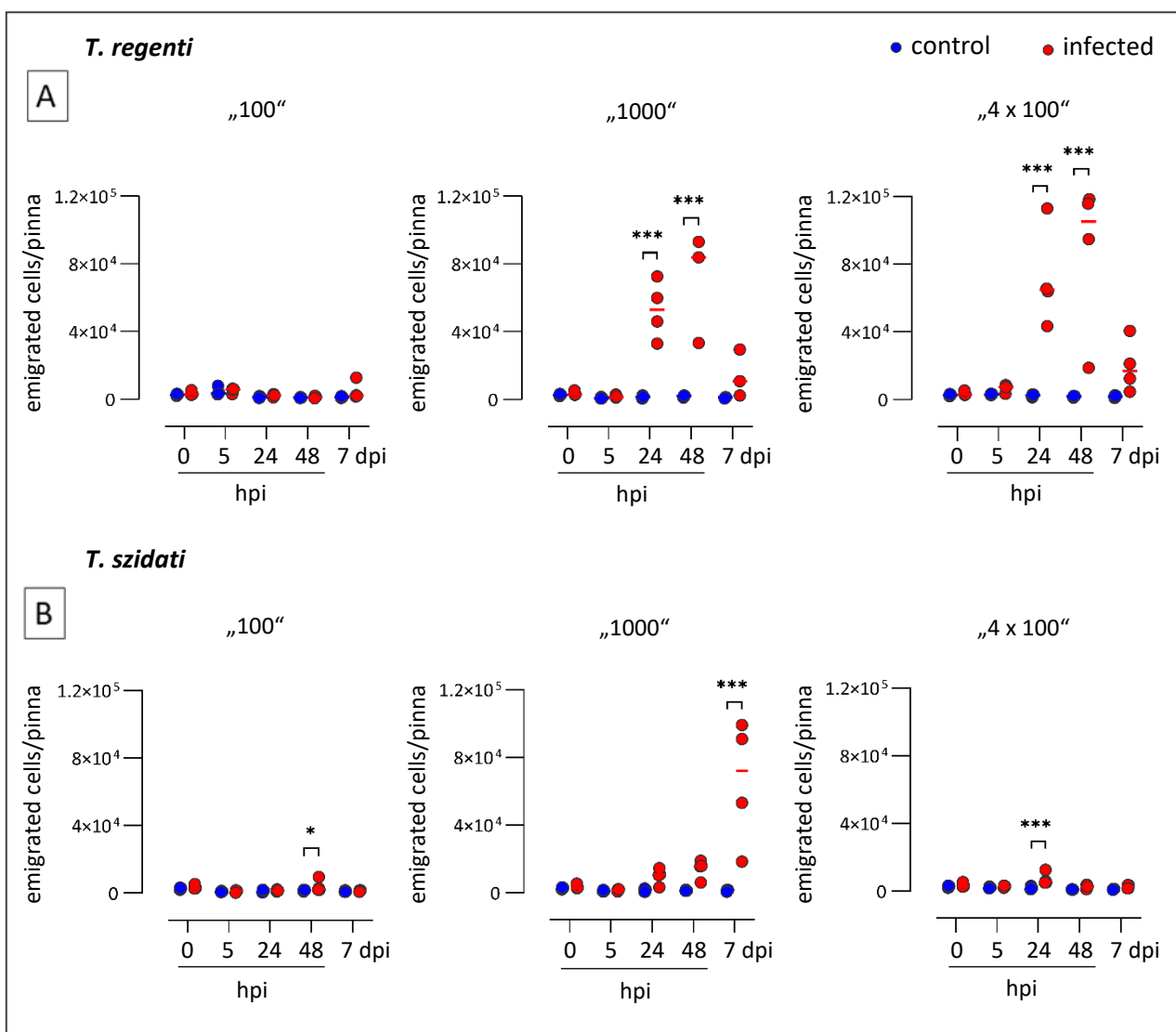


**Figure 14.** The effect of infection by 100, 1000 and 4x100 cercariae of *T. regenti* (A) and cercariae of *T. szidati* (B) on cell-emigration from cultivated mouse pinnae. Released cells were counted after 18h of incubation of mouse pinnae, which were infected by cercariae or unexposed. Significant mean differences between infected and contralateral control pinnae are shown for each group. 1-way ANOVA; Sidak test;  $n = 3-4$ ; hpi – hours post infection; dpi – days post infection

#### 4.6.2. *In vitro* cytokine secretion from cultivated mouse pinnae

Infection by *T. regenti* but not *T. szidati* was marked by the production of the alarmin TSLP (Figure 15). The fastest onset of the TSLP production was observed in supernatants from *in vitro* cultivated mouse pinnae after infection by 1000 cercariae of *T. regenti*. Already 5 hpi, secretion of TSLP arose and the production significantly increased later. At 24 hpi and 48 hpi, the levels exceeded top standard which ruled out the possibility of further description of the dynamics. High level of TSLP was detected also 48 hpi after reinfection by *T. regenti* but low infection dose did not trigger release of this alarmin. Nonetheless, these results indicate rapid production of TSLP in response to *T. regenti* which was not observed at all from pinnae infected by *T. szidati*. Even though generally low cytokine concentrations were measured in supernatants from cultivated mouse pinnae, several trends were noticed. In *T. regenti*-infected mouse pinnae, cytokine production peaked 24 hpi and then rapidly declined (Figure 16A, p. 50). While single high dose of *T. regenti* cercariae triggered secretion of pro-inflammatory TNF, multiple exposures induced higher production of Th2-associated and regulatory cytokines such as IL-4 and IL-10. Later, only weak cytokine production was detected. On the contrary, higher levels of cytokines were not detected in cultivated pinnae infected by *T. szidati* (Figure 16B), until the late phase. As for *T. regenti*, the late phase of pinnae infected by 1000 cercariae was marked by the secretion of IFN- $\gamma$ , but also more IL-4 and IL-10 were produced, indicating mixed polarization. Interestingly, significantly reduced IL-5 production was detected from *T. szidati*-infected pinnae and the similar trend was present also in the case of *T. regenti*. No remarkable cytokine production was detected in samples from mice infected by 100 cercariae of either species. Taken together, *T. regenti* triggers earlier and more prominent *in vitro* cytokine secretion compared to *T. szidati*.

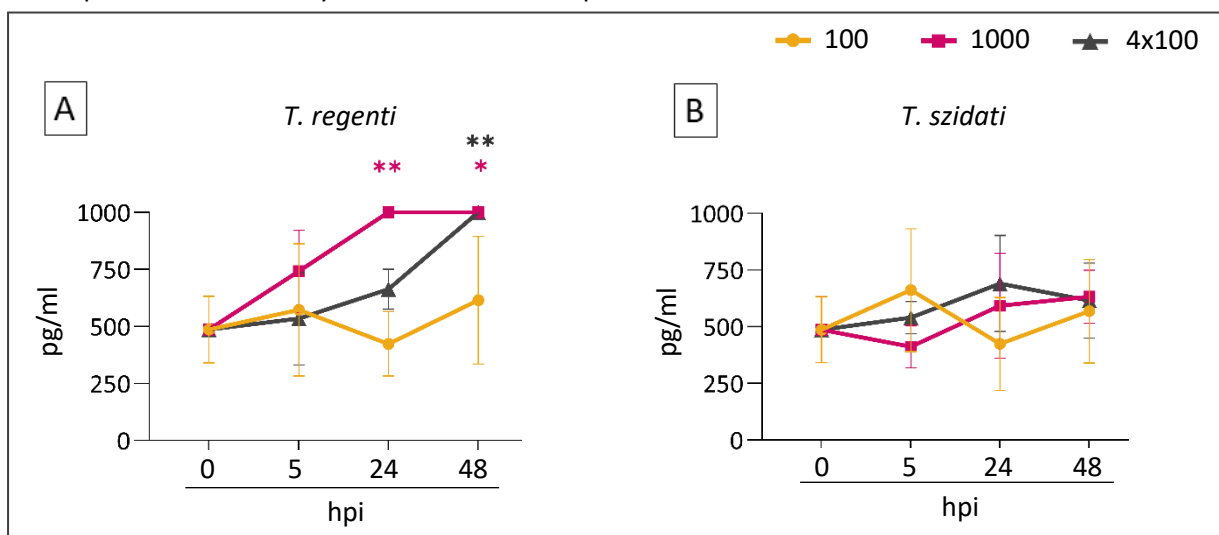


**Figure 15.** Concentration of TSLP in supernatants from cultivated mouse pinnae after infection by 100, 1000 or 4x100 cercariae of *T. regenti* (A) and *T. szidati* (B). TSLP was detected by ELISA in supernatants from cultivated mouse pinnae. Significant mean differences between the groups at the particular timepoints and the control group 0 hpi are shown with the corresponding color code. Two-way ANOVA; Sidak test;  $n = 3-4$ ; hpi – hours post infection

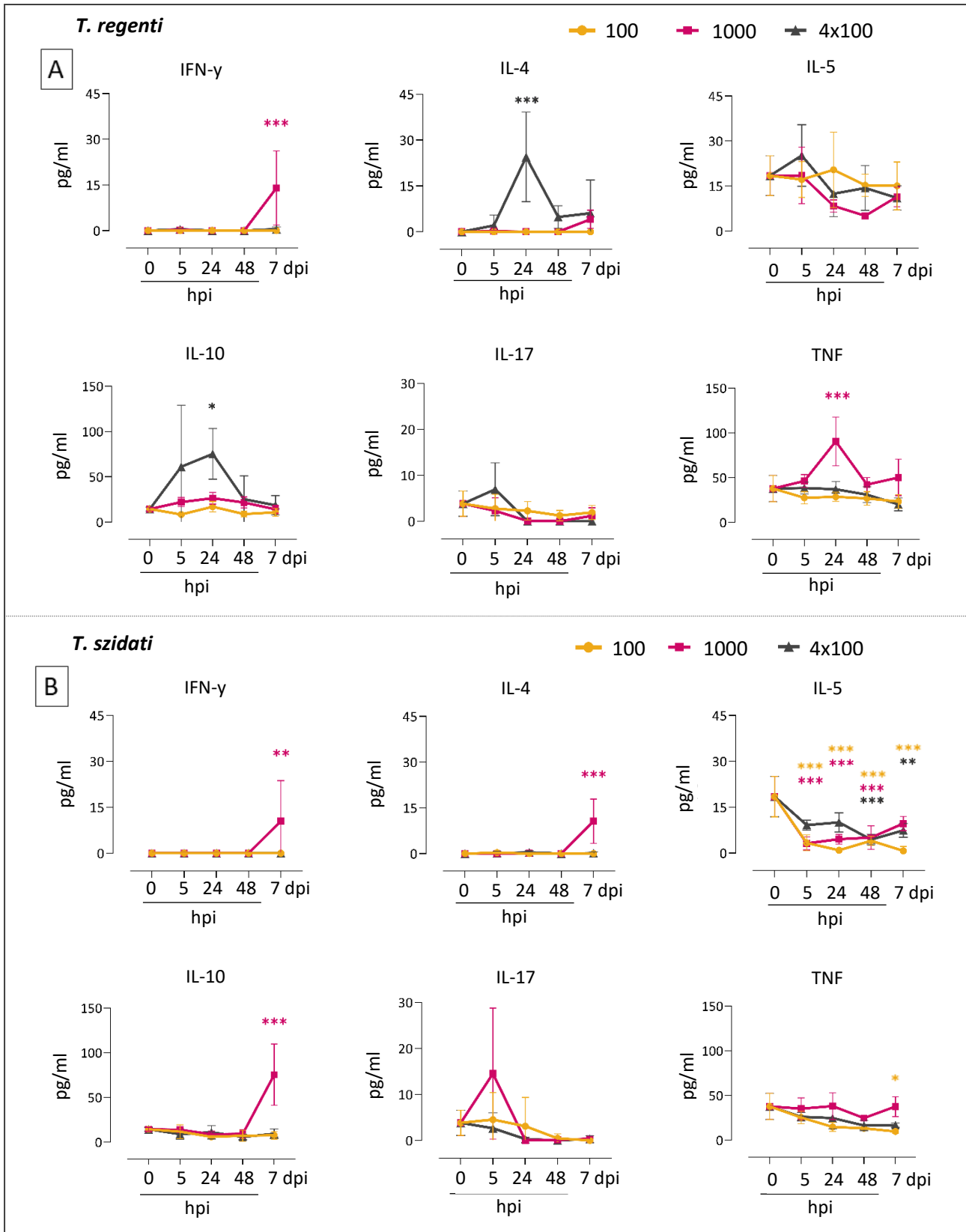


**Figure 16.** Concentration of cytokines in supernatants of mice infected by 100, 1000 or 4x100 cercariae of *T. regenti* (A) and *T. szidati* (B). Cytokines IFN- $\gamma$ , IL-4, IL-5, IL-10, IL-17 and TNF were detected simultaneously by cytokine bead array. Significant mean differences between the groups at the particular timepoints and the control group 0 hpi are shown with the corresponding color code; means  $\pm$  SD is shown; 2-way ANOVA; Sidak test;  $n = 3-4$ ; hpi – hours post infection; dpi – days post infection

## 5. Discussion

Cercarial dermatitis is considered as the allergic reaction towards penetrating cercariae, affecting mostly sensitized individuals. Although the immunological background of the individuals and the number of prior exposures on the intensity of immune response is commonly discussed, the impact of infection dose and the specific infective species is overlooked despite the possibility of clinical relevance. Thus, to examine the role of the abovementioned factors, infection doses of 100, 1000 and 4x100 cercariae of *T. szidati* or *T. regenti* were used to infect mouse pinnae. Skin immune response, along with the systemic inflammation, was studied at different timepoints (5, 24, 48 hpi and 7 dpi) by combining *in vivo* and *in vitro* approaches.

Our data demonstrated that skin pathology evoked by penetration of *Trichobilharzia* spp. cercariae is largely dose-dependent. Although dose-dependency of pathologies was proved for several other helminths (*Nippostrongylus brasiliensis* (Simaren and Ogunyoye, 1973), *Toxocara canis* (Pinelli et al., 2007), *Ancylostoma ceylanicum* (Bungiro et al., 2022)), this has not been studied in the skin infected by avian schistosomes. While in human volunteers infected by *S. mansoni*, addition of only 10 cercariae (2-fold increase) exaggerated the symptoms during skin and acute phase of infection (Langenberg et al., 2020), such effects were not published for migration-related (non-skin) pathology caused by *Trichobilharzia* spp. E.g., Olivier (1953) noticed that numbers of lung hemorrhages nor adults correlated with the infection doses of *T. szidati*. As for *T. regenti* infected mice, the severity of neural pathologies (leg paresis) did not reflect the infection dose either (Horák et al., 1999). However, our complex investigation revealed that the cercarial infection dose greatly impacted the severity of skin pathology and also the host immune response. While in all our experiments hardly any effect (except for histopathology) was observed after exposure to 100 cercariae, mice exposed to 1000 cercariae responded to the infection by noteworthy production of specific IgM antibodies, detectable cellular immune response, cytokine production, parotid LN enlargement and visible macroscopic changes of the infected tissue. Interestingly, the effect of repeated exposures with the small infection dose (4x100) was not so consistent. Below, specific dose-dependent trends observed in our data are discussed.

The activation of adaptive immune response was detected by the production of parasite-specific antibodies. Reinfections clearly increased the production of parasite-specific IgM, and in mice infected by *T. regenti* also production of IgG 7 dpi. This timepoint was chosen according to Majer et al. (2020), who did not detect significant production of IgG in the earlier phases of infection. Enhanced specific IgM and IgG production after repeated exposures of mice to *T. regenti* is well-documented and our results correlate with the previous observations (Kouřilová et al., 2004b; Lichtenbergová et al., 2008). However, contrary to Majer et al. (2020), we did not detect elevated levels of specific IgG in primary-

infected mice. We ascribe this to the higher infection dose and to the mode of infection performed by Majer et al. (2020). They infected mice by a “water-bath” method (through the legs and tail, thus, exposing more areas for penetration), during twice longer exposure time, and, possibly most importantly, with twice as much cercariae (infection dose of 2000). Indeed, the production of specific IgG subsets or specific overall IgG levels were also dose-dependent in mice infected by *T. canis* (Pinelli et al., 2007), by filaria *Litomosoides sigmodontis* (Babayán et al., 2005) or even in rats infected by *Nippostrongylus brasiliensis* (Yamada et al., 1992). Despite undetectable levels of IgG, the activation of adaptive immune response at 7 dpi by single high dose of infection was evident by the striking leukocytes expansion in parotid LNs, supporting the observation of Majer et al. (2020), who noted a peak in cellular response (based on T-cells expansion) in LNs around that time. However, we have observed enormous proliferation of B-cells rather than T-cells in the infected parotid LNs. Such an expansion likely explains the increased antibody production. Presumably, if mice infected by high dose of *T. regenti* cercariae would be sampled at later timepoints, the conversion of IgM into IgG would occur. As already mentioned, marked T-cell proliferation in the parotid LNs and neither the influx of CD4+ T-cells in the infected skin was observed. This is in contrast with the published results of Kouřilová (2004b) from *T. regenti*-infected skin, who observed infiltration of CD4+ T-cells, especially after reinfections. We propose, that after exposure to 1000 cercariae, CD4+ T-cell influx could occur in later, not examined, timepoints. Repeated infection by 100 cercariae did not seem to stimulate extensive DCs accumulation in LNs, thus probably did not suffice to induce antigen-specific CD4+ T-cell proliferation. Interestingly, in experiments of Kouřilová (2004b) infection dose of 300-400 cercaria effectively activated CD4+ T-cells. Nevertheless, limitations of the methodological approaches that we used are discussed later (see Limitations, p. 60). To conclude, B-cells predominantly responded to the infection in the infected parotid LNs by the production of antibodies, but the cells of adaptive immunity were not specifically detected at the infection site.

The infection scheme and dose markedly affected the cytokine production in infected mice, which was prominent especially in sera. Considering generally low serum cytokine levels detected in mice infected by 2000 cercariae of *T. regenti* by Majer et al. (2020), we analyzed only sera from mice infected by 1000 cercariae and from reinfected animals. Unexpectedly, our results from mice infected by *T. regenti* differed from their observation. Whereas in their experiment the level of IFN- $\gamma$  reached the peak at 3 dpi, we observed the highest production of IFN- $\gamma$  in the early phase of infection (5 hpi, 24 hpi) which was followed by rapid decline. However, these observations are not necessarily contradictory and we do not reject the possibility of fluctuation between 48 hpi and 7 dpi. Majer et al. (2020), suggested, that the immune response detected at 3 dpi mostly reflects the skin inflammation during destruction of schistosomula. We speculate, that increased production of cytokines that was detected in sera

almost immediately after primary-infection by high number of cercariae, reflects a reaction upon mechanical skin injury with recognition of antigens of both the parasites and microbiota. Likely, such an early inflammation is induced by tissue-resident cells, rather than by newly infiltrated leukocytes, which we only hardly detected by flow cytometry or observed during histological examination at that timepoint. In epidermis of mice infected by human schistosomes, higher expression of various cytokines was detected (He et al., 2002) even at 1 hpi when no leukocytes were recruited (Angeli et al., 2001). Indeed, keratinocytes *in vitro* reacted to ES products of *S. mansoni* by detectable production of cytokines already 6 hpi, suggesting their capacity to recognize parasite antigens (Bourke et al., 2015). Likewise, keratinocytes in *Leishmania* spp.-infected skin were proved to produce cytokines soon after infection (Jafarzadeh et al., 2021). Additionally, Di Domizio et al. (2020) showed, that commensal bacteria of skin microbiota, carried into wounds of mechanically injured skin, trigger inflammation via activation of neutrophils. Actually, already in 1955, Kagan and Meranze (1955) hypothesized, that not only cercariae, but also contaminants on their surface could possibly evoke inflammation. However, abovementioned innate responses are just few examples how skin-resident cells can mediate inflammation almost immediately after pathogen invasion. One of the possible explanation, how cytokines production by tissue-resident cells can be reflected in sera was recently provided by Dudeck et al. (2021), who showed, that mast cells, which are able to degranulate in 15 min upon stimulus (De Filippo et al., 2013), may secrete its content directly into the bloodstream. However, in our model, these hypotheses were not tested. Insofar of the current knowledge, we can not define the source of cytokines detected in sera. We suggest stimulating a layer of epidermal cells, keratinocytes, and mast cells by different stimuli, such as cercarial ES products, cercarial antigens by to detect source of cytokines. Moreover, intracellular staining of cytokines for flow cytometry in combination with extracellular markers could be used as well as single-cell RNA sequencing. Furthermore, repetition of percutaneous infection of germ-free mice could reveal the role of skin microbiota in the infection.

With higher infection dose, not only higher amount of antigens activates immune system but also, specifically, more cercarial proteases disrupt skin components (Dolečková et al., 2009; Kašný et al., 2007). Proteases of *Necator americanus*, another skin-penetrating helminth, weakened cellular junctions in dose-dependent manner *in vitro* (Souadkia et al., 2010). Moreover, in the presence of higher concentration of *S. mansoni* proteases, more schistosomula successfully matured in mice, probably thanks to the facilitated migration (Fallon et al., 1996). Although not frequently, we have noticed penetration of several cercariae in vicinity of each other, similarly to observations of Haas and Van De Roemer (1998). In the light of ES products, we can not exclude the possibility, that larger quantity of cercariae/schistosomula and their ES products could facilitate the penetration. On the other hand, it could also result in faster passage of antigens to deeper layers of skin due to the

increased permeability. Indeed, schistosomula of *T. szidati* contain more ES products than *S. mansoni* (Nevhutalu et al., 1993) and such a high amount of proteases could be double-edged sword, especially if more cercariae penetrate at the same site. In fact, *in vitro* stimulation of human keratinocytes by ES products of *T. szidati* evoked secretion of pro-inflammatory IL-1 $\alpha$  as high as stimulation by bacterial lipopolysaccharide (Ramaswamy et al., 1996). As for *T. regenti*, recombinant cathepsin B2 was shown to activate DCs and trigger expression of inflammation promoting genes, such as *Cxcl10* or *Il12* (Majer et al., 2020). Hence, we speculate, that not only the tissue damage, and microbiota (both dependent on the infection dose) but also the quantity of parasite antigens, including immunogenic proteases, could participate in triggering the skin pathology and host immune response.

Inflammation intensity is reflected by the quantity of leukocyte recruitment from blood and by leukocyte emigration from the infected site, presumably to the skin-draining LNs. Cells from infected pinnae were released during separation of epidermis and dermis, which was observed visually from the cell-richness of DEC and on the cellular-level by flow cytometry. Interestingly, even this phenomenon was the most evident in pinnae exposed to high infection dose. Regarding DCs (CD45+ CD11c+ MHCII+) in DEC from mice infected by *T. regenti*, we hypothesize, that these cells could have higher migratory potential as higher proportion of them expressed the activation marker CD80. Besides, slightly higher numbers of F4/80+ macrophages/DCs were found in DEC from *T. regenti*-infected pinnae by 1000 cercariae. Possibly, these could be migratory LCs or DCs, although we do not have direct evidence for this. Unfortunately, we have not found any link between number of LCs (nor DCs), and their counts in the parotid LNs. Of note, *S. mansoni* and *L. major* alter migratory capacity of LCs, regardless of their activation status, as one of the immune evasion strategies (Angeli et al., 2001) (Ponte-Sucre et al., 2001). Nevertheless, even during these infections, dermal DCs were found to migrate from infected skin and act as Ag-presenting cells (Cook et al., 2011; Paveley et al., 2009). Interestingly, we have not observed decreasing numbers of F4/80+ cells in the skin, neither in epidermis nor dermis. We hypothesize, that it could be a consequence of monocytes infiltration and differentiation. Monocytes, with a potential of differentiating into monocyte-derived DCs or monocyte-derived macrophages (Coillard et al., 2021), were infiltrated into dermis in large quantities 24 and 48 hpi, and noteworthy, the significant increase in DCs in dermis and DEC followed later, 48 hpi and 7 dpi. However, these monocytes-derived DC and macrophages are indistinguishable from other macrophages or DCs by the markers used in this work.

Our data suggest that reinfections mirror more into systemic than local (skin) inflammation. In a sensitized human, only 4 cercariae of avian schistosome induced skin edema and prolonged pruritus (Macfarlane, 1949). In contrast, repeated exposures to 100 cercariae of *T. szidati* and *T. regenti* in our experiments did not seem to trigger extensive local leukocytic response in mice. However,

concentrations of serum cytokines of mice infected by *T. regenti* were significantly elevated at all the examined timepoints. We speculate, that faster destruction of schistosomula in reinfected skin (Kouřilová et al., 2004b), lies in antigen-specificity (“quality”) rather than in abundance (“quantity”) of leukocytes. As the literature indicates, in sensitized skin, different immune mechanisms can be employed. For example, memory T-cells readily respond to reinfection by *Leishmania* sp., even at previously unexposed site, by producing cytokines and inducing influx of leukocytes (Scott, 2020). Additionally, interesting study was published by Hervé et al. (2021), who observed faster processing of antigens by skin Ag-presenting cells and higher frequency of these specific Ag-presenting cells in LNs of previously sensitized mice. Notably, this was efficient in mice which received sera of previously sensitized mice, or even if only IgG antibodies from sensitized animals were transferred. Involvement of systemic immune response through the course of *T. regenti* infection was indicated also by Majer et al. (2020) when they observed fluctuations in numbers of T-lymphocytes in spleen and increased cytokine production from splenocytes in response to antigens of cercariae. Perhaps, multiple exposures by low infection dose activated systemic immune response but this was not mirrored into strong local inflammation. Therefore, we hypothesize, that reaction in sensitized individuals reflects not only the number of prior exposures but also their intensity. Of note, reinfected tissue did not show erythema despite papule formation. Regarding the papules we suggest that they could result from cercarial penetration at the previously affected site. Thickened epidermal layer could serve as an extra barrier, leading to the retardation of schistosomula migration. Indeed, we noticed proliferation of keratinocytes in *stratum basale*, which was previously described also after penetration of *Trichobilharzia* sp. by (Appleton and Brock, 1986), *S. douthitti* (Batten, 1956) or by (Bourke et al., 2015) in the skin infected by *S. mansoni* around hair follicles. We conclude, that the immune response in sensitized individuals also depends on the intensity (of all the exposures) and not only on the counts. Besides, even in hamsters infected by *A. ceylanicum*, Davey et al. (2013) observed, that the course of infection is affected by the number, intensity and also frequency of previous exposures. Additionally, low infection dose could possibly trigger antigen-specific immune response rather than strong innate reaction.

Despite that reinfection (4x100) changes the course of infection, our results from reinfected skin did not confirm the previous observations of strong and efficient leukocyte immune response. In the skin (4x) reinfected by *T. regenti* (300 – 400 cercariae), Kouřilová et al. (2004b) undoubtedly proved stronger immune response in comparison to the primary-infected skin. Interestingly, our results from different methodological approaches provided contradictory outcomes regarding the intensity of local immune response after infection by 4x100 cercariae. While only weak cellular infiltration was detected by flow cytometry, extensive cell emigration during pinnae cultivation was observed. Nonetheless,

there are more possible explanations for this discrepancy. In flow cytometry, cells were stained for leukocyte-specific markers, thus epithelial cells, such as keratinocytes and fibroblasts, were not included in the analysis. However, leukocytes as well as epithelial cells could be loosened during *in vitro* pinnae cultivation and manually counted (resulting in the virtual increase of cell emigration). In fact, approximately 20% of the cells from cultivated pinnae of mice infected by *S. mansoni* were not leukocytes (Cook et al., 2011). Moreover, by flow cytometry, only live cells were analyzed, but emigrated cells were counted regardless of their viability. Indeed, apoptosis was observed in *T. regenti*-infected skin by Parohová (2020), who suggested, that those apoptotic cells, especially due to their location in the epidermis, are keratinocytes. In view of our histopathological examination, we support this observation and further extend this hypothesis. We assume, that apoptotic cells, transiently detected by immunohistochemistry in the early phase of infection (8 hpi) (Parohová, 2020), could later, as dead keratinocytes, form hyperkeratotic lesions. These keratinocytes could separate from the infected tissue more easily and therefore, they could be counted after *in vitro* skin cultivation. Apoptosis in larger-scale during reinfection also cannot be excluded. In fact, *S. mansoni* affects apoptosis of emigrated Ag-presenting cells during *in vitro* cultivation of skin (Cook et al., 2011) and, especially after multiple exposures, schistosomula of *S. mansoni*, were shown to induce apoptosis of T-lymphocytes in the skin-draining LNs (Chen et al., 2002; Prendergast et al., 2015). Furthermore, apoptosis and necrosis of the epidermal cells could explain conspicuous pathology of (primary infected) epidermis which was not detected to such an extent by flow cytometry. In short, we suggest, that reinfection either affected the epithelial cells more than leukocytes, or caused cellular death (of any cell type) at higher rate.

Considering the lack of evidence for IgE-mediated hypersensitivity (Lichtenbergová et al., 2008; Macháček et al., 2018) and the absence of vasodilation in reinfected pinnae through our experiments, the question of mast cell degranulation arises. Kouřilová et al. (2004b) observed almost immediate mast cell degranulation in *T. regenti*-infected skin and elevated histamine production especially after reinfections. Hoppe et al. (2020) showed that the presence of extracellular adenosine triphosphate (ATP) and IL-33 enhances the mast cell degranulation and histamine production after epicutaneous application of allergens. ATP and IL-33 were shown to promptly induce vasodilation and edema in the mouse pinnae. Later Jordan et al. (2021) concluded, that simultaneous stimulation by these mediators induce fast mast cell degranulation independently of IgE antibodies. Notably, increased expression of IL-33 in epidermis of mice was detected in response to the infection by *S. mansoni* (Bourke et al., 2015) or by *Strongyloides venezuelensis* (Koida et al., 2021). Cercarial cathepsin B2 of *T. regenti* induced expression of *IL33* in DCs after *in vitro* stimulation (Majer et al., 2020). Therefore, it is tempting to speculate that while single high dose of cercariae of *Trichobilharzia* spp. causes severe injury along

with abrupt release of stress related mediators followed by mast cells degranulation and vasodilation, damage caused by 100 cercariae is less extensive, possibly causing weaker release of ATP and IL-33 from damaged cells or possibly weaker stimulation of DCs. Even if more damaged or dead cells are present in reinfecting skin, as we previously suggested, stress mediators could be released gradually thus not inducing rapid mast cell degranulation.

Regardless of the effort to stimulate natural infections, many factors can only be approximated. Ecological factors such as temperature, light, snail density and species impact the infection. Prolonged exposure of cercariae may potentially decrease their infectivity, but on the other hand, more cercariae may accumulate through the day and infect the host (Soldánová et al., 2013). The infection doses in our experiments were based on the literature while respecting ethic principles of animal handling (prevention of excessive injury and pathology). Assuming that infection dose of 2000 cercariae is used to study peripheral and neural immune response of mice infected by *T. regenti* (Macháček et al., 2022; Majer et al., 2020), to study skin, as the site of first host-pathogen interaction, infection dose of 1000 cercariae was chosen. However, we are not able to determine the infection dose during natural infections. According to (Olivier, 1949), the infection dose can be assumed from the number of skin lesions, but in our (histo)pathological examination, papules did not reflect the actual number of penetrated cercariae. Based on the histological examination, we suggest, that schistosomula entrapped in epidermis triggered strong immune response to form macroscopic lesions. Batten (1956) came to similar conclusion during histopathological examination of skin of mice infected by *G. huronensis*, when schistosomula were found only in dermis and no macroscopic lesions were noticed. While epidermis of mice on some body parts consists of only one clearly defined layer of living keratinocytes, epidermis of humans is multilayered. Despite that, similar histopathological changes, such as hyperkeratosis and abscess formation, were observed in the skin of *Trichobilharzia* sp. infected mice and human, but in humans, schistosomula were noticed almost exclusively in the epidermis (Brackett, 1940; Kouřilová et al., 2004b; Macfarlane, 1949). Therefore, we hypothesize, that breaching more layers of keratinocytes in human skin would cause slowing down the migration of schistosomula which results in more time for host's immune response along with pushing schistosomula towards the outer layers. Consequently, the penetration of equal number of cercariae could be possibly accompanied by more lesions in human skin than in mice.

Skin immune response evoked by penetrating schistosomula of the genus *Trichobilharzia* is species-specific. Firstly, our histopathological observation did not reveal qualitative differences between *T. regenti* and *T. szidati*-infected skin and it agreed with descriptions of infected skin by *T. regenti* or *T. szidati*, published by Kouřilová et al. (2004b) or Olivier (1949), respectively. Besides, thickening of the skin, vasodilation, cellular influx and even formation of epidermal abscesses was noted also in the skin

infected by different genera and species of the family Schistosomatidae (Batten, 1956; Incani and McLaren, 1984; Olivier, 1949). Later, despite this primary resemblance, great differences in the skin immune response evoked by *T. regenti* and *T. szidati* were revealed, especially in terms of intensity and dynamics. Although species might be closely related, there can be differences regarding their biology. He et al. (2005) pointed out differences between *S. mansoni*, *S. haematobium* and *S. japonicum*, in terms of host-finding and skin penetration. Likewise in our observations, cytokines were produced in species-specific manner (He et al., 2002). Cercariae of *T. regenti* induced faster cellular immune response than cercariae of *T. szidati*. Despite the absence of complete data from flow cytometry from mice 7 dpi infected by 1000 cercariae of *T. szidati*, number of total leukocytes and counts of emigrated cells indicated that the strongest cellular immune response occurred at that timepoint. On the contrary, highest number of cells from *T. regenti*-infected pinnae were detected between 24 and 48 hpi. Such differences in dynamics of cellular infiltration could explain discrepancies in the previous studies regarding the composition of leukocytes which were based solely on the histological examination of the skin infected by *Trichobilharzia* spp. (Appleton and Brock, 1986; Gay et al., 1999; Kouřilová et al., 2004b).

Unexpectedly, *T. regenti* induced remarkably stronger skin immune response which was especially evident by the rapid cytokine production. Epidermal cells were shown to produce multiple cytokines, including alarmins, in response to helminth infections. Particularly, increased expression of alarmin TSLP, a potential inducer of Th2 polarization, was detected in the early phase after infection by *S. mansoni* (Bourke et al., 2015), *N. brasiliensis* (Connor et al., 2017) and *S. venezuelensis* (Koida et al., 2021). While *S. mansoni*, species related to our experimental models *Trichobilharzia* spp., induced only transiently increased expression of TSLP 24 hpi, *T. regenti* induced rapid production that was detectable even 48 hpi. In contrast, increased production of TSLP was not detected from *T. szidati*-infected pinnae. Along with the weaker leukocyte infiltration observed in *T. szidati*-infected skin, we suggest, that TSLP can be a factor dictating the intensity of the immune reaction. Nevertheless, the production of other alarmins (IL-33, IL-25), triggered by either species, can not be excluded. Eventually, broad spectrum of cytokines was detected from cultivated mouse pinnae from mice infected by *T. regenti*, both in our study as well as in study of Kouřilová et al. (2004b). Currently, we can only hypothesize about their roles. However, while discussing the intensity of immune response, penetration rate of cercariae should be considered. Penetration rate of *T. regenti* cercariae was consistent with the results of Kouřilová et al. (2004a), however, when compared to *T. szidati*, cercariae of *T. regenti* penetrated at higher rate. As previously mentioned, penetration of more cercariae would result in higher antigen load, more severe injury, and higher contamination by microbiota. Although we estimated the penetration rate of cercariae based on the number of non-penetrant cercariae,

completion of penetration of individual cercariae were not examined. Appleton and Brock (1986) observed, that out of “penetrated” *Trichobilharzia* sp. cercariae, 41% were only attached to the skin of mice after 60 min of exposure but also this does not mean that the cercariae did not penetrate afterwards. Clearly, our calculation of penetration rate provides only approximate estimation of the cercarial penetration. Despite that, we do not assume that variability in penetration rate would cause such a striking difference in the skin immune response. To control for this, the infection time could be prolonged to see if the penetration rate would equalize between species or would really stay uneven indicating true interspecific differences.

Currently, the literature does not provide any explanations for the abovementioned interspecific differences occurring during skin phase in terms of pathology and the host immune response. We speculate that the generally lower pathogenicity of *T. szidati* compared to *T. regenti* can be a result of coevolution between the parasite and its hosts. Cercariae of *T. szidati* may emerge from its intermediate host *L. stagnalis* in dramatically higher quantities than cercariae of *T. regenti* from smaller snail species of the genus *Radix* (Soldánová et al., 2016, 2022). Therefore, we hypothesize that highly pathogenic strains of *T. szidati* were eliminated by the means of natural selection because highly pathogenic cercariae in high numbers caused the death of (or at least a severe injury to) the definitive host, thus restraining maturation of parasite. However, we are aware, that our results were obtained from infection of accidental hosts and the comparative study about the immune response in the skin of aquatic bird is needed. We suggest to cultivate duck skin *in vitro* or to stain leukocytes for flow cytometry to allow quantification and comparison of cellular immune response in the skin of definitive hosts infected by *T. regenti* or by *T. szidati*. Furthermore, we are aware, that higher pathogenicity of schistosomula in the skin does not necessarily mean higher pathogenicity upon the escape from the skin. Of note, Turjanicová (2012) detected the production of cercarial specific IgY in ducks infected by *T. regenti* but not by *T. szidati*, (despite that higher infection dose of *T. szidati* was used) which support our observation about lower immunogenicity of *T. szidati* cercariae. Whether this variability lies in the composition of ES products, glycocalyx or in immune evasion strategies of the particular *Trichobilharzia* sp. remains to be answered.

Collectively, our results showed that the cercariae of *T. regenti* and *T. szidati* evokes skin immune response in a dose-dependent manner. Single high dose infection induced severe skin pathologies, which were conspicuous by both macroscopic and microscopic examinations. Besides, extensive leukocytes infiltration, elevation of cytokine concentrations, activated humoral immune response, and skin-draining LN enlargement were observed. However, infection by 100 cercariae did not induce detectable immune response by the chosen methods and even repeated exposures did not seem to dramatically affect the site of infection but rather mirror into systemic inflammation. Furthermore, our

results indicate noteworthy immunogenicity of *T. regenti* cercariae which elicit severe skin-pathology. Our comparative study showed that the skin immune response differs between *Trichobilharzia* spp. and the results obtained from one species can not be generalized for the entire genus. However, the major cause for such a remarkable difference in induction of skin inflammation needs to be examined.

#### Limitations of the study

Due to poor quality of histological processing, sections of the mouse pinnae were lost thereby not all the sections were examined. For the description, representative areas were chosen which could lead to the bias. Because of strong cellular influx, individual leukocytes were poorly distinguishable, therefore flow cytometry analysis was used for leukocytes characterization and quantification. Migration of LCs or DCs was not successfully examined due to the low yield of DCs from parotid LNs caused by the unsuitable extraction technique. Higher yield of DCs from LNs could be acquired by enzymatic digestion (Kashem and Kaplan, 2018). To study DCs migration from skin, more immunophenotyping markers, (e.g. CD103, CD64, PDCA-1), should be used in combination with the markers of our choice (CD11b, CD11c, MHCII, CD207 and F4/80) to correctly define specific DCs subsets (Sheng et al., 2021) therefore, we suggest performing the experiment with different set of markers, which would focus on the phenotype rather than activation status of Ag-presenting cells, as poorly defined cell population restrain proper interpretation, and just as importantly, to use enzymatic digestion for LNs. To isolate leukocytes from the skin, enzymatic digestion was used. Although dispase was proved to cleave some extracellular markers on leukocytes, including CD4 (Autengruber et al., 2012), we believe this was not the case as dispase was used only to separate epidermis and dermis. Prior to mechanical digestion, dispase would unlikely reach the individuals T-cells and cleave CD4 out of their surface. Collagenase does not negatively impact extracellular markers (Autengruber et al., 2012).

Inbred C57BL/6J01aHsd mice of the same age were used to limit biological variability. However, the biggest limitation of the study is the number of animals per group. Usually, four mice per group were processed for quantitative experiments which is not sufficient for proper statistical analysis. Furthermore, low quality of some samples, especially because of poor acquisition by flow cytometer, required their exclusion from the analysis. Although statistical analysis was performed, its validity needs to be taken cautiously. Even more cautions must be taken to interpret our results and translate them comparatively into natural infections. Nevertheless, the value of the presented screening study lies in its complexity which provides preliminary data needed for design of further research.

## 6. Conclusion

The skin phase of the host invasion by cercariae of the genus *Trichobilharzia* is believed to be conserved over the entire genus. However, comparative studies regarding the species-specific differences in the pathology and host immune response are lacking, leaving the researchers to extrapolate results obtained from a single species to the entire genus. Moreover, the role of infection dose on the course of skin-immune response towards *Trichobilharzia* spp. has not been experimentally evaluated yet, despite the frequent association of CD with previous sensitization. Therefore, this thesis aimed to elucidate the skin immune response in mice infected by *T. regenti* and *T. szidati*, to determine the species-specific differences and to examine the effect of infection doses.

In this thesis, these main results were obtained:

- The infection dose greatly impacted the skin immune response. In primary infected pinnae, 1000 cercariae triggered extensive skin immune response along with severe histopathology which was very mild in pinnae infected by 100 cercariae.
- The low infection dose even after repeated exposures (4x100) did not trigger an intensive local immune response but rather resulted in systemic inflammation which was detected as the production of parasite-specific antibodies and in mice infected by *T. regenti* also as the persistent increase of cytokine concentrations in sera.
- Examination of infected mouse pinnae revealed similar histopathological changes and influx of identical cell types into infected skin after infection by cercariae of either *T. regenti* or *T. szidati*. However, the intensity of the immune response was much weaker in *T. szidati*-infected skin, indicating its lower immunopathogenicity. Moreover, different patterns in cytokine production, in terms of quantity as well as dynamics, were observed.
- Predominantly, granulocytes and monocytes infiltrated infected skin since 24 hpi. In the pinnae-draining (parotid) lymph nodes, mostly B-cells expansion occurred, especially 7 dpi, presumably resulting in the production of parasite-specific antibodies.

The results revealed that the skin and local immune response towards *Trichobilharzia* spp. during the early phase after parasite invasion is species-specific and dose-dependent. The studied factors will be therefore considered in further plans and experiments. This thesis provided complex insight into the skin pathology evoked by the penetration of *T. regenti* and *T. szidati* cercariae.

## References

- Al-Jubury A., Kania P., Bygum A. and Buchmann K.** (2020). Temperature and light effects on *Trichobilharzia szidati* cercariae with implications for a risk analysis. *Acta Vet. Scand.* 62, 54.
- Al-Jubury A., Bygum A., Susannatracz E., Koch C.N. and Buchmann K.** (2021). Cercarial dermatitis at public bathing sites (Region Zealand, Denmark): A case series and literature Review. *Case Rep. Dermatol.* 13, 360–365.
- Aldhoun J., Kment P. and Horák P.** (2016). Historical analysis of the type species of the genus *Trichobilharzia* Skrjabin et Zakharov, 1920 (Platyhelminthes: Schistosomatidae). *Zootaxa* 4084, 593–595.
- Anderson N.J., Blankespoor C.L. and DeJong R.J.** (2022). The tails of two avian schistosomes: Paired exposure study demonstrates *Trichobilharzia stagnicolae* penetrates human skin more readily than a novel avian schistosome from *Planorbella*. *Pathogens* 11, 651.
- Angeli V., Faveeuw C., Roye O., Fontaine J., Teissier E., Capron A., Wolowczuk I., Capron M. and Trottein F.** (2001). Role of the parasite-derived prostaglandin D2 in the inhibition of epidermal Langerhans cell migration during schistosomiasis infection. *J. Exp. Med.* 193, 1135–1147.
- Appleton C.C. and Brock K.** (1986). The penetration of mammalian skin by cercariae of *Trichobilharzia* sp. (Trematoda: Schistosomatidae) from South Africa. *Onderstepoort J. Vet. Res.* 53, 209–211.
- Appleton C.C. and Lethbridge R.C.** (1979). Schistosome dermatitis in the Swan estuary, western Australia. *Med. J. Aust.* 1, 141–144.
- Ashrafi K., Nouroosta A., Sharifdini M., Mahmoudi M.R., Rahmati B. and Brant S. V.** (2018). Genetic diversity of an avian nasal schistosome causing cercarial dermatitis in the Black Sea-Mediterranean migratory route. *Parasitol. Res.* 117, 3821–3833.
- Autengruber A., Gereke M., Hansen G., Hennig C. and Bruder D.** (2012). Impact of enzymatic tissue disintegration on the level of surface molecule expression and immune cell function. *Eur. J. Microbiol. Immunol.* 2, 112–120.
- Babayán S., Attout T., Specht S., Hoerauf A., Snounou G., Rénia L., Korenaga M., Bain O. and Martin C.** (2005). Increased early local immune responses and altered worm development in high-dose infections of mice susceptible to the filaria *Litomosoides sigmodontis*. *Med. Microbiol. Immunol.* 194, 151–162.
- Batten P.J.** (1956). The histopathology of swimmers' itch. I. The skin lesions of *Schistosomatium douthitti* and *Gigantobilharzia huronensis* in the unsensitized mouse. *Am. J. Pathol.* 32, 363–377.
- Blažová K. and Horák P.** (2005). *Trichobilharzia regenti*: The developmental differences in natural and abnormal hosts. *Parasitol. Int.* 54, 167–172.
- Bourke C.D., Prendergast C.T., Sanin D.E., Oulton T.E., Hall R.J. and Mountford A.P.** (2015). Epidermal keratinocytes initiate wound healing and pro-inflammatory immune responses following percutaneous schistosome infection. *Int. J. Parasitol.* 45, 215–224.
- Bourns T.K., Ellis F.C. and Rau M.E.** (1973). Migration and development of *Trichobilharzia ocellata* (Trematoda: Schistosomatidae) in its duck hosts. *Can. J. Zool.* 51, 1021–1030.
- Brackett S.** (1940). Pathology of schistosome dermatitis. *Arch. Dermatol.* 42, 410–418.
- Bungiro R.D., Harrison L.M., Dondji B. and Cappello M.** (2022). Comparison of percutaneous vs oral infection of hamsters with the hookworm *Ancylostoma ceylanicum*: Parasite development, pathology and primary immune response. *PLoS Negl. Trop. Dis.* 16, e0010098.

- Caron Y., Cabaraux A., Marechal F. and Losson B.** (2017). Swimmer's itch in Belgium: First recorded outbreaks, molecular identification of the parasite species and intermediate hosts. *Vector-Borne Zoonotic Dis.* 17, 190–194.
- Chanová M., Vuong S. and Horák P.** (2007). *Trichobilharzia szidati*: The lung phase of migration within avian and mammalian hosts. *Parasitol. Res.* 100, 1243–1247.
- Chen L., Rao K.V.N., He Y.X. and Ramaswamy K.** (2002). Skin-stage schistosomula of *Schistosoma mansoni* produce an apoptosis-inducing factor that can cause apoptosis of T cells. *J. Biol. Chem.* 277, 34329–34335.
- Coillard A., Guyonnet L., de Juan A., Cros A. and Segura E.** (2021). TLR or NOD receptor signaling skews monocyte fate decision via distinct mechanisms driven by mTOR and miR-155. *Proc. Natl. Acad. Sci. U. S. A.* 118, e2109225118.
- Connor L.M., Tang S.C., Cognard E., Ochiai S., Hilligan K.L., Old S.I., Pellefigues C., White R.F., Patel D., Smith A.A.T. et al.** (2017). Th2 responses are primed by skin dendritic cells with distinct transcriptional profiles. *J. Exp. Med.* 214, 125–142.
- Cook P.C., Aynsley S.A., Turner J.D., Jenkins G.R., Van Rooijen N., Leeto M., Brombacher F. and Mountford A.P.** (2011). Multiple helminth infection of the skin causes lymphocyte hypo-responsiveness mediated by Th2 conditioning of dermal myeloid cells. *PLoS Pathog.* 7, e1001323.
- Cort W.W.** (1928). Schistosome dermatitis in the United States (Michigan). *J. Am. Med. Assoc.* 90, 1027–1029.
- Davey D., Manickam N., Simms B.T., Harrison L.M., Vermeire J.J. and Cappello M.** (2013). Frequency and intensity of exposure mediate resistance to experimental infection with the hookworm, *Ancylostoma ceylanicum*. *Exp. Parasitol.* 133, 243–249.
- Davis N.E., Blair D. and Brant S. V.** (2022). Diversity of *Trichobilharzia* New Zealand with a new species and a redescription, and their likely contribution to cercarial dermatitis. *Parasitology* 149, 380–395.
- De Liberato C., Berrilli F., Bossù T., Magliano A., Montalbano Di Filippo M., Di Cave D., Sigismondi M., Cannavacciuolo A. and Scaramozzino P.** (2019). Outbreak of swimmer's itch in Central Italy: Description, causative agent and preventive measures. *Zoonoses Public Health* 66, 377–381.
- Dolečková K., Kašný M., Mikeš L., Cartwright J., Jedelský P., Schneider E.L., Dvořák J., Mountford A.P., Craik C.S. and Horák P.** (2009). The functional expression and characterisation of a cysteine peptidase from the invasive stage of the neuropathogenic schistosome *Trichobilharzia regenti*. *Int. J. Parasitol.* 39, 201–211.
- Dolečková K., Albrecht T., Mikeš L. and Horák P.** (2010). Cathepsins B1 and B2 in the neuropathogenic schistosome *Trichobilharzia regenti*: Distinct gene expression profiles and presumptive roles throughout the life cycle. *Parasitol. Res.* 107, 751–755.
- Di Domizio J., Belkhdja C., Chenuet P., Fries A., Murray T., Mondéjar P.M., Demaria O., Conrad C., Homey B., Werner S. et al.** (2020). The commensal skin microbiota triggers type I IFN-dependent innate repair responses in injured skin. *Nat. Immunol.* 21, 1034–1045.
- Dudeck J., Kotrba J., Immler R., Hoffmann A., Voss M., Alexaki V.I., Morton L., Jahn S.R., Katsoulis-Dimitriou K., Winzer S. et al.** (2021). Directional mast cell degranulation of tumor necrosis factor into blood vessels primes neutrophil extravasation. *Immunity* 54, 468-483.e5.
- Fallon P.G., Teixeira M.M., Neice C.M., Williams T.J., Hellewell P.G. and Doenhoff M.J.** (1996). Enhancement of *Schistosoma mansoni* infectivity by intradermal injections of larval extracts: A putative role for larval proteases. *J. Infect. Dis.* 173, 1460–1466.

- Feiler W. and Haas W.** (1988a). Host-finding in *Trichobilharzia ocellata* cercariae: Swimming and attachment to the host. *Parasitology* 96, 493–505.
- Feiler W. and Haas W.** (1988b). *Trichobilharzia ocellata*: Chemical stimuli of duck skin for cercarial attachment. *Parasitology* 96, 507–517.
- De Filippo K., Dudeck A., Hasenberg M., Nye E., Van Rooijen N., Hartmann K., Gunzer M., Roers A. and Hogg N.** (2013). Mast cell and macrophage chemokines CXCL1/CXCL2 control the early stage of neutrophil recruitment during tissue inflammation. *Blood* 121, 4930–4937.
- Frey A., Di Canzio J. and Zurakowski D.** (1998). A statistically defined endpoint titer determination method for immunoassays. *J. Immunol. Methods* 221, 35–41.
- Gay P., Bayssade-Dufour C., Grenouillet F., Bourezane Y. and Dubois J.P.** (1999). Étude expérimentale de dermatites cercariennes provoquées par *Trichobilharzia* en France. *Med. Mal. Infect.* 29, 629–637.
- Grabe K. and Haas W.** (2004a). Navigation within host tissues: Cercariae orientate towards dark after penetration. *Parasitol. Res.* 93, 111–113.
- Grabe K. and Haas W.** (2004b). Navigation within host tissues: *Schistosoma mansoni* and *Trichobilharzia ocellata* schistosomula respond to chemical gradients. *Int. J. Parasitol.* 34, 927–934.
- Gulyás K., Soldánová M., Orosová M. and Oros M.** (2020). Confirmation of the presence of zoonotic *Trichobilharzia franki* following a human cercarial dermatitis outbreak in recreational water in Slovakia. *Parasitol. Res.* 119, 2531–2537.
- Haas W.** (1994). Physiological analyses of host-finding behaviour in trematode cercariae: Adaptations for transmission success. *Parasitology* 109, S15–S29.
- Haas W.** (2003). Parasitic worms: Strategies of host finding, recognition and invasion. *Zoology* 106, 349–364.
- Haas W. and Pietsch U.** (1991). Migration of *Trichobilharzia ocellata* schistosomula in the duck and in the abnormal murine host. *Parasitol. Res.* 77, 642–644.
- Haas W. and Van De Roemer A.** (1998). Invasion of the vertebrate skin by cercariae of *Trichobilharzia ocellata*: Penetration processes and stimulating host signals. *Parasitol. Res.* 84, 787–795.
- He Y.X., Chen L. and Ramaswamy K.** (2002). *Schistosoma mansoni*, *S. haematobium*, and *S. japonicum*: early events associated with penetration and migration of schistosomula through human skin. *Exp. Parasitol.* 102, 99–108.
- He Y.X., Salafsky B. and Ramaswamy K.** (2005). Comparison of skin invasion among three major species of *Schistosoma*. *Trends Parasitol.* 21, 201–203.
- Helmer N., Blatterer H., Hörweg C., Reier S., Sattmann H., Schindelar J., Szucsich N.U. and Haring E.** (2021). First record of *Trichobilharzia physellae* (Talbot, 1936) in Europe, a possible causative agent of cercarial dermatitis. *Pathogens* 10, 1473.
- Hervé P.L., Plaquet C., Assoun N., Oreal N., Gaulme L., Perrin A., Bouzereau A., Dhelft V., Labernardière J.L., Mondoulet L. et al.** (2021). Pre-existing humoral immunity enhances epicutaneously-administered allergen capture by skin DC and their migration to local lymph nodes. *Front. Immunol.* 12, 1–10.
- Hoppe A., Katsoulis-Dimitriou K., Edler H.J., Dudeck J., Drube S. and Dudeck A.** (2020). Mast cells initiate the vascular response to contact allergens by sensing cell stress. *J. Allergy Clin. Immunol.* 145, 1476-1479.e3.
- Horák P.** (1995). Developmentally regulated expression of surface carbohydrate residues on larval

stages of the avian schistosome *Trichobilharzia szidati*. *Folia Parasitol. (Praha)*. 42, 255–265.

**Horák P., Kolářová L. and Dvořák J.** (1998a). *Trichobilharzia regenti* n. sp. (Schistosomatidae, Bilharziellinae), a new nasal schistosome from Europe. *Parasite* 5, 349–357.

**Horák P., Kovář L., Kolářová L. and Nebesářová J.** (1998b). Cercaria-schistosomulum surface transformation of *Trichobilharzia szidati* and its putative immunological impact. *Parasitology* 116, 139–147.

**Horák P., Dvořák J., Kolářová L. and Trefil L.** (1999). *Trichobilharzia regenti*, a pathogen of the avian and mammalian central nervous systems. *Parasitology* 119, 577–581.

**Horák P., Kolářová L. and Adema C.M.** (2002). Biology of the schistosome genus *Trichobilharzia*. *Adv. Parasitol.* 52, 155–233.

**Horák P., Mikeš L., Lichtenbergová L., Skála V., Soldánová M. and Brant S.V.** (2015). Avian schistosomes and outbreaks of cercarial dermatitis. *Clin. Microbiol. Rev.* 28, 165–190.

**Hrádková K. and Horák P.** (2002). Neurotropic behaviour of *Trichobilharzia regenti* in ducks and mice. *J. Helminthol.* 76, 137–141.

**Hunter G.W.** (1951). The epidemiology of schistosome dermatitis (“koganbyo”) in Japan. *Trans. R. Soc. Trop. Med. Hyg.* 45, 103–112.

**Incáni R.N. and McLaren D.J.** (1984). Histopathological and ultrastructural studies of cutaneous reactions elicited in naive and chronically infected mice by invading schistosomula of *Schistosoma mansoni*. *Int. J. Parasitol.* 14, 259–276.

**Jafarzadeh A., Nair A., Jafarzadeh S., Nemati M., Sharifi I. and Saha B.** (2021). Immunological role of keratinocytes in leishmaniasis. *Parasite Immunol.* 43, e12870.

**Jordan P.M., Andreas N., Groth M., Wegner P., Weber F., Jäger U., Kuchler C., Werz O., Serfling E., Kamradt T. et al.** (2021). ATP/IL-33-triggered hyperactivation of mast cells results in an amplified production of pro-inflammatory cytokines and eicosanoids. *Immunology* 164, 541–554.

**Juhász A., Dán Á., Dénes B., Kucsera I., Danko J. and Majoros G.** (2016). Egy ritka zoonosis: A *Schistosoma turkestanicum* vérmétely által okozott cercaria dermatitis Magyarországon. *Orv. Hetil.* 157, 1579–1586.

**Juhász A., Majoros G. and Cech G.** (2022). Threat of cercarial dermatitis in Hungary: A first report of *Trichobilharzia franki* from the mallard (*Anas platyrhynchos*) and European ear snail (*Radix auricularia*) using molecular methods. *Int. J. Parasitol. Parasites Wildl.* 18, 92–100.

**Kagan I.G. and Meranze D.R.** (1955). The histopathology of immune and normal mouse skin exposed to cercariae of *Schistosomatium douthitti* (Trematoda : Schistosomatidae). *J. Infect. Dis.* 97, 187–193.

**Karvonen A., Pauku S., Valtonen E.T. and Hudson P.J.** (2003). Transmission, infectivity and survival of *Diplostomum spathaceum* cercariae. *Parasitology* 127, 217–224.

**Kashem S.W. and Kaplan D.H.** (2018). Isolation of murine skin resident and migratory dendritic cells via enzymatic digestion. *Curr. Protoc. Immunol.* 121, 139–148.

**Kašný M., Mikeš L., Dalton J.P., Mountford A.P. and Horák P.** (2007). Comparison of cysteine peptidase activities in *Trichobilharzia regenti* and *Schistosoma mansoni* cercariae. *Parasitology* 134, 1599–1609.

**Kia lashaki E., Gholami S., Fakhar M., Karamian M. and Daryani A.** (2021). Association between human cercarial dermatitis (HCD) and the occurrence of *Trichibilarizia* in duck and snail in main wetlands from Mazandaran Province, northern Iran. *Parasite Epidemiol. Control* 13, e00211.

- Koida A., Yasuda K., Adachi T., Matsushita K., Yasuda M., Hirano S. and Kuroda E.** (2021). Thymic stromal lymphopoietin contributes to protection of mice from *Strongyloides venezuelensis* infection by CD4+ T cell-dependent and -independent pathways. *Biochem. Biophys. Res. Commun.* 555, 168–174.
- Kolářová L.** (2007). Schistosomes causing cercarial dermatitis: A mini-review of current trends in systematics and of host specificity and pathogenicity. *Folia Parasitol. (Praha)*. 54, 81–87.
- Kolářová L., Horák P. and Sítko J.** (1997). Cercarial dermatitis in focus: Schistosomes in the Czech Republic. *Helminthologia* 34, 127–139.
- Korycińska J., Rybak-D'obyrn J., Kubiak D., Kubiak K. and Dzika E.** (2021). Dermatological and molecular evidence of human cercarial dermatitis in north-eastern Poland. *Vector-Borne Zoonotic Dis.* 21, 269–274.
- Kouřilová P., Syrůček M. and Kolářová L.** (2004a). The severity of mouse pathologies caused by the bird schistosome *Trichobilharzia regenti* in relation to host immune status. *Parasitol. Res.* 93, 8–16.
- Kouřilová P., Hogg K.G., Kolářová L. and Mountford A.P.** (2004b). Cercarial dermatitis caused by bird schistosomes comprises both immediate and late phase cutaneous hypersensitivity reactions. *J. Immunol.* 172, 3766–3774.
- Langenberg M.C.C., Hoogerwerf M.A., Koopman J.P.R., Janse J.J., Kos-van Oosterhoud J., Feijt C., Jochems S.P., de Dood C.J., van Schuijlenburg R., Ozir-Fazalalikhani A. et al.** (2020). A controlled human *Schistosoma mansoni* infection model to advance novel drugs, vaccines and diagnostics. *Nat. Med.* 26, 326–332.
- Leontovyč R., Young N.D., Korhonen P.K., Hall R.S., Tan P., Mikeš L., Kašný M., Horák P. and Gasser R.B.** (2016). Comparative transcriptomic exploration reveals unique molecular adaptations of neuropathogenic *Trichobilharzia* to invade and parasitize its avian definitive host. *PLoS Negl. Trop. Dis.* 10, e0004406.
- Lichtenbergová L., Kolbeková P., Kouřilová P., Kašný M., Mikeš L., Haas H., Schramm G., Horák P., Kolářová L. and Mountford A.P.** (2008). Antibody responses induced by *Trichobilharzia regenti* antigens in murine and human hosts exhibiting cercarial dermatitis. *Parasite Immunol.* 30, 585–595.
- Ligasová A., Bulantová J., Šebesta O., Kašný M., Koberna K. and Mikeš L.** (2011). Secretory glands in cercaria of the neuropathogenic schistosome *Trichobilharzia regenti* - Ultrastructural characterization, 3-D modelling, volume and pH estimations. *Parasites and Vectors* 4, 162.
- Liu Z., Liu Z., Gu Y., Shin A., Zhang S. and Ginhoux F.** (2020). Protocol analysis of myeloid cells in mouse tissues with flow cytometry protocol analysis of myeloid cells in mouse tissues with flow cytometry. *STAR Protoc.* 1, 100029.
- Loker E.S., DeJong R.J. and Brant S. V.** (2022). Scratching the itch: Updated perspectives on the schistosomes responsible for swimmer's itch around the world. *Pathogens* 11, 587.
- Lorenti E., Brant S. V., Gilardoni C., Diaz J.I. and Cremonte F.** (2022). Two new genera and species of avian schistosomes from Argentina with proposed recommendations and discussion of the polyphyletic genus *Gigantobilharzia* (Trematoda, Schistosomatidae). *Parasitology* 149, 1–59.
- Lowenberger C.A. and Rau M.E.** (1994). *Plagiorchis elegans*: Emergence, longevity and infectivity of cercariae, and host behavioural modifications during cercarial emergence. *Parasitology* 109, 65–72.
- Macfarlane W. V.** (1949). Schistosome dermatitis in New Zealand: Part II. Pathology and immunology of cercarial lesions. *Am. J. Epidemiol.* 50, 152–167.
- Macháček T., Turjanicová L., Bulantová J., Hrdý J., Horák P. and Mikeš L.** (2018). Cercarial dermatitis: a systematic follow-up study of human cases with implications for diagnostics. *Parasitol. Res.* 117,

3881–3895.

**Macháček T., Leontovyč R., Šmídová B., Majer M., Vondráček O., Vojtěchová I., Petrásek T. and Horák P.** (2022). Mechanisms of the host immune response and helminth-induced pathology during *Trichobilharzia regenti* (Schistosomatidae) neuroinvasion in mice.

**Majer M., Macháček T., Súkeníková L., Hrdý J. and Horák P.** (2020). The peripheral immune response of mice infected with a neuropathogenic schistosome. *Parasite Immunol.* 42, e12710.

**Marszewska A., Strzała T., Cichy A., Dąbrowska G.B. and Żbikowska E.** (2018). Agents of swimmer's itch—dangerous minority in the Digenea invasion of Lymnaeidae in water bodies and the first report of *Trichobilharzia regenti* in Poland. *Parasitol. Res.* 117, 3695–3704.

**Mduluza-Jokonya T.L., Vengesai A., Midzi H., Kasambala M., Jokonya L., Naicker T. and Mduluza T.** (2021). Algorithm for diagnosis of early *Schistosoma haematobium* using prodromal signs and symptoms in pre-school age children in an endemic district in Zimbabwe. *PLoS Negl. Trop. Dis.* 15, e0009599.

**Mikeš L., Židková L., Kašný M., Dvořák J. and Horák P.** (2005). In vitro stimulation of penetration gland emptying by *Trichobilharzia szidati* and *T. regenti* (Schistosomatidae) cercariae. Quantitative collection and partial characterization of the products. *Parasitol. Res.* 96, 230–241.

**Neuhaus W.** (1952). Biologie und entwicklung von *Trichobilharzia szidati* n. sp. (Trematoda, Schistosomatidae), einem Erreger von dermatitis beim Menschen. *Zeitschrift Für Parasitenkd.* 15, 203–266.

**Nevhutalu P.A., Salafsky B., Haas W. and Conway T.** (1993). *Schistosoma mansoni* and *Trichobilharzia ocellata*: Comparison of secreted cercarial eicosanoids. *J. Parasitol.* 79, 130–133.

**Olivier L.** (1949). Schistosome dermatitis, a sensitization phenomenon. *Am. J. Epidemiol.* 49, 290–302.

**Olivier L.** (1953). Observations on the migration of avian schistosomes in mammals previously unexposed to cercariae. *J. Parasitol.* 39, 237–246.

**Oyarzún-Ruiz P., Thomas R., Santodomingo A., Collado G., Muñoz P. and Moreno L.** (2022). Morphological, behavioral, and molecular characterization of avian schistosomes (Digenea: Schistosomatidae) in the native snail *Chilina dombeyana* (Chiliniidae) from southern Chile. *Pathogens* 11, 332.

**Parohová I.** (2020). Parazitem indukovaná apoptóza u myši infikovaných neuropatogenní schistosomou *Trichobilharzia regenti*. Master's thesis. Charles University.

**Paveley R.A., Aynsley S.A., Cook P.C., Turner J.D. and Mountford A.P.** (2009). Fluorescent imaging of antigen released by a skin-invading helminth reveals differential uptake and activation profiles by antigen presenting cells. *PLoS Negl. Trop. Dis.* 3, e528.

**Pinelli E., Brandes S., Dormans J., Fonville M., Hamilton C.M. and der Giessen J. van** (2007). *Toxocara canis*: Effect of inoculum size on pulmonary pathology and cytokine expression in BALB/c mice. *Exp. Parasitol.* 115, 76–82.

**Pinto H.A., Mati V.L.T., Melo A.L. and Brant S. V.** (2022). A putative new genus of avian schistosome transmitted by *Biomphalaria straminea* (Gastropoda: Planorbidae) in Brazil, with a discussion on the potential involvement in human cercarial dermatitis. *Parasitol. Int.* 90, 102607.

**Ponte-Sucre A., Heise D. and Moll H.** (2001). *Leishmania major* lipophosphoglycan modulates the phenotype and inhibits migration of murine Langerhans cells. *Immunology* 104, 462–467.

**Prendergast C.T., Sanin D.E., Cook P.C. and Mountford A.P.** (2015). CD4+ T cell hyporesponsiveness

after repeated exposure to *Schistosoma mansoni* larvae is dependent upon interleukin-10. *Infect. Immun.* 83, 1418–1430.

**Ramaswamy K., Salafsky B., Potluri S., He Y.X., Li J.W. and Shibuya T.** (1996). Secretion of an anti-inflammatory, immunomodulatory factor by schistosomulae of *Schistosoma mansoni*. *J. Inflamm.* 46, 13–22.

**Rao V.G., Dash A.P., Agrawal M.C., Yadav R.S., Anvikar A.R., Vohra S., Bhondeley M.K., Ukey M.J., Das S.K., Minocha R.K. et al.** (2007). Cercarial dermatitis in central India: An emerging health problem among tribal communities. *Ann. Trop. Med. Parasitol.* 101, 409–413.

**Reier S., Haring E., Billinger F., Blatterer H., Duda M., Gorofsky C., Grasser H.P., Heinisch W., Hörweg C., Kruckenhauser L. et al.** (2020). First confirmed record of *Trichobilharzia franki* Müller & Kimmig, 1994, from *Radix auricularia* (Linnaeus, 1758) for Austria. *Parasitol. Res.* 119, 4135–4141.

**Římnáčová J., Mikeš L., Turjanicová L., Bulantová J. and Horák P.** (2017). Changes in surface glycosylation and glycocalyx shedding in *Trichobilharzia regenti* (Schistosomatidae) during the transformation of cercaria to schistosomulum. *PLoS One* 12, e0173217.

**Rudolfová J., Hampl V., Bayssade-Dufour C., Lockyer A.E., Littlewood D.T.J. and Horák P.** (2005). Validity reassessment of *Trichobilharzia* species using *Lymnaea stagnalis* as the intermediate host. *Parasitol. Res.* 95, 79–89.

**Scott P.** (2020). Long-lived skin-resident memory T cells contribute to concomitant immunity in cutaneous leishmaniasis. *Cold Spring Harb. Perspect. Biol.* 12, a038059.

**Selbach C., Soldánová M. and Sures B.** (2016). Estimating the risk of swimmer's itch in surface waters – A case study from Lake Baldeney, River Ruhr. *Int. J. Hyg. Environ. Health* 219, 693–699.

**Sheng J., Chen Q., Wu X., Dong Y.W., Mayer J., Zhang J., Wang L., Bai X., Liang T., Sung Y.H. et al.** (2021). Fate mapping analysis reveals a novel murine dermal migratory Langerhans-like cell population. *Elife* 10, e65412.

**Simaren J.O. and Ogunyoye A.O.** (1973). Worm burden, pathophysiology and indirect nutritional effect of *Nippostrongylus brasiliensis* on the host. *Ann. Parasitol. Hum. Comp.* 48, 105–116.

**Soldánová M., Selbach C., Kalbe M., Kostadinova A. and Sures B.** (2013). Swimmer's itch: Etiology, impact, and risk factors in Europe. *Trends Parasitol.* 29, 65–74.

**Soldánová M., Selbach C. and Sures B.** (2016). The early worm catches the bird? Productivity and patterns of *Trichobilharzia szidati* cercarial emission from *Lymnaea stagnalis*. *PLoS One* 11, e0149678.

**Soldánová M., Born-Torrijos A., Kristoffersen R., Knudsen R., Amundsen P.A. and Scholz T.** (2022). Cercariae of a bird schistosome follow a similar emergence pattern under different subarctic conditions: First experimental study. *Pathogens* 11, 647.

**Souadkia N., Brown A., Leach L. and Pritchard D.I.** (2010). Hookworm (*Necator americanus*) larval enzymes disrupt human vascular endothelium. *Am. J. Trop. Med. Hyg.* 83, 549–558.

**Tracz E.S., Al-Jubury A., Buchmann K. and Bygum A.** (2019). Outbreak of swimmer's itch in Denmark. *Acta Derm. Venereol.* 99, 1116–1120.

**Turjanicová L.** (2012). Protilátková odpověď specifických hostitelů vůči antigenům ptačích schistosom. Master's thesis. Charles University.

**Vondráček O., Mikeš L., Talacko P., Leontovych R., Bulantová J. and Horák P.** (2022). Differential proteomic analysis of laser-microdissected penetration glands of avian schistosome cercariae with a focus on proteins involved in host invasion. *Int. J. Parasitol.* 52, 343–358.

**Whitfield P.J., Bartlett A., Khammo N. and Clothier R.H.** (2003). Age-dependent survival and infectivity of *Schistosoma mansoni* cercariae. *Parasitology* 127, 29–35.

**Yamada M., Nakazawa M., Kamata I. and Arizono N.** (1992). Low-level infection with the nematode *Nippostrongylus brasiliensis* induces significant and sustained specific and non-specific IgE antibody responses in rats. *Immunology* 75, 36–40.